Mitochondrial motility during synapse development

Pinho da Silva, Cátia Alexandra

2022

document version
Publisher's PDF, also known as Version of record

Mitochondrial motility during synapse development

Cátia A. P. Silva

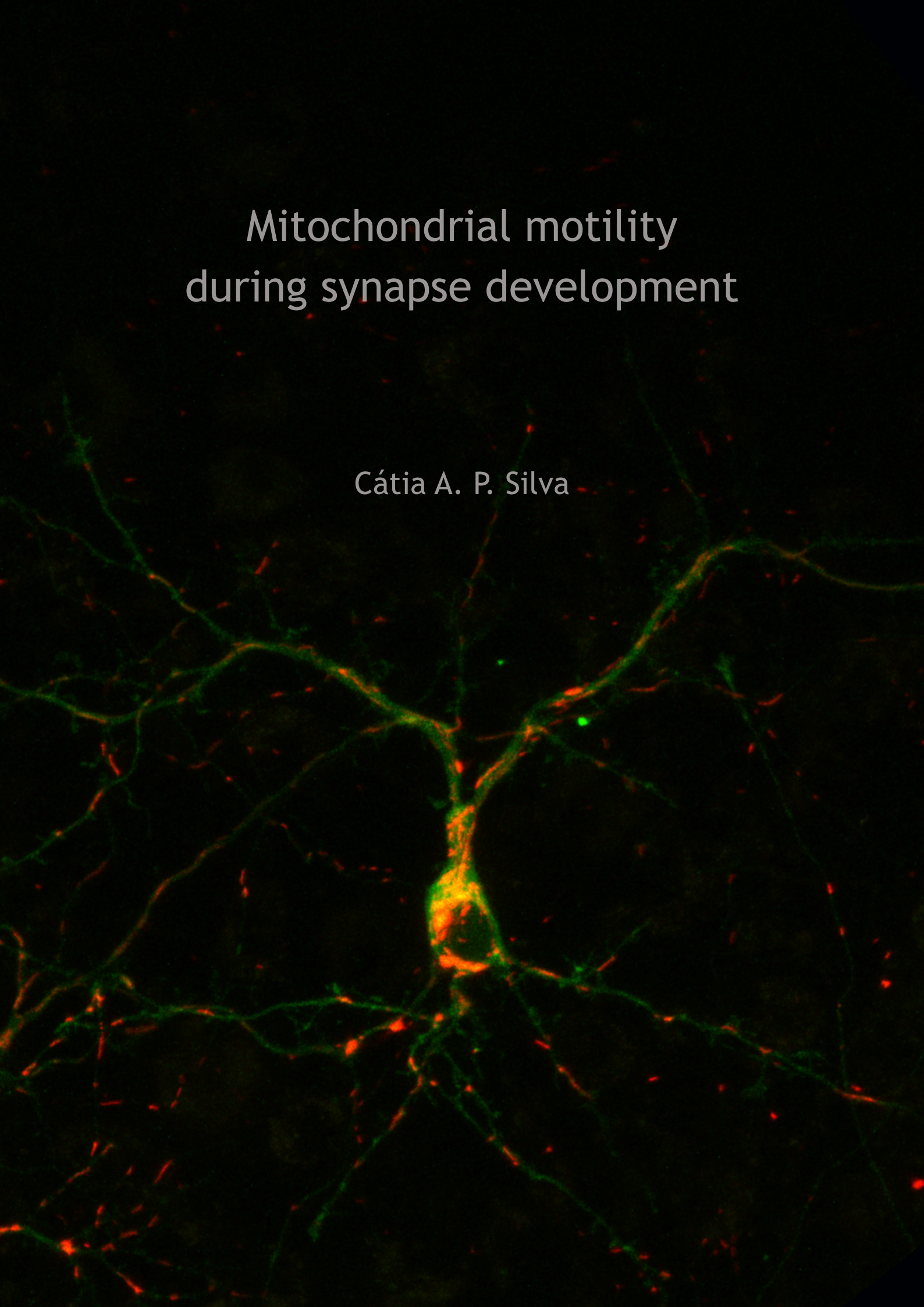

Mitochondrial motility during synapse development

Cátia A. P. Silva

The research conducted and described in this thesis was done in the Synapse and Network Development Department at the Netherlands Institute for Neuroscience, an Institute of the Royal Netherlands Academy for Arts and Sciences, Amsterdam, The Netherlands.

Layout and design by Cátia A. P. Silva

VRIJE UNIVERSITEIT

MITOCHONDRIAL MOTILITY DURING SYNAPSE DEVELOPMENT

ACADEMISCH PROEFSCHRIFT

ter verkrijging van de graad Doctor of Philosophy aan
de Vrije Universiteit Amsterdam,
op gezag van de rector magnificus
prof.dr. J.J.G. Geurts,
in het openbaar te verdedigen
ten overstaan van de promotiecommissie
van de Faculteit der Bètawetenschappen
op woensdag 15 juni 2022 om 11.45 uur
in een bijeenkomst van de universiteit,
De Boelelaan 1105

door

Cátia Alexandra Pinho Da Silva

geboren te Santa Maria da Feira, Portugal

promotor:	prof.dr. M. Verhage
copromotor:	prof.dr. C.N. Levelt
promotiecommissie:	prof.dr. A.B. Smit prof.dr. C.I. de Zeeuw prof.dr. A. Luisa Carvalho dr. J. Cheyne dr. J.A. Heimel

Contents

General abstract

Mammals are able to make sense of the external environment soon after they are born. How incredible is that, considering that they had not experienced anything like it before? I and others have studied young brains to understand the neuronal mechanisms that allow for this incredible feat of nature.

During early brain development, connectivity between neurons is dynamic, with synaptic contacts continuously being formed and eliminated. The refinement of these synaptic connections depends on neuronal 1) activity, 2) energy, and 3) morphological changes. These are extremely important processes, as the correct synaptic contacts must be made to ensure that functional and healthy neuronal networks are formed. The work described in this thesis was conducted in the primary visual cortex of mice during the first two postnatal weeks. In this model, we are able to study 1) spontaneous activity, which is neuronal activity without sensory input nor artificial manipulations; 2) the presence and motility of mitochondria, the main energy- producing organelles in neurons; and 3) the dynamics of microtubules, the organelles responsible for neuronal morphological changes; as well as their relationship to each other.

Previous work has shown that neuronal activity modulates mitochondria, and that mitochondria affect synapses. Despite their obvious importance, these studies had some experimental limitations and resulted in some apparently conflicting conclusions.

In this thesis, we used an improved methodological and experimental approach, and found unifying theories for previous literature. Specifically, we showed that *in vivo*, mitochondrial motility decreases over development, stabilising around the second postnatal week in the visual cortex (simultaneous with eye opening). We did not find any evidence supporting the hypothesis that neuronal activity that affects the whole neuron is able to modulate mitochondrial motility during early postnatal development. And lastly, we found synaptic activity to be able to modulate mitochondrial motility, which most likely explains the developmental decrease in mitochondrial motility.

Investing in learning the rules of connectivity between neurons is important and necessary. It expands humanity's knowledge, allows for a better understanding of neurodevelopmental disorders and how to tackle them, and will certainly contribute to a reduction in the use of animal models for scientific research.

List of abbreviations

aCSF	Artificial cerebrospinal fluid
ADP	Adenosine diphosphate
ANT	Adenine nucleotide translocase
ATP	Adenosine triphosphate
CamKII	Calcium/ calmodulin-dependent kinase II
CFP	Cyan fluorescent protein
CNQX	Cyanquixaline (6-cyano-7-nitroquinoxaline-2,3-dione)
COXVIII	Cytochrome C oxidase subunit 8
DIV	Days *in vitro*
DNA	Deoxyribonucleic acid
DRP1	Dynamin-1-like protein
DsRed	Discosoma red fluorescent protein
E	Embryonic day
EB3	Microtubule end-binding protein 3
FCCP	Carbonyl cyanide p-(tri-fluromethoxy)phenyl-hydrazone
Fis1	Mitochondrial fission protein 1
FM1-43	N-(3-triethylammoniumpropyl)-4-(p-dibutylaminostyryl)pyridinium dibromide
GABA	Gamma-aminobutyric acid
GABAA	Gamma-aminobutyric acid receptor subunit A
GFP	Green fluorescent protein<
GTPases	Hydrolase enzymes that bind to the nucleotide guanosine triphosphate
HBSS	Hank's balanced salt solution
i.p.	Intraperitoneal injection
IVC	Individually ventilated cages
Kif5a	Kinesin family member 5a

LPZ	Lesion projection zone
LTX	Latrotoxin
MCU	Mitochondrial calcium uniporter
Mfn1	Mitofusin 1
Miro1	Mitochondrial RHO
NCX	Sodium/ calcium exchanger
NMDA	N-methyl-D-aspartate
NR2B	N-methyl-D-aspartate receptor subunit 2b
Opa1	Optic atrophy protein 1
P	Postnatal day
PSD95	Postsynaptic density protein 95
Ras	Rat sarcoma virus protein
s.c.	Subcutaneous injection
Trak	Trafficking kinesin protein, aka Milton
TTX	Tetrodotoxin
V1	Primary visual cortex
YFP	Yellow fluorescent protein

Chapter 1

General introduction

List of figures

1. The developing nervous system

Newborn mammals can successfully interact with their environment very soon after birth, despite the lack of patterned sensory input in the womb. To understand how the neonatal brain is prepared for the onset of sensory information input, the processes that shape neuronal connectivity in the developing nervous system have been studied intensively. Besides providing insight into the healthy brain, such research also contributes to our understanding and subsequent treatment of neurodevelopmental disorders.

During early brain development, connectivity between neurons is in a dynamic state, with synaptic contacts continuously being formed and eliminated (Li et al., 2010). Initial connectivity is established by molecular guidance cues, and further refinement of these synaptic connections is activity dependent (Clause et al., 2014; Simon and O'Leary, 1992).

There is little sensory input to drive activity; instead, the necessary activity is spontaneously generated by the brain. Spontaneous activity occurs throughout the developing nervous system and in many animals. The best studied example is the mouse visual system. It develops after birth and the computations are well known (Leighton and Lohmann, 2016). Mice are born blind, and the eyes remain closed during the first two postnatal weeks (Figure 1). When the eyes open, neuronal connections in the visual system have already been made and are immediately ready to receive and process sensory information from the outside world. Experiments suggest that it is because before this, neuronal circuits generate spontaneous activity that helps setting up and refining early connections between neurons (Katz and Shatz, 1996). This activity is generated by pacemaker cells present in the immature retina, even before photoreceptors are present (Galli and Maffei, 1988; Meister et al., 1991). Spontaneous activity propagates along the optic nerve, through the thalamus and into the visual cortex. This spontaneous activity most likely serves to test-run and fine-tune the synaptic connections of visual pathways downstream of the retina (Huberman et al., 2008; Kleindienst et al., 2011). Spontaneous activity is also generated in the thalamus and/ or the cortex (Siegel and Lohmann, 2009). Typically, spontaneous activity occurs in bursts, where many neurons are active together. These activity patterns are known to be important for connecting neurons properly during this period of development, because synapses between neurons that are frequently active together are potentiated and synapses between neurons that fire out-of-sync become weakened or eliminated (Leighton and Lohmann, 2016).

Both neuronal plasticity during synaptogenesis and spontaneous activity are energetically expensive (Attwell and Laughlin, 2001; Harris et al., 2012). In fact, the ability of synapses to undergo plasticity depends on energy availability (Attwell and Laughlin, 2001; Lohmann and Kessels, 2014). The molecular unit of currency of intracellular energy is adenosine triphosphate (ATP), and mitochondria are the main ATP producers in the central nervous system (Silver and Erecinska, 1994). Mitochondrial energy provision is crucial for adequate network activity and connectivity (Li et al., 2004; Mattson et al., 2008).

Both synaptic development and spontaneous activity need tightly regulated energy provision and also calcium handling (discussed next). As mitochondria perform both functions, in this thesis I explore the relationship between mitochondrial distribution, synaptic development, and spontaneous activity in functional neuronal networks. In the next sections I will first introduce some background information on mitochondria, and then discuss their relationship to brain development and neuronal activity.

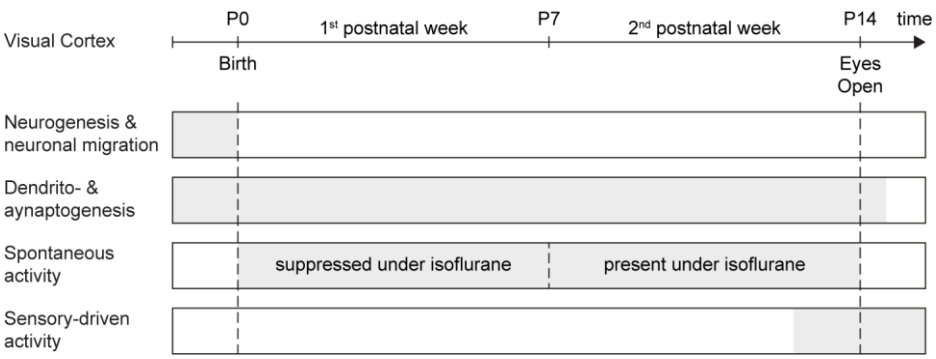

Figure 1. Timeline of some relevant events in the developing primary visual cortex of mice. All experiments in this thesis were performed during the first two postnatal weeks (see * in section 6).

2. Mitochondria

Neuronal mitochondria are organelles of approximately 0.5 up to 5 µm in length, with a characteristic elongated, oval shape. Mitochondria most likely originated approximately 1.5 billion years ago, when previously independent organisms formed an endosymbiotic relationship with eukaryotic cells. Mitochondria became organelles, providing mechanisms for cellular respiration and an evolutionary advantage to their host cells (Martin et al., 2015). Of the many functions they perform within the cell (MacAskill et al., 2010), arguably the most important ones are ATP production and calcium buffering. To optimally perform these functions, mitochondria are dynamic: they undergo fusion and fission (to create larger mitochondria or split in two as necessary), and are motile (transported to all parts of the cell to locally execute their functions).

2.1 Mitochondrial ATP production

Mitochondria are composed of two lipid bilayer membranes. The outer one is thought to have been originated by the original prokaryote when it became enveloped within the host cell. Having this outer membrane gives mitochondria an intermembrane space (Gellerich et al., 2000), which encapsulates the energy-production processes of the inner membrane (Figure 2). The inner membrane contains the electron transport chain and ATP synthase necessary to produce energy by oxidative phosphorylation (Figure 3) (Fernie et al., 2004). This is the machinery used to produce ATP from glucose and oxygen. An adenosine nucleotide translocator (ANT) transports adenosine diphosphate (ADP, an ATP precursor) from the cytoplasm to the mitochondrial matrix (the space inside the inner mitochondrial membrane), and conversely, transports newly generated ATP from the mitochondrial matrix back to the cytoplasm.

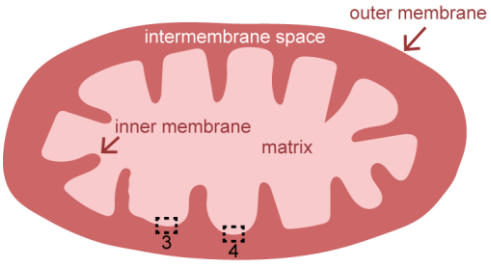

Figure 2. Representation of a mitochondrion with outer membrane, intermembrane space, inner membrane, and mitochondrial matrix. Indication of insets for Figures 3 and 4.

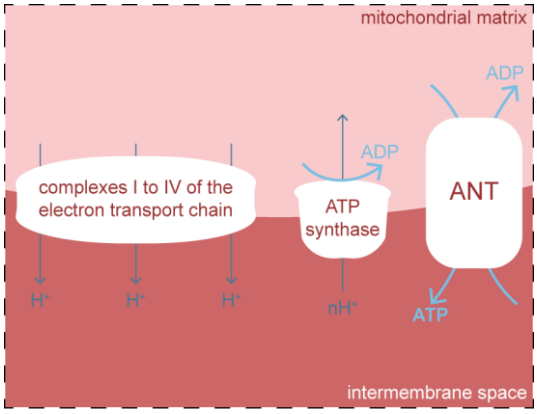

Figure 3. Mitochondrial machinery for ATP production. In the presence of oxygen, glucose is transformed through glycolysis and then the Krebs cycle. The sub-products enter the electron transport chain in the mitochondrion, forming a proton gradient that enables the ATP synthase to phosphorylate ADP into ATP. ATP is the cellular currency for energy.

2.2 Mitochondrial calcium buffering

Tight regulation of intracellular calcium is crucial for many cellular processes, including survival. Large amounts of calcium can enter neurons via activated neurotransmitter receptors, such as the ionotropic glutamatergic N-methyl D-aspartate (NMDA) receptor, or through voltage-gated calcium channels during action potential firing. Simultaneously, neurons rely on local increases in calcium for intracellular communication, for instance as second messengers in signal transduction at the postsynaptic site (Brini et al., 2014). Prolonged high global calcium levels activate cytotoxic signaling cascades that can damage or even kill the cell. To prevent calcium-induced cytotoxicity, mitochondria buffer the intracellular calcium concentration via

the mitochondrial calcium uniporter (MCU) (Figure 4) (Mammucari et al., 2018). Mitochondria can then release calcium via de sodium/ calcium exchanger (NCX, which moves sodium into the mitochondrial matrix in exchange for calcium) (Luongo et al., 2017). By taking up and releasing calcium locally and in a controlled way, mitochondria help modulate intracellular calcium signals to control metabolism, transcription, secretion, and programmed cell death. Thus, mitochondrial influence allows neurons to maintain global calcium homeostasis (Knott and Holtmaat, 2008; MacAskill and Kittler, 2009; MacAskill et al., 2010; Mattson et al., 2008).

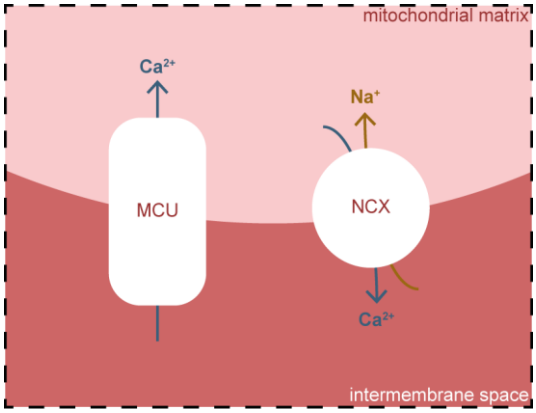

Figure 4. The Mitochondrial Calcium Uniporter (MCU) passively transports calcium into the mitochondrial matrix. The Sodium/ Calcium exchanger (NCX) moves calcium outside of the mitochondrion (from the matrix to the intermembrane space), in exchange for sodium into the matrix.

2.3 Mitochondrial fusion and fission

Mitochondrial fusion and fission events (Figure 5) occur in coordinated cycles and help determine the number and size of mitochondria (Cagalinec et al., 2013; Tilokani et al., 2018). Mitochondrial fusion occurs when two mitochondria fuse into one bigger one and is regulated by OPA1 (Dominant optic atrophy protein 1) and MFN1 (Mitofusin 1) (Tilokani et al., 2018). It is most likely to occur when mitochondria are motile (Cagalinec et al., 2013). Fission, mostly under the control of FIS1 (Mitochondrial fission 1 protein) and DRP1 (Dynamin-1-like protein), occurs when mitochondria are too long and ought to be divided into two (Cagalinec et al., 2013; Tilokani et al., 2018). These processes protect mitochondrial function by enabling the mixing and exchange of small molecules, proteins, and mitochondrial DNA between mitochondria (Cagalinec et al., 2013).

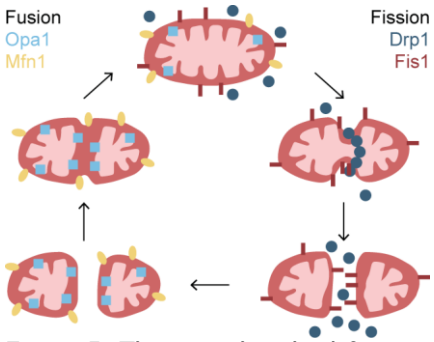

Figure 5. The mitochondrial fusion-fission cycle. Mitochondrial fusion is mostly regulated by OPA1 and MFN1; and mitochondrial fission by FIS1 and DRP1.

2.4 Mitochondrial motility

Mitochondrial transport, or motility, occurs via the microtubule network, together with motor and adaptor proteins (Figure 6).

Microtubules, together with actin filaments and neurofilaments, form the major parts of the neuronal cytoskeleton. Microtubules are dynamic, as they are continuously being formed and dismantled (Gu and Zheng, 2009). They are also polarized, with the plus-end undergoing polymerization and therefore growth, and the minus-end undergoing disassembly leading to shrinkage. In axons, microtubules are uniformly oriented with their plus poles towards the distal ends. In dendrites, microtubules show both orientations, with only the most distal dendrites showing the axon-like unidirectional orientation (Gu and Zheng, 2009).

Two families of motor proteins execute microtubule-dependent mitochondrial transport: kinesins (which move from minus- to plus-ends), and dyneins (which move from plus- to minus-ends) (Frederick and Shaw, 2007). In axons, kinesins are the most abundant, as transport occurs mainly from the soma (where mitochondria are initially generated) to the distal ends. In dendrites, mitochondrial transport can switch rapidly between retrograde and anterograde directions, due to both microtubule organization and the presence of both dyneins and kinesin family member 5a (KIF5a) on single mitochondria (Toba et al., 2006).

Adaptor proteins link mitochondria to motor proteins, or directly to microtubules (MacAskill et al., 2009). MIRO (mitochondrial RHO) is an adaptor protein localized in the mitochondrial outer membrane (Fransson et al., 2003). MIRO1 can bind to a second adaptor protein, TRAK (trafficking kinesin protein) (Schwarz, 2013); or directly to kinesin KIF5 (MacAskill et al., 2009). MIRO1 is a key protein for regulating mitochondrial motility, most likely due to a calcium sensing domain (section 2.5, Figure 6) (MacAskill et al., 2009).

Microtubules are essential for mitochondrial motility, as disruption of microtubule dynamics (with colchicine or nocodazole) reduced mitochondrial motility (Muller et al., 2005). Conversely, mitochondrial function is also essential for microtubule dynamics, as disrupting mitochondrial ATP production (with FCCP, cyanide, or oligomycin) also reduced mitochondrial motility (Mironov, 2007; Muller et al., 2005). Thus, intact microtubule- and mitochondrial function are necessary for mitochondrial motility, suggesting interplay between mitochondrial function and microtubule dynamics.

2.5 Mitochondrial stabilization

In-between transportation, mitochondria can temporarily stop (for seconds to minutes) at positions along the neuronal processes, and also sometimes undergo long-term stabilization (at least for several days) (Chang et al., 2006; Li et al., 2004; MacAskill et al., 2009).Temporary arrest of mitochondria appears to occur mainly through local rises in calcium (Yi et al., 2004), that bind to MIRO1 (section 2.4, Figure 6) (MacAskill et al., 2009; Vaccaro et al., 2017; Wang and Schwarz, 2009). Pull-down assays show that calcium binding leads to a conformational change that unbinds MIRO1 from the adaptor protein TRAK (Wang and Schwarz, 2009), and/ or the motor protein kinesin KIF5 (MacAskill et al., 2009), preventing mitochondria from continuing motility along the axon or dendrite (Figure 6B). This link to MIRO1 was confirmed by overexpression of calcium-insensitive MIRO1, which prevented calcium-dependent inhibition of mitochondrial motility (MacAskill et al., 2009; Vaccaro et al., 2017; Wang and Schwarz, 2009).

Reduced mitochondrial motility has also been linked to a decrease in local intracellular ATP, as injection of ADP (a readout for low ATP, as it lowers the ATP/ADP ratio) decreased mitochondrial motility in cultures of respiratory neurons (Mironov, 2007). Moreover, mitochondria are known to localize to subcellular compartments with high ATP consumption, such as synapses (Wong-Riley, 1989). Thus, it is widely believed that mitochondria localize near synapses to buffer local calcium increases and provide the necessary ATP (Mironov, 2006, 2007; Sheng, 2014).

Both high calcium and low ATP are signals to stop mitochondria and are also characteristics common to the synaptic environment. When near synapses, mitochondria could buffer the resulting calcium, and produce the necessary ATP to fuel synaptic transmission. Both these functions could be of particular importance as synapses form during early development, as the presence of mitochondria may be necessary for synapse stabilization and thus (co-) determine where and which synaptic contacts are established and/ or maintained.

Long term stabilization of mitochondria seems to require mitochondrial binding to the cytoskeleton. In axons, the synaptic protein syntaphilin has been shown to be necessary and sufficient to dock mitochondria to the microtubule network (Kang et al., 2008). It is not yet clear how long-term mitochondrial immobilization occurs in dendrites, but it seems to include a direct binding to the actin cytoskeleton (Boldogh and Pon, 2006). For example, myosin V has been suggested as a dendritic mitochondrial tether (Yi et al., 2004), as myosin V depletion increased axonal mitochondrial motility (Pathak et al.,

2010), and is present in dendrites (Konietzny et al., 2019) where it may play a similar role as in axons.

In summary, mitochondrial motility and their temporary arrest are crucial processes for the proper functioning of the neuron, and their potential regulation by (synaptic) calcium must be studied under more physiological conditions.

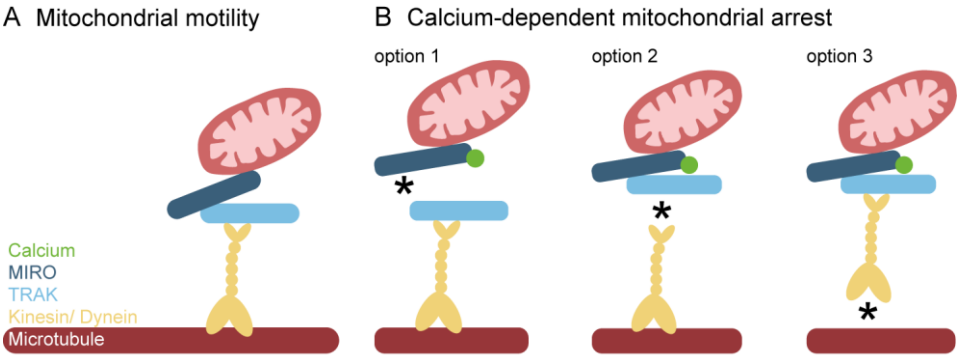

Figure 6.
A. Microtubule-dependent mitochondrial motility, including motor proteins (kinesins and dyneins), and adaptor proteins (MIRO and TRAK).
B. Calcium-dependent mitochondrial arrest occurs through binding of calcium to MIRO that unbinds (*) mitochondria from the adaptor protein (option 1), the motor protein (option 2), and/ or the microtubule (option 3).

3. Mitochondria in neurite and synapse development

The transport of mitochondria to distal parts of neurons occurs concomitantly with neurite growth and branching, as well as synaptogenesis (Kimura and Murakami, 2014). Mitochondria appear to limit neurite growth and branching, as hindering mitochondrial presence or function in neurites increased neurite branching and lengthening (Gioran et al., 2014; Kimura and Murakami, 2014). In contrast, mitochondrial presence seems positively correlated with synapse formation. Neurons grown in culture show a progressive decrease in mitochondrial motility with age, which is associated with an increase in synaptic density (Chang and Reynolds, 2006), and an increase in mitochondrial presence at synapses (Lewis et al., 2016). Furthermore, increasing dendritic mitochondrial density (by overexpressing DRP1) or function (with creatine) led to the formation of new excitatory synapses (Li et al., 2004). Conversely, decreasing dendritic mitochondrial density (with OPA1 overexpression or a dominant DRP1 mutant) was followed by a reduction in the number of excitatory synapses in spines (Li et al., 2004). Removing mitochondria from axon terminals results in aberrant synaptic transmission, likely due to insufficient ATP supply and/ or altered calcium transients (Sheng, 2014). Moreover, boutons with nearby mitochondria were found to be bigger and with more vesicles (Li et al., 2008).

Altogether, it seems that as mitochondria are transported to distal locations, and mitochondrial motility is typically high, mitochondria negatively regulate neurite branching and length (Kimura and Murakami, 2014). Over time, mitochondrial motility decreases, and mitochondrial presence positively modulates synaptogenesis (Li et al., 2004). Interestingly, though mitochondria affect neurite and synapse development, synapses in turn reciprocally affect mitochondria, both function and localization (Kimura and Murakami, 2014; Li et al., 2004). This has been mostly investigated in the context of neuronal activity, which I discuss next.

4. Mitochondria and neuronal activity

One of the physiological principles that have been described to regulate the accumulation of mitochondria at synapses is neuronal activity (Chang et al., 2006; Li et al., 2004; MacAskill et al., 2009). Neuronal activity can be categorized in many ways, but for the purpose of this thesis I will distinguish between global and local activity. 'Global activity' refers to a calcium transient that affects a large portion of the dendritic tree, typically as the result of back-propagating action potentials. In contrast, 'local activity' refers to activity in subcellular compartments, such as synapses, and results from synaptic activity. Both global and local activity involve increases in intracellular calcium and both affect mitochondrial dynamics and function (sections 2.4 and 2.5).

4.1 Global activity

Decreased mitochondrial motility has been found using various methods to artificially increase global neuronal activity; activating NMDA receptors with either high extracellular potassium, glutamate, or tetanic electrical stimulation (Chang et al., 2006; Li et al., 2004; MacAskill and Kittler, 2009; Wang and Schwarz, 2009), using a sodium channel agonist (veratridine) (Chang et al., 2006); and using a GABAA receptor blocker (bicuculline) (Chang et al., 2006; MacAskill et al., 2009). Conversely, mitochondrial motility was increased by blocking neuronal activity (with tetrodotoxin, TTX) (Chang et al., 2006; Li et al., 2004). Hence, many studies showed an anti-correlation between neuronal activity and mitochondrial motility.

However, one study failed to replicate these results. In their hands, blocking the GABAA receptor (with bicuculline), activating adenylyl cyclase (with forskolin), or increasing intracellular calcium (with thapsigargin), did not decrease mitochondrial

motility (Beltran-Parrazal et al., 2006). Similarly, blocking activity (with TTX), or blocking glutamate receptors (using CNQX + MK801), did not increase mitochondrial motility (Beltran-Parrazal et al., 2006). The discrepancy with previously mentioned studies is probably due to differences in methodological approaches, such as age of neurons (E17-P0 vs E16), and/ or concentrations of drugs used (e.g. 50-100 µM vs 10 µM of glutamate or bicuculline). As this study was mostly overlooked in the field, it remains generally accepted that neuronal activity negatively modulates mitochondrial motility.

The abovementioned studies used pharmacological and other artificial manipulations, often inducing dramatic changes in neuronal activity, and mostly in cultured rodent neurons. Understanding the effect of physiological activity on mitochondrial motility requires more nuanced experiments. The strongest suggestion that manipulations of neuronal activity do not tell the full story of the relationship between neuronal activity and mitochondrial motility comes from a more recent study in retinal explants (Faits et al., 2016). High extracellular potassium decreased mitochondrial motility as in previous studies (Faits et al., 2016). In contrast, physiological activity (both spontaneous and sensory-evoked) did not affect mitochondrial motility (Faits et al., 2016). Moreover, a model of hyperactive retina (Cone-rod Homeobox knockout) not only did not show decreased mitochondrial motility, but instead had even higher motility than age-matched controls (Faits et al., 2016).

In conclusion, most studies showed that artificial, extreme manipulations of global activity affect mitochondrial motility. For physiologically relevant spontaneous neuronal activity, however, this relationship is less clear. We hypothesized that the key to understanding this discrepancy might be in the study of local physiological synaptic activity, instead of global, artificial activity.

4.2 Local (synaptic) activity

As the need for calcium buffering and ATP production is particularly high at synapses, the relationship between synapses and synaptic activity, and mitochondrial distribution must be examined. The two questions here are whether mitochondria are preferentially found close to synapses, and whether synaptic activity regulates mitochondrial motility and distribution.

Some studies have reported mitochondria co-localizing more often with excitatory post-synaptic sites than expected by chance, or when compared with non-synaptic sites (Chang et al., 2006; Mironov, 2006). Other studies have shown that under basal

conditions mitochondria do not preferably localize near synapses, as distances between them were similar to those found in a random distribution (MacAskill et al., 2009). This discrepancy might be due to different relationships between mitochondria and synapses in different types of neurons, and/ or their developmental stage. Young neurons can have mitochondria preferentially close to synapses but as they age, mitochondrial and synaptic density increase (Defelipe et al., 2002; Kimura and Murakami, 2014), and the bias can no longer be observed. Interestingly, some of the abovementioned studies found mitochondria to localize closer to synapses when synaptic activity was mimicked (Li et al., 2004; MacAskill et al., 2009). Specifically, they found that upon glutamate application (30 μM), moving mitochondria preferably stopped in the vicinity of synaptophysin-GFP puncta (pre-synaptic marker tagged with a green fluorescent protein), suggesting arrest at postsynaptic sites (MacAskill et al., 2009). In a different experiment, tetanic electrical stimulation of spines (compared to unstimulated ones within the same dendritic stretch) lead to spine enlargement and mitochondrial recruitment to the activated spines (Li et al., 2004). Similarly, spontaneous decreases of FM1-43 fluorescence (indicative of exocytosis of synaptic vesicles) were followed by a decrease in mitochondrial speed around these synapses (Mironov, 2006). Moreover, mitochondria move more slowly around synapses than outside these regions (Mironov, 2007).

Taken together, we still lack clear conclusions on the role of physiological neuronal activity on mitochondrial distribution, as well as on mitochondrial distribution relative to synapses. These are important questions to understand brain development, as spontaneous activity and energy availability must be tightly regulated to form proper neuronal circuits.

In conclusion, neuronal activity, probably through synaptic activation, seems to arrest mitochondrial motility, most likely due to the influx of calcium in the post-synapse which binds to MIRO1, disconnecting mitochondria from their transportation machinery (section 2.5) (MacAskill et al., 2009; Wang and Schwarz, 2009).

5. Summary

Mitochondria are ATP-producing, calcium-sensing and -buffering organelles, that are transported via microtubules to reach distal parts of neurons. In the context of the developing brain, their presence and function have been linked to synaptogenesis and synaptic function, and their motility has been mostly anti-correlated with neuronal and

synaptic activity. These arguments point towards an important role for mitochondria in the regulation of synaptic plasticity mechanisms during development.

There are two important limitations among almost all the studies that build up this current body of knowledge. First, most studies were performed in dissociated neuronal cultures, which are immature when dissociated and mature *in vitro* in the absence of the typical *in vivo* environment. Secondly, many artificial manipulations of activity affected mitochondria, but physiological activity or activity within the physiological range did not. Moreover, synaptic activity seems to affect mitochondria more consistently, which might be the missing link to the developmental profile of mitochondrial motility (as mitochondrial motility decreases over early brain development). All in all, we hypothesized that finding a unifying theory between these studies may lie in the use of intact study systems (such as brain slices and the *in vivo* brain) and more physiologically relevant protocols that provide new and more complete data that can help solve discrepancies in the current literature and expand on it.

6. Thesis outline

Here, I investigated how neuronal activity patterns, both global and local, affect mitochondrial motility. To integrate previous findings in the field, I tested both artificial manipulations and spontaneous activity, and used *in vivo* and *in vitro* experimental models. I aim to present a thorough view of mitochondrial motility and its relationship to synapses, neuronal activity, and microtubules. I aimed to answer the following research questions in the mouse visual cortex*:

* The mouse visual cortex and methods overview

The most common experimental protocol and model used thus far to answer these questions have been artificial manipulations of activity or proteins in cultures of dissociated neurons. Despite their inarguable value, we now need more natural activity and experimental models to draw conclusions that extend to the intact brain. All experiments in the following chapters were performed on the mouse visual cortex during the first two postnatal weeks. Before eye opening at 14 days old, activity observed in pyramidal neurons of layer II/III of the visual cortex is mostly spontaneous (section 1, Figure 1). We used the in utero electroporation technique, which enables the delivery of genetic constructs to prenatal pups in the uterus, to sparsely deliver a calcium indicator and a mitochondrial marker (chapters 3 and 4). The calcium indicator is used as readout for spontaneous neuronal activity in single neurons, which we then characterize as global or local calcium transients (section 4). We performed experiments both *in vivo* and in cortical slice cultures.

Chapter 2: How do presynaptic mitochondria relate to synaptic plasticity?

As outlined above, mitochondria and synapses influence each other in multiple ways, at least in dissociated neurons. In chapter 2, we studied the relationship between mitochondrial motility and synaptic plasticity in cortical axons *in vivo*. The first surprising finding was that mitochondrial motility was much lower than previously reported. We found that mitochondrial motility decreases over development, and a positive spatial relationship between mitochondria and putative boutons. We did not find, however, a relationship between mitochondria and structural synaptic plasticity. These findings are crucial for interpreting the current body of literature, as previous studies relied on immature neurons.

Chapter 3: How does spontaneous activity affect mitochondrial motility?

In chapter 3, we present the first study to image dendritic mitochondrial motility and spontaneously occurring activity *in vivo*. We show that mitochondrial motility decreases with age, while spontaneous activity increases. However, one does not seem to affect the other, as only an anti-correlation and no causal relationship between these two developmental changes was observed. Furthermore, in cultured slices, a relationship between local spontaneous synaptic activity and mitochondrial motility was observed. We found that synaptic activity precedes a temporary arrest of nearby mitochondria. Such a relationship was not observed for global calcium activity. Finally, we used a computational model to conclude that the relationship between mitochondria and synaptic activity likely contributes to stabilization of mitochondria over development.

Chapter 4: How do different patterns of neuronal activity affect mitochondrial motility and distribution?

Several studies show that mitochondrial motility is affected by artificial changes in activity, but not by spontaneously occurring neuronal activity. In contrast, other studies show that mitochondrial motility is also affected by local, synaptic activity. We imaged spontaneous activity and dendritic mitochondria *in vivo* and in slice cultures, and showed that global activity manipulations in the near physiological range do not affect mitochondrial motility. Then we investigated local activity and we did not find mitochondria to be closer to putative synapses (active spines). However, mitochondria preferentially accumulated in the dendritic shaft where repetitive local calcium transients, likely synaptic, occurred. Thus, stable mitochondria can be correlated to spontaneous activity, but the mechanisms by which this phenomenon occurs are still unclear.

Chapter 5: Can we simultaneously study microtubule- and mitochondrial dynamics?

To zoom in upon mitochondrial distribution during synapse development, we aimed at studying the relationship between microtubule and mitochondrial dynamics within developing neurons. We used a transgenic mouse line that expressed a fluorescent protein bound to a microtubule-specific protein (EB3), and another to mitochondria; only to discover that individual cortical pyramidal neurons did not show double fluorescent expression. This prevented the use of this mouse line for our research. We discuss possible solutions that will enable future studies.

Finally, in **Chapter 6**, I discuss the main findings in chapters 2 to 5 in the context of available literature and draw three main general conclusions, as well as two unresolved issues. I also discuss some of the most relevant questions to pursue in future studies.

References

Attwell, D., and Laughlin, S.B. (2001). An Energy Budget for Signaling in the Grey Matter of the Brain. J Cereb Blood Flow Metab 21, 1133–1145.

Beltran-Parrazal, L., López-Valdés, H.E., Brennan, K.C., Díaz-Muñoz, M., de Vellis, J., and Charles, A.C. (2006). Mitochondrial transport in processes of cortical neurons is independent of intracellular calcium. Am. J. Physiol. Cell Physiol. 291, C1193-1197.

Boldogh, I.R., and Pon, L.A. (2006). Interactions of mitochondria with the actin cytoskeleton. Biochim. Biophys. Acta 1763, 450–462.

Brini, M., Calì, T., Ottolini, D., and Carafoli, E. (2014). Neuronal calcium signaling: function and dysfunction. Cell. Mol. Life Sci. 71, 2787–2814.

Cagalinec, M., Safiulina, D., Liiv, M., Liiv, J., Choubey, V., Wareski, P., Veksler, V., and Kaasik, A. (2013). Principles of the mitochondrial fusion and fission cycle in neurons. J Cell Sci 126, 2187–2197.

Chang, D.T.W., and Reynolds, I.J. (2006). Differences in mitochondrial movement and morphology in young and mature primary cortical neurons in culture. Neuroscience 141, 727–736.

Chang, D.T.W., Honick, A.S., and Reynolds, I.J. (2006). Mitochondrial Trafficking to Synapses in Cultured Primary Cortical Neurons. J. Neurosci. 26, 7035–7045.

Clause, A., Kim, G., Sonntag, M., Weisz, C.J.C., Vetter, D.E., Rűbsamen, R., and Kandler, K. (2014). The Precise Temporal Pattern of Prehearing Spontaneous Activity Is Necessary for Tonotopic Map Refinement. Neuron 82, 822–835.

Defelipe, J., Elston, G.N., Fujita, I., Fuster, J., Harrison, K.H., Hof, P.R., Kawaguchi, Y., Martin, K.A., Rockland, K.S., Thomson, A.M., et al. (2002). Neocortical circuits: evolutionary aspects and specificity versus non-specificity of synaptic connections. Remarks, main conclusions and general comments and discussion. J.Neurocytol. 31, 387–416.

Faits, M.C., Zhang, C., Soto, F., and Kerschensteiner, D. (2016). Dendritic mitochondria reach stable positions during circuit development. ELife 5.

Fernie, A.R., Carrari, F., and Sweetlove, L.J. (2004). Respiratory metabolism: glycolysis , the TCA cycle and mitochondrial electron transport. Curr. Opin. Plant Biol. 7, 254–261.

Fransson, Å., Ruusala, A., and Aspenström, P. (2003). Atypical Rho GTPases Have Roles in Mitochondrial Homeostasis and Apoptosis*. J. Biol. Chem. 278, 6495–6502.

Frederick, R.L., and Shaw, J.M. (2007). Moving Mitochondria: Establishing Distribution of an Essential Organelle. Traffic Cph. Den. 8, 1668–1675.

Galli, L., and Maffei, L. (1988). Spontaneous impulse activity of rat retinal ganglion cells in prenatal life. Science 242, 90–91.

Gellerich, F.N., Trumbeckaite, S., Opalka, J.R., Seppet, E., Rasmussen, H.N., Neuhoff, C., and Zierz, S. (2000). Function of the mitochondrial outer membrane as a diffusion barrier in health and diseases. Biochem. Soc. Trans. 28, 64–69.

Gioran, A., Nicotera, P., and Bano, D. (2014). Impaired mitochondrial respiration promotes dendritic branching via the AMPK signaling pathway. Cell Death Dis. 5, e1175.

Gu, J., and Zheng, J.Q. (2009). Microtubules in Dendritic Spine Development and Plasticity. OpenNeurosci J 3, 128–133.

Harris, J.J., Jolivet, R., and Attwell, D. (2012). Synaptic energy use and supply. Neuron 75, 762–777.

Huberman, A.D., Feller, M.B., and Chapman, B. (2008). Mechanisms Underlying Development of Visual Maps and Receptive Fields. Annu. Neurosci 31, 479–509.

Kang, J.-S., Tian, J.-H., Pan, P.-Y., Zald, P., Li, C., Deng, C., and Sheng, Z.-H. (2008). Docking of Axonal Mitochondria by Syntaphilin Controls Their Mobility and Affects Short-Term Facilitation. Cell 132, 137–148.

Katz, L.C., and Shatz, C.J. (1996). Synaptic activity and the construction of cortical circuits. Science 274, 1133–1138.

Kimura, T., and Murakami, F. (2014). Evidence that dendritic mitochondria negatively regulate dendritic branching in pyramidal neurons in the neocortex. J. Neurosci. 34, 6938–6951.

Kleindienst, T., Winnubst, J., Roth-Alpermann, C., Bonhoeffer, T., and Lohmann, C. (2011). Activity-dependent clustering of functional synaptic inputs on developing hippocampal dendrites. Neuron 72, 1012–1024.

Knott, G., and Holtmaat, A. (2008). Dendritic spine plasticity-Current understanding from *in vivo* studies. Brain ResRev .

Konietzny, A., González-Gallego, J., Bär, J., Perez-Alvarez, A., Drakew, A., Demmers, J.A.A., Dekkers, D.H.W., Hammer, J.A., Frotscher, M., Oertner, T.G., et al. (2019). Myosin V regulates synaptopodin clustering and localization in the dendrites of hippocampal neurons. J. Cell Sci. 132, 3790–3798.

Leighton, A.H., and Lohmann, C. (2016). The Wiring of Developing Sensory Circuits-From Patterned Spontaneous Activity to Synaptic Plasticity Mechanisms. Front. Neural Circuits 10, 71.

Lewis, T.L., Turi, G.F., Kwon, S.-K., Losonczy, A., and Polleux, F. (2016). Progressive Decrease of Mitochondrial Motility during Maturation of Cortical Axons *In vitro* and *In vivo*. Curr. Biol. 26, 2602–2608.

Li, M., Cui, Z., Niu, Y., Liu, B., Fan, W., Yu, D., and Deng, J. (2010). Synaptogenesis in the developing mouse visual cortex. Brain Res. Bull. 81, 107–113.

Li, Y., Van Hooser, S.D., Mazurek, M., White, L.E., and Fitzpatrick, D. (2008). Experience with moving visual stimuli drives the early development of cortical direction selectivity. Nature.

Li, Z., Okamoto, K., Hayashi, Y., and Sheng, M. (2004). The Importance of Dendritic Mitochondria in the Morphogenesis and Plasticity of Spines and Synapses. Cell 119, 873–887.

Lohmann, C., and Kessels, H.W. (2014). The developmental stages of synaptic plasticity. J. Physiol. 592, 13–31.

Luongo, T.S., Lambert, J.P., Gross, P., Nwokedi, M., Lombardi, A.A., Shanmughapriya, S., Carpenter, A.C., Kolmetzky, D., Gao, E., van Berlo, J.H., et al.

(2017). The mitochondrial Na+/Ca2+ exchanger is essential for Ca2+ homeostasis and viability. Nature 545, 93–97.

MacAskill, A.F., and Kittler, J.T. (2009). Control of mitochondrial transport and localization in neurons. Cell 20, 102–112.

MacAskill, A.F., Rinholm, J.E., Twelvetrees, A.E., Arancibia-carcamo, I.L., Muir, J., Fransson, A., Aspenstrom, P., Attwell, D., and Kittler, J.T. (2009). Miro1 Is a Calcium Sensor for Glutamate Receptor-Dependent Localization of Mitochondria at Synapses. Neuron 61, 541–555.

MacAskill, A.F., Atkin, T.A., and Kittler, J.T. (2010). Mitochondrial trafficking and the provision of energy and calcium buffering at excitatory synapses. Eur.J.Neurosci 32, 231–240.

Mammucari, C., Raffaello, A., Vecellio Reane, D., Gherardi, G., De Mario, A., and Rizzuto, R. (2018). Mitochondrial calcium uptake in organ physiology: from molecular mechanism to animal models. Pflugers Arch. 470, 1165–1179.

Martin, W.F., Garg, S., and Zimorski, V. (2015). Endosymbiotic theories for eukaryote origin. Philos. Trans. R. Soc. B Biol. Sci. 370.

Mattson, M.P., Gleichmann, M., and Cheng, A. (2008). Mitochondria in neuroplasticity and neurological disorders. Neuron 60, 748–766.

Meister, M., Wong, R.O.L., Baylor, D.A., and Shatz, C.J. (1991). Synchronous bursts of action potentials in ganglion cells of the developing mammalian retina. Science 252, 939–943.

Mironov, S.L. (2006). Spontaneous and evoked neuronal activities regulate movements of single neuronal mitochondria. Synapse. 59, 403–411.

Mironov, S.L. (2007). ADP regulates movements of mitochondria in neurons. Biophys. J. 92, 2944–2952.

Muller, M., Mironov, S.L., Ivannikov, M.V., Schmidt, J., and Richter, D.W. (2005). Mitochondrial organization and motility probed by two-photon microscopy in cultured mouse brainstem neurons. ExpCell Res 303, 114–127.

Pathak, D., Sepp, K.J., and Hollenbeck, P.J. (2010). Evidence that myosin activity opposes microtubule-based axonal transport of mitochondria. J. Neurosci. 30, 8984–8992.

Schwarz, T.L. (2013). Mitochondrial Trafficking in Neurons. Cold Spring Harb. Perspect. Biol. 5, a011304.

Sheng, Z.-H. (2014). Mitochondrial trafficking and anchoring in neurons: New insight and implications. J Cell Biol 204, 1087–1098.

Siegel, F., and Lohmann, C. (2009). *In vivo* imaging of spontaneous activity patterns in the developing mouse visual cortex. Proc. G”ttingen Neurobiol. Conf.

Silver, I.A., and Erecinska, M. (1994). Extracellular glucose concentration in mammalian brain: continuous monitoring of changes during increased neuronal activity and upon limitation in oxygen supply in normo-, hypo-, and hyperglycemic animals. J. Neurosci. 14, 5068–5076.

Simon, D.K., and O’Leary, D.D. (1992). Development of topographic order in the mammalian retinocollicular projection. J. Neurosci. 12, 1212–1232.

Tilokani, L., Nagashima, S., Paupe, V., and Prudent, J. (2018). Mitochondrial dynamics: overview of molecular mechanisms. Essays Biochem. 62, 341–360.

Toba, S., Watanabe, T.M., Yamaguchi-Okimoto, L., Toyoshima, Y.Y., and Higuchi, H. (2006). Overlapping hand-over-hand mechanism of single molecular motility of cytoplasmic dynein. Proc. Natl. Acad. Sci. 103, 5741–5745.

Vaccaro, V., Devine, M.J., Higgs, N.F., and Kittler, J.T. (2017). Miro1-dependent mitochondrial positioning drives the rescaling of presynaptic Ca2+ signals during homeostatic plasticity. EMBO Rep. 18, 231–240.

Wang, X., and Schwarz, T.L. (2009). The mechanism of Ca2+ -dependent regulation of kinesin-mediated mitochondrial motility. Cell 136, 163–174.

Wong-Riley, M.T. (1989). Cytochrome oxidase: an endogenous metabolic marker for neuronal activity. Trends Neurosci 12, 94–101.

Yi, M., Weaver, D., and Hajnóczky, G. (2004). Control of mitochondrial motility and distribution by the calcium signal a homeostatic circuit. J. Cell Biol. 167, 661–672.

Chapter 2

Mitochondrial dynamics in adult visual cortex are limited and not affected by axonal structural plasticity

Laura Smit-Rigter*, Rajeev Rajendran*, **Cátia A. P. Silva**, Liselot Spierenburg, Femke Groeneweg, Emma M. Ruimschotel, Danielle van Versendaal, Chris van der Togt, Ulf T. Eysel, J. Alexander Heimel, Christian Lohmann, Christiaan N. Levelt

*These authors contributed equally

Smit-Rigter et al., 2016. Current Biology

CAPS contribution: performed and analyzed experiments in Figure 1A-B.

List of figures

Abstract

Mitochondria buffer intracellular Ca^{2+} and provide energy [1]. Because synaptic structures with high Ca^{2+} buffering [2-4] or energy demand [5] are often localized far away from the soma, mitochondria are actively transported to these sites [6-11]. Also, the removal and degradation of mitochondria are tightly regulated [9, 12, 13], because dysfunctional mitochondria are a source of reactive oxygen species, which can damage the cell [14]. Deficits in mitochondrial trafficking have been proposed to contribute to the pathogenesis of Parkinson's disease, schizophrenia, amyotrophic lateral sclerosis, optic atrophy, and Alzheimer's disease [13, 15-19]. In neuronal cultures, about a third of mitochondria are motile, whereas the majority remains stationary for several days [8, 20]. Activity-dependent mechanisms cause mitochondria to stop at synaptic sites [7, 8, 20, 21], which affects synapse function and maintenance. Reducing mitochondrial content in dendrites decreases spine density [22, 23], whereas increasing mitochondrial content or activity increases it [7]. These bidirectional interactions between synaptic activity and mitochondrial trafficking suggest that mitochondria may regulate synaptic plasticity. Here we investigated the dynamics of mitochondria in relation to axonal boutons of neocortical pyramidal neurons for the first time *in vivo*. We find that under these circumstances practically all mitochondria are stationary, both during development and in adulthood. In adult visual cortex, mitochondria are preferentially localized at putative boutons, where they remain for several days. Retinal-lesion-induced cortical plasticity increases turnover of putative boutons but leaves mitochondrial turnover unaffected. We conclude that in visual cortex *in vivo*, mitochondria are less dynamic than *in vitro*, and that structural plasticity does not affect mitochondrial dynamics.

Introduction

Mitochondria buffer intracellular calcium and provide energy [1]. Because synaptic structures with high calcium-buffering [2-4] or energy demand [5] are often localized far away from the soma, mitochondria are actively transported to these sites [6-11]. Also the removal and degradation of mitochondria are tightly regulated [9,12,13] because dysfunctional mitochondria are a source of reactive oxygen species which can damage the cell [14]. Deficits in mitochondrial trafficking have been proposed to contribute to the pathogenesis of Parkinson’s disease, schizophrenia, amyotrophic lateral sclerosis, optic atrophy and Alzheimer’s disease [13,15-19].

In neuronal cultures, about a third of mitochondria are motile while the majority remain stationary for several days [8,20]. Activity-dependent mechanisms cause mitochondria to stop at synaptic sites [7,8,20,21], which affects synapse function and maintenance. Reducing mitochondrial content in dendrites decreases spine density [22,23] while increasing mitochondrial content or activity increases it [7]. These bidirectional interactions between synaptic activity and mitochondrial trafficking suggest that mitochondria may regulate synaptic plasticity.

Here we investigated the dynamics of mitochondria in relation to axonal boutons of neocortical pyramidal neurons for the first time *in vivo*. We find that under these circumstances practically all mitochondria are stationary, both during development and in adulthood. In adult visual cortex, mitochondria are preferentially localized at putative boutons where they remain for several days. Retinal-lesion-induced cortical plasticity increases turnover of putative boutons but leaves mitochondrial turnover unaffected. We conclude that in the visual cortex *in vivo*, mitochondria are less dynamic than *in vitro*, and that structural plasticity does not affect mitochondrial dynamics.

Results and Discussion

Few motile mitochondria in axons of pyramidal neurons in visual cortex *in vivo*

To fluorescently label mitochondria and neuronal structures in which they are localized, we performed in utero electroporation with two DNA constructs driving expression of Mito-mTurquoise2 and membrane-associated YFP. A cranial window was implanted once the mice had reached the age of 8-10 weeks. This allowed us to visualize mitochondria in axonal arbors of layer 2/3 pyramidal neurons in V1 *in vivo* using two-photon microscopy (Figure 1A-C, Movie S1). Two to three weeks after cranial window implantation, optical imaging of intrinsic imaging was performed to localize monocular V1. One week later, axonal branches in layer 1 and upper layer 2 were imaged using *in vivo* two-photon microscopy. We found that the density of mitochondria was 0.09 per µm (Figure 1D). Surprisingly, the fraction of axonal mitochondria that were motile was only 0.83% (Figure 1E), much lower than the 10-30% previously observed in neuronal cultures [6-10]. We therefore asked whether the difference in mitochondrial motility was caused by the different experimental condition (*in vivo* versus *in vitro*) or by the difference in the age of the imaged neurons. We assessed mitochondrial motility

in axons imaged in developing V1, both *in vivo* and *in vitro* (Movies S2 and S3). For this purpose, we again used in utero electroporation to fluorescently label mitochondria and axons of layer 2/3 pyramidal neurons. Axonal branches were imaged within layers 1 and 2 of the visual cortex either *in vivo* at postnatal day 10-13 or in slice cultures prepared at postnatal day 5 and imaged 7-8 days later. Representative kymographs (Figure 1C) already show that mitochondria in slice cultures were more dynamic than *in vivo*. The fraction of mitochondria undergoing trafficking during 2 minutes of imaging was 15.3% in slice cultures, similar to what was observed previously in hippocampal slice cultures [20] and significantly different from what we observed in adult V1 ($p<0.0001$, Figure 1E). The density was 0.09 per µm, similar to that *in vivo* ($p>0.05$, Figure 1D). In the developing visual cortex *in vivo*, the situation was not significantly different from what we observed in adult V1. The fraction of mitochondria that were motile was 1.06% and the density was 0.12 per µm (Figure 1D, E). A lack of motile mitochondria was recently observed in dendrites of *ex vivo* retinal ganglion cells from adult mice [24]. In retinal ganglion cell dendrites, the reduction of mitochondrial motility appeared to be related to the age of the neurons. Our data suggest that the culture conditions influence mitochondrial motility. Possibly, this apparent discrepancy is caused by the different cell type or neuronal compartment studied.

Mitochondrial localization in relation to putative boutons

Previous work has shown that about 40% of all mitochondria are localized close to synaptic boutons [25] and that mitochondria close to a bouton are more stable than other mitochondria in an axon [20]. Considering the large difference between the mitochondrial dynamics *in vivo* and *in vitro*, we wondered whether the previously observed relationships between mitochondrial dynamics and synaptic boutons were also different.

We therefore studied how mitochondria were distributed in relation to putative boutons in axons of adult V1 pyramidal neurons and at what rate mitochondria appeared or disappeared. Axonal branches in layer 1 and upper layer 2 were imaged 11 times at 4-day intervals (Figure 1A). Putative boutons were present at a density of 0.10 +/- 0.01 per µm. Of all mitochondria, 49% were found in the direct vicinity (<2 µm) of a putative bouton, and 29% of all putative boutons had a mitochondrion nearby (Figure 2A). This is similar to what has been observed previously cortical cultures and somewhat lower than in hippocampus *in vitro* (43%) [20] or *ex vivo* (41%) [25]. To test whether the distribution of mitochondria localization relative to the position of putative boutons was

random, we randomly repositioned boutons on each axon 1000x. When we compared the distribution of distances between mitochondria and the nearest putative bouton in the actual measurements to that in the shuffled data we found that it was skewed significantly towards localization closer to putative boutons ($p<0.001$, Figure 2B).

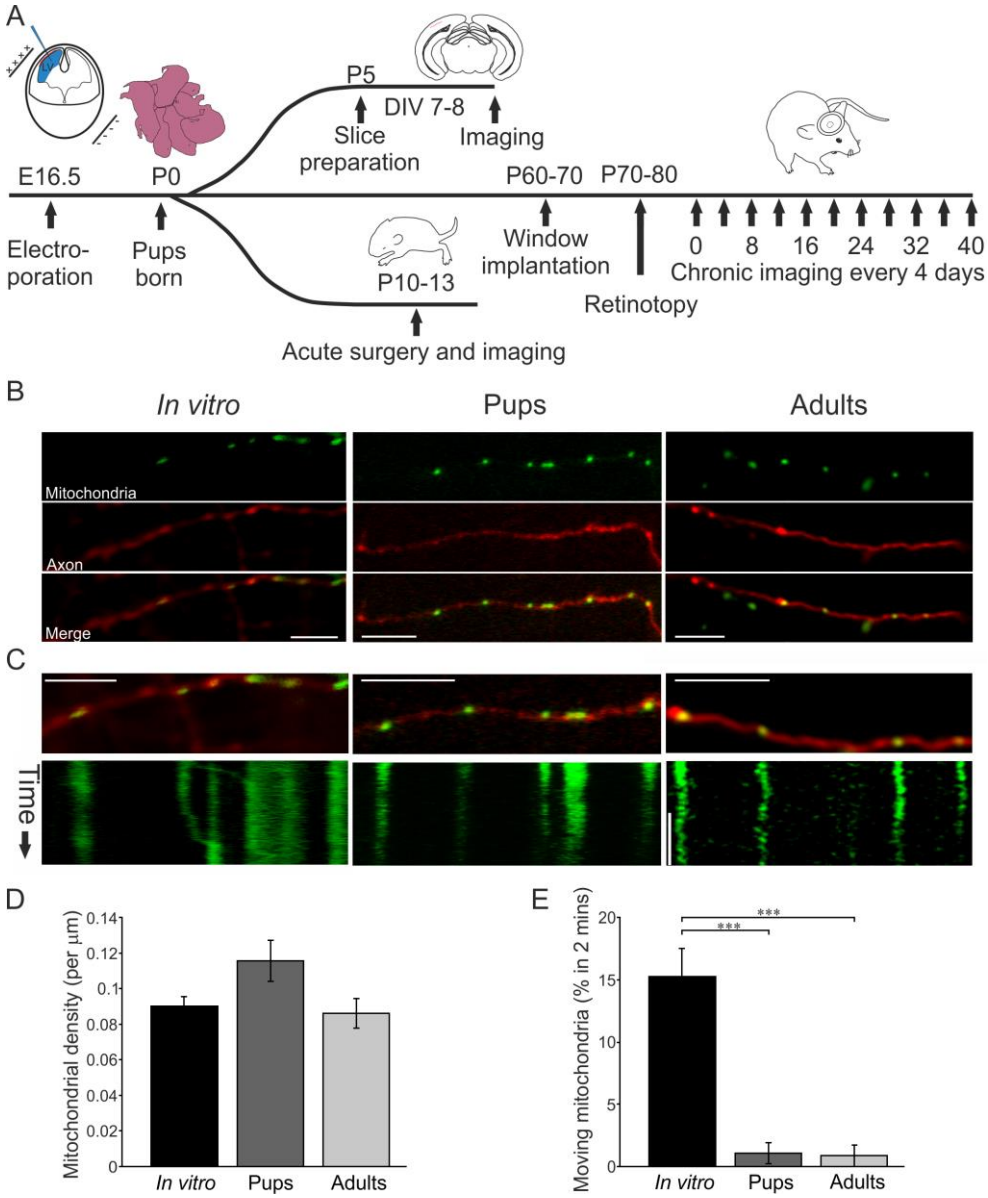

Figure 1. Mitochondrial density and motility differ *in vitro* and *in vivo*.
A. Timeline of experiment. Embryos at stage 16.5 days post gestation (E16.5) were electroporated to fluorescently label sparse layer 2/3 V1 pyramidal neurons and their mitochondria. For *in vitro* experiments, brain slices from postnatal day 2 (P2) pups were cultured for 6-10 days prior to imaging. P10-13 pups were used for acute two-photon imaging. For chronic *in vivo* experiments, adult mice were window implanted, retinotopy was determined and V1 repeatedly imaged every 4 days.
B. Representative pseudo-colored fluorescence micrographs showing mitochondrial and axonal labeling.
C. An example axon with pseudo colored mitochondria (green, top panel) is used to generate kymograph (bottom panel) showing motility during a two-minute window. Representative time series images of mitochondrial motility *in vivo* in adults, pups and in slice cultures are shown in supplementary movies S1, S2 and S3 respectively.
D. Mitochondrial density in axons of neurons in slice cultures is not different than in *in vivo* visual

cortex of pups or adult mice (slice culture 0.09 ± 0.004 mitochondria per µm, n=51 axons vs pups 0.12 ± 0.012 per µm, n=23, Kruskal-Wallis p=0.18 followed by post-hoc Dunn's test, p>0.05, vs adults 0.09 ± 0.008 per µm, n=20, Dunn's test p>0.05).
E. Fraction of motile mitochondria in axons of neurons in slice cultures is higher than in *in vivo* visual cortex of pups or adult mice (chi-squared= 53.97, p<0.0001; slice culture 15.31 ± 2.18 %, n=51 axons, vs pups 1.06 ± 0.78 %, n=23, pcorr(Bonferroni)<0.0001, vs adults 0.83 ± 0.83%, n=20, pcorr(Bonferroni)<0.0001). Motility in pups and adults do not differ significantly. Horizontal scale bars in B and C = 10 µm, vertical scale bar in C=1 min. Bar graphs are presented as mean ± SEM. *** p-value<0.001.

Relationships between the turnover of putative boutons and mitochondria

Chronic imaging of putative boutons in V1 revealed that they were lost and gained at a rate of 6-8% (loss 7.26 +/- 0.86% (SEM), n = 42 axons; gain 6.39+/- 0.8%, n = 42) every 4 days, similar to what was previously observed by others [26]. Despite the very small fraction of motile mitochondria in axons of adult V1, we found that mitochondria did not remain stationary for more than several days. Of all mitochondria, 63.8% had moved away from their initial location, defined by a 1.2 µm circle, after 4 days and 61.8% of mitochondria newly appeared during the same time interval (Figure 2C). These turnover rates are similar to what was observed in hippocampal slices *in vitro* [20]. When we analyzed the persistence of mitochondria we found that the data could be fitted with an exponential curve towards zero (Figure 2D) indicating that there was no persistent subpopulation of mitochondria. Over 95% of all mitochondria had moved or disappeared in a period of 16 days.

We then analyzed whether there was a relationship between the dynamics of mitochondria and boutons. We asked whether the presence of a putative bouton made it more likely for a mitochondrion to appear. We found that mitochondria were not significantly more likely to appear near a putative bouton than elsewhere (Figure 2E). However, the percentage of mitochondria close to a putative bouton that remained 4 days later was 41% compared to 28% of those that were not close to a putative bouton (p<0.01, Figure. 2F). Next we tested whether putative boutons that had a mitochondrion close by were more stable than those without a mitochondrion. We found that the percentage of putative boutons with a mitochondrion that were lost 4 days later was 5.7% compared to 8.7% of the putative boutons without a mitochondrion (p<0.05, Figure 2G). We conclude that putative boutons keep hold of mitochondria, and that putative boutons with mitochondria are more stable.

Previous studies have found that mitochondria in the direct vicinity of synaptic boutons alter synaptic function. Short-term plasticity is reduced [2,3,27] probably due to the Ca2+ buffering capacity of mitochondria. Mitochondria passing by presynaptic

boutons can cause changes in synaptic transmission [28]. The slow but continuous gain and loss of mitochondria at putative boutons we observed suggests that mitochondria-induced synaptic effects will also occur in the adult cortex but on a much slower timescale.

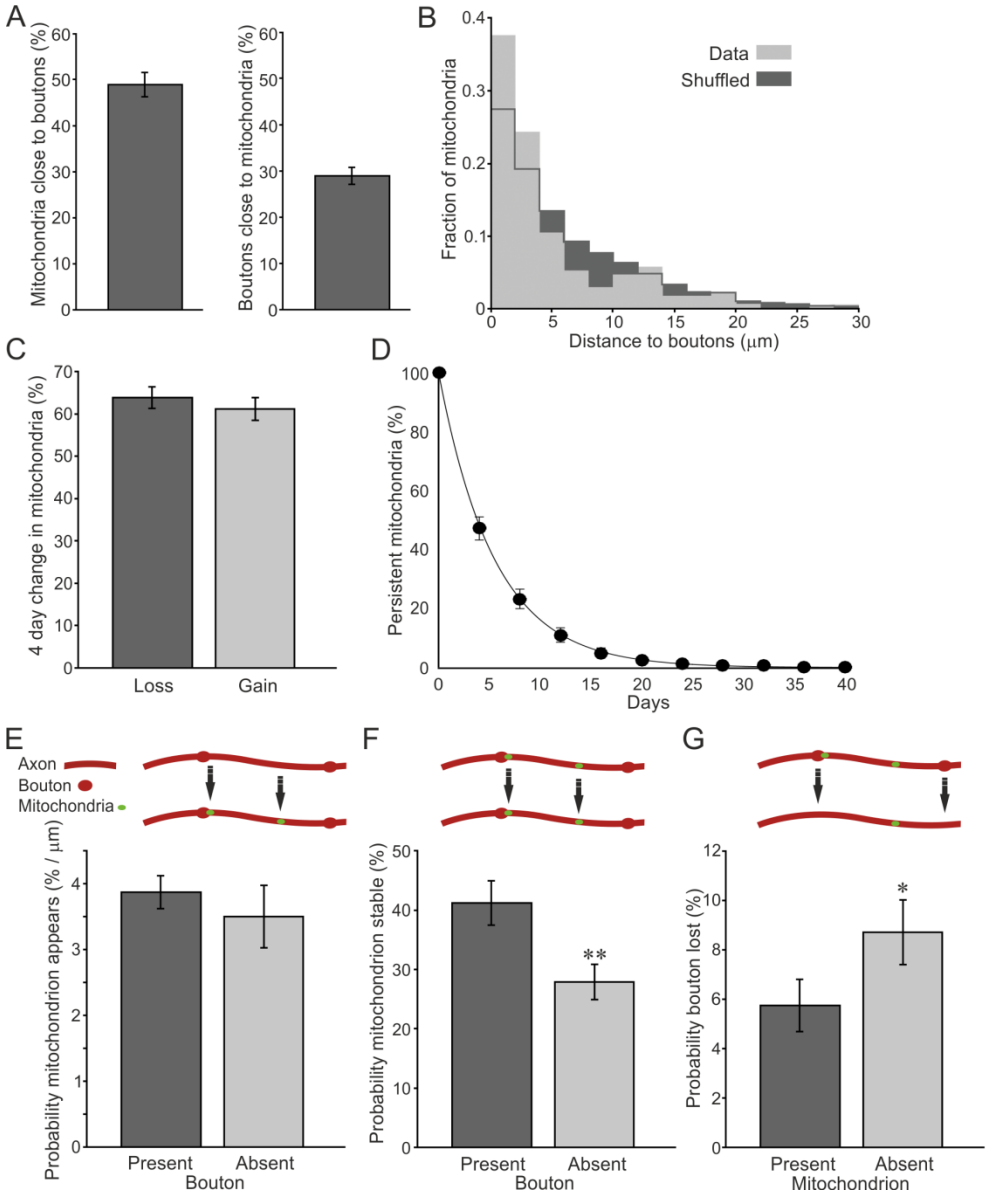

Figure 2. Dynamics of mitochondria in adult V1 are influenced by the presence of putative boutons.

A. Fraction of mitochondria near a putative bouton (left panel, 49.0 ± 2.6%, n=110 axons) and of putative boutons near a mitochondrion (right, 28.9 ± 1.8%, n=41 axons). Examples of putative boutons and proximity of a mitochondrion to a bouton is shown in Figure S1.

B. The distribution of distances of mitochondria to the nearest bouton (light gray, 3.65 ± 0.22 μm, n=468 axons) is shown in comparison with the distribution when boutons on each axon were randomly redistributed 1000 times (dark gray, 4.64 ± 0.001 μm, n=468000). The mean distance of mitochondria to the nearest bouton in the actual measurements is lower than in this shuffled data ($p<0.001$, Kolmogorov-Smirnov).

C. The majority of mitochondria did not remain at the same location, defined by a 1.2 μm circle, during a 4-day period (4-day loss 63.8 ± 2.5%, n=41 axons, gain 61.8 ± 2.7%, n=41).

D. Mean survival fraction of mitochondria (mitochondria persistent from day 0) at different time-points (black circles) perfectly fits an exponential curve (black trace). The top panels of E-G are

schematic representations of the dynamics quantified in the bar graphs (bottom panel), left and right arrows represents left and right bars respectively.
E. Probability that mitochondria appear per unit length of axon does not depend on the presence of a putative bouton (present: 3.9 ± 0.3%, n=41 axons, vs absent 3.5 ± 0.5%, n=41; Wilcoxon signed rank test, p=0.24, W=522).
F. The fraction of mitochondria close to putative boutons that is stable over a 4-day period is larger than that of mitochondria more than 2 µm away from putative boutons (close-by: 41.5 ± 3.8%, n=40 axons vs remote: 27.9 ± 3.0%, n=40; Wilcoxon signed rank test, p-value < 0.01, W = 561.5).
G. Fraction of putative boutons that is lost is lower when a mitochondrion is close (<2 µm away) over a 4-day period than those without a mitochondrion close-by (close-by: 5.7 ± 1.1%, n=41 axons vs remote: 8.7 ± 1.3%, n=41; Wilcoxon signed rank test, p < 0.05, W = 242.5). Data presented as mean + SEM. *p-value<0.05, **p-value<0.01.

Induction of structural plasticity in V1 induced by retinal lesions does not alter mitochondrial dynamics

The bidirectional interaction between mitochondrial motility and synaptic activity raises the question whether mitochondrial transportation is also involved in long-term plasticity in the visual cortex. We therefore wanted to understand whether changes in synaptic activity resulting in cortical plasticity would affect mitochondrial dynamics. To address this question, we performed monocular lesions in the part of the retina projecting to the monocular area of V1 (Figure 3A). The procedure eliminates all feedforward visual input to the corresponding lesion projection zone (LPZ) in V1. It causes a prolonged period of increased bouton and dendritic spine turnover [29,30], eventually resulting in increased responsiveness of the LPZ to stimuli in neighboring visual-field positions [31,32]. The loss of putative boutons measured during the time points after retinal lesioning increased 1.8-fold ($p<0.001$, Figure 3B). The gain of putative boutons also showed an upwards trend which was however not significant (Figure 3C). Despite the change in putative bouton turnover, neither the loss nor the gain of mitochondria changed upon retinal lesioning (Figure 3D-E). We conclude that structural plasticity of axonal boutons is not associated with altered turnover of mitochondria.

This does not contradict previous findings that mitochondrial function is important for synapse stability, but opposes the idea that activity-regulated recruitment or removal of mitochondria contributes to bouton turnover during cortical plasticity. Several studies have implicated mitochondria in postsynaptic plasticity mechanisms [7,22,22]. Furthermore, neuronal activity had different effects on mitochondrial motility in axons and dendrites [8]. The very high density of mitochondria in dendrites of cortical pyramidal neurons *in vivo* unfortunately prohibited us from studying postsynaptic changes in mitochondrial dynamics.

Other *in vivo* studies examining mitochondrial trafficking in axon tracts reported a larger proportion of motile mitochondria. In spinal cord of zebrafish this fraction was approximately 10% [33], similar to what was observed in mouse peripheral nerves [34] or optic nerve [35]. The absence of boutons in the imaged axons tract may explain the difference between our *in vivo* data, obtained in cortical axons forming many synapses, and these previously published *in vivo* data.

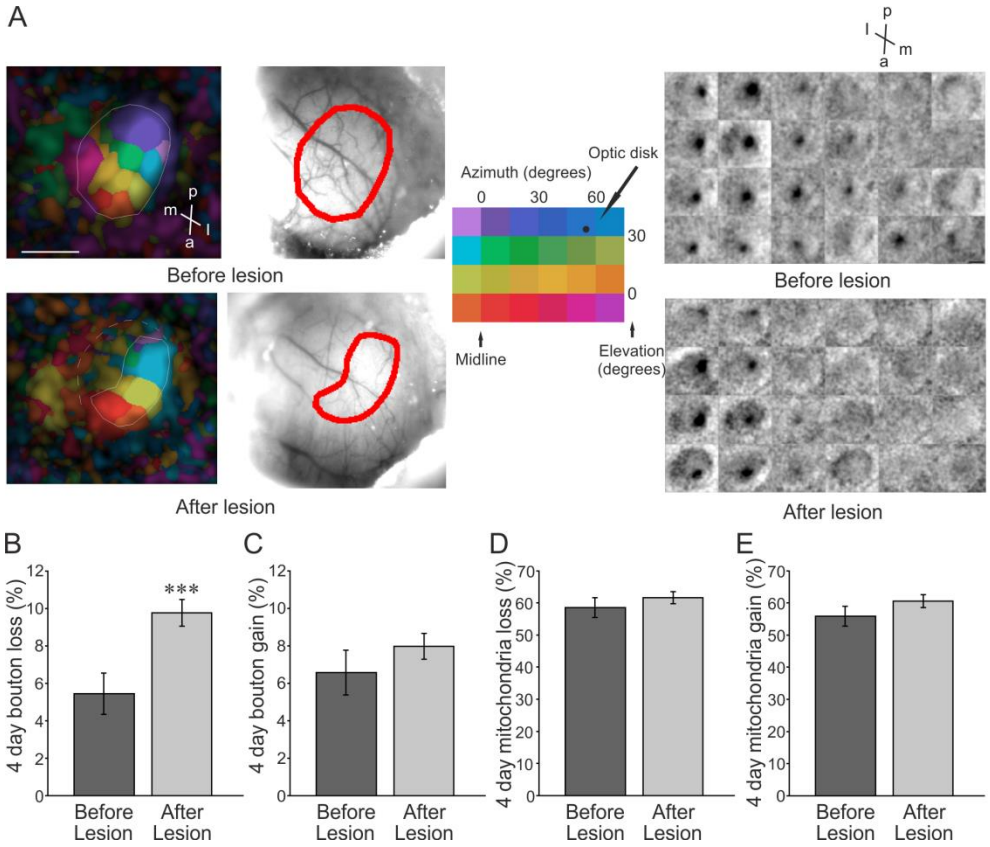

Figure 3. Mitochondrial dynamics in adult V1 are unaltered after retinal lesions.
A. Intrinsic signal retinotopic responses in V1 were recorded (left) through a cranial glass window (middle left) upon serially showing drifting gratings on a 6x4 grid on the screen. Cortical areas responding to the stimuli are depicted by a white margin. Color code of visual stimuli presentation (middle right) also shows the elevation and azimuth of presented stimuli. Each small square subtends 15˚ in the visual field. Mice were imaged again, 6 days following retinal lesions (bottom panel) of size ranging from 20˚x10˚ to 40˚x30˚ dorsal to the optical disk, showing loss of responses in V1 corresponding to retinal lesion (dashed lines show outline of the full retinotopy similar to top panel). Right panel shows recorded responses in each of the 6x4 squares before (top) and after (bottom) retinal lesions.
B. Retinal lesioning results in an increased loss of putative boutons (before lesion 5.5 ± 1.1%, n=65 axons, after lesion 9.8 ± 0.7%, n=65; Wilcoxon signed rank test, p-value < 0.001, W = 523.5).
C. Retinal lesioning causes no significant change in gain of putative boutons (before lesion 6.6 ± 1.20%, n=65 axons, after lesion 8.0 ± 0.7%, n=65, Wilcoxon signed rank test p = 0.11, W = 748).
D, E. Retinal lesioning did not result in any significant change in mitochondrial loss (D, before lesion 59.1 ± 3.0%, n=65 axons vs after lesion 62.9 ± 1.8%, n=65, Wilcoxon signed rank test, p = 0.25 W = 868, or gain (E, before lesion 55.9 ± 3.0%, n=64 axons, after lesion 60.7 ± 1.7%, n=64, Wilcoxon signed rank test p = 0.11, W = 775. a = anterior; p = posterior; m = medial; l = lateral. Scale bars = 1 mm. Data presented as mean + SEM. ***p-value<0.001.

It appears unlikely that the presence or absence of boutons also explains the difference in mitochondrial motility we observe between *in vitro* and *in vivo* preparations. We have no clear indications that axonal boutons in slice cultures are less active or dense than *in vivo*. Interestingly, high glucose concentrations reduce mitochondrial motility through activation of the enzyme O-Linked N-acetylglucosamine transferase [36]. *In vivo*, this enzyme is strongly enriched in synaptic boutons [37]. Possibly, glucose concentrations are distributed more unevenly *in vivo* than *in vitro* and peak preferentially in synaptic boutons, thus keeping mitochondria in place through O-Linked N-acetylglucosamine activation.

In summary, our results show that in adult V1, the fraction of motile mitochondria is much lower than observed *in vitro* and that plasticity-induced bouton turnover is not accompanied by altered mitochondrial dynamics. It will be highly informative to use the experimental strategy we employed here to study the proposed involvement of mitochondria in brain diseases such as Alzheimer's disease, Parkinson's disease and Schizophrenia.

Materials and Methods

Animals

All animal procedures were carried out with the approval of the institutional animal care and use committee of the Royal Netherlands Academy of Arts and Sciences. Animal experiments were carried out on C57BL/6J mice or F1 progenies of CBA/CaJ female mice crossed with C57BL/6J males.

In utero electroporation

CBA/CaJ (for adult *in vivo* experiments) or C57Bl/6J (all other experiments) female mice were mated with C57BL/6J males and timed for pregnancy. Pregnant mice at 16.5 days gestation were anesthetized using 5 % isoflurane mixed with 0.8 L/min oxygen and kept under anesthesia with 2 % isoflurane. The same procedures were used as described previously [S1]. In brief, a midline incision was made and uterine horns were exposed. Plasmid DNA (0.1-3 µg/µl) for expression of fluorescent proteins was used, dissolved in 10 mM Tris and 0.02 % Fast Green. Approximately 1-2 µl of this mixture was injected through a pulled capillary pipette in the lateral ventricle of each embryo using a picospritzer (PLI-100, BTX Harvard Apparatus, MA, USA). To electroporate layer 2/3 pyramidal neurons in the developing visual cortex, a custom-made square wave isolated pulse generator (5 pulses, pulse width 50 ms, frequency 1 Hz and voltage 30 V) was

used. Plasmids that drove expression of mito-mTurquoise2 and YFP-F were used for all adult *in vivo* experiments. For *in vivo* experiments in pups and *in vitro* experiments, mito-DsRed was used together with a green fluorescent cytoplasmic label (GCaMP6 for *in vivo* experiments in pups and GFP for *in vitro* experiments). Expression of fluorescent proteins was driven by the pCAG promoter. Mito-mTurquoise2 and mito-DsRed contained the mitochondrial targeting sequence from subunit VIII of human cytochrome c oxidase (COXVIII) causing mitochondrial localization as previously described [S2-4]. After electroporation, the uterine horns were carefully placed back in the abdominal cavity and the abdomen was sutured. During the surgery embryos were kept moist with warm saline and the mothers were kept warm using a euthermic pad. After surgery the animal was allowed to recover after Lidocaine ointment was applied on the wound for analgesia and Metacam (1 mg/kg s.c.) was administered for post-operative analgesia. Once the pups were born they were checked before postnatal day 3 for expression and targeting of V1. Only animals that had proper expression in V1 were used for further experiments.

Window implantation

Cranial window implantation was performed as previously described [S1]. Once the animals with proper expression were approximately 2-3 months of age, they were anesthetized using 5% isoflurane mixed with 0.8L/min oxygen and kept under anesthesia with 1.8% isoflurane. Mice (controls: n=4, lesioned: n=7) were placed on a euthermic pad and head-fixed in a stereotaxic apparatus and the scalp was incised and fascia of the skull was removed. A circular metal ring was glued on the skull centered on V1 and fixed with dental cement. A circular window (diameter 3 mm) was made on the skull covering V1 using a dental drill. Care was taken not to damage the dura. Once the skull was removed, the area exposed was kept moist with aCSF. A 5 mm diameter round glass coverslip with a layer of silicon oil (Fluka Analytical UK) was applied on top of the exposed area and fixed using dental cement. After the surgery the animal was allowed to recover after Metacam (1 mg/kg s.c.), Cefotaxim (40 mg/kg s.c.) and dexamethasone (5 mg/kg s.c.) were administered.

Retinal lesions

Monocular retinal lesions were made as described previously [S6,7]. In brief, animals were anesthetized with a mixture of ketamine and xylazine (100mg/kg and 10 mg/kg i.p.) and the pupil was dilated using a drop of atropine. The retina contralateral to where the cranial window was placed was focally photo-coagulated with multiple lesions, using an 805 nm infrared diode laser (2-10 laser pulses of 350-400 mW, duration

150-200 ms) through a laser adapted operating microscope. The resulting retinal lesions were 20°x10° to 40°x30° in size and localized dorsally above the optic disc. After lesioning, the animals were allowed to recover for at least two days. Intrinsic signal imaging to determine the lesioned area was performed 6-8 days after the retina was lesioned. Optic disk projection on the visual field (Figure 3A) was positioned as previously described [S8]. For control group, mice underwent sham treatment.

Optical imaging of intrinsic signal

Using optical imaging of intrinsic signals, the retinotopic map of V1 from each mouse before and after retinal lesioning was determined as described [S9]. Imaging was done under a tungsten-halogen lamp filtered through a 700 nm transmission filter. Images were acquired with a cooled CCD camera (Optical Imaging) focused 300 µm below the dura surface. Two weeks after the cranial window was placed and approximately one week before the onset of the two-photon experiment, animals were imaged under 1.6 % isoflurane mixed with 0.8 L/min oxygen anesthesia.

Visual stimuli consisted of rectangular square-wave drifting gratings (0.03-0.05 cycles per degree, 2 cycles, moving in a random selection of 12 directions each for 0.6 s) presented on a gamma-corrected LCD screen, in front of the mouse. To obtain a retinotopic map, 6 s of such sequences were presented 4 times in each of the 24 separate areas on the screen (6x4 equal squares covering the visual field from -15 to +45o elevation and -15 to +75°azimuth). An image of the blood vessel pattern was first made using a green transmission filter and later overlaid on the produced retinotopic map.

In vivo two-photon microscopy in adult mice

To visualize boutons and mitochondria in the lesioned and non-lesioned areas in V1, at least three weeks after the cranial window implant, animals (P90-P120) were anesthetized with a mixture of ketamine and xylazine (100 mg/kg and 10 mg/kg i.p.) and fixed on a custom-made magnetic head-stage positioned in the two-photon setup. Two-photon laser scanning microscopy was performed on a modified Olympus BX61WI confocal microscope, using a 1.5 W Ti-sapphire laser at 850 nm and at a power of 10-30 % (Mai-Tai Spectraphysics, CA, USA). Axons expressing YFP-F in layer 1 until 100 µm under the dura were selected for chronic image acquisition. One to three regions of interest (~100 x 100 µm) were selected. Image stack (40-50 sections, spaced 1 µm apart) of these regions of interest were acquired at 512x512 pixels, 197 nm per pixel, through a water immersion Olympus 20x/0.95 objective at 7x zoom. The head stage was

controlled by a xyz micro-motor (Sutter Instruments, CA, USA). Imaging was carried out every 4 days in epochs of in total 11 imaging sessions.

Acute *in vivo* two-photon microscopy during development

P10 to P13 animals (n=3) were anesthetized with isoflurane (2 % in 1 L/min O2) and transferred to the imaging setup. Xylocaine cream was applied to the scalp, which was then cut followed by transection of the neck muscles. A head bar with an opening (Ø 4 mm) was attached to the skull above the visual cortex (0.5–2.5 mm rostral from lambda and 1– 3 mm lateral from the midline) with superglue (Pattex) and dental cement (Heraeus Kulzer). For axonal imaging, a small craniotomy above the visual cortex (approximately 1– 2 mm) was performed with spring scissors, forceps and a scalpel. Care was taken not to damage the dura and the exposed cortical surface was kept moist with cortex buffer (125 mM NaCl, 5 mM KCl, 10 mM glucose, 10 mM HEPES, 2 mM $MgSO_4$ and 2 mM $CaCl_2$ [pH 7.4]). For additional stability, a thin layer of 2 % high electroendosmosis agarose (Biomol) was applied to the cortical surface. To monitor mitochondrial dynamics on axonal stretches, isoflurane was decreased to 0.8 % and xyzt-stacks were acquired with a Nikon two-photon microscope, with a 3 W Ti-sapphire laser at 900 nm and at a power of 5-15 %. A 25x water-immersion objective (1.10 NA, Nikon) with 6x zoom was used to obtain time-lapse recordings with the following parameters: 512 x 256 pixels, frame rate of approximately 1 Hz, z-step size of 2 µm, pixel size of 170 nm, for 2 minutes. Throughout the entire experiment, physiological parameters such as heartbeat and body temperature were monitored, and temperature was maintained at 36˚C using a heating pad.

Organotypic slice cultures

Organotypic slice cultures were prepared as described [S5]. At postnatal day 5, the animals (n=3) were decapitated quickly and brains were placed in ice-cold Gay's balanced salt solution under sterile conditions. Cortical slices (400 µm) were cut using a tissue chopper (McIlwain) and incubated with serum-containing medium on Millicell culture inserts (Millipore). The slices were used for imaging 7-8 days after plating.

In vitro two-photon imaging

After incubation for seven to eight days, organotypic slices from V1 were cut out of the Millicel insert and placed in a microscope chamber perfused with modified Hank's balanced salt solution (HBSS, Life Technologies; 3.26 mM CaCl2, 0.493 mM $MgCl_2$, 0.406 mM $MgSO_4$, 5.33 mM KCl, 0.441 mM KH_2PO_4, 4.17 mM $NaHCO_3$, 138 mM NaCl, 0.336 mM Na_2HPO_4, and 5.56 mM D-glucose) kept at 30˚C. Images were obtained with the same

Nikon two-photon microscope, with the same laser and power range as used for *in vivo* imaging in pups (3 W at 5-15 %). A 16x water-immersion objective (0.80 NA, Nikon) with 8x zoom was used to obtain time-lapse recordings with the following parameters: 512 x 256 pixels, frame rate of approximately 1 Hz, pixel size of 210 nm, for 2 minutes.

Statistics

For statistical comparisons between two groups students t-test was used for normally distributed data (tested using the Kolmogorov-Smirnov method), with equal standard deviations (SDs). For comparison between randomly shuffled and actual data Kolmogorov-Smirnov test was used. For all paired tests Wilcoxon Signed Rank test was used. Statistical significance was determined at p value <0.05. For tests with more than two groups, the Kruskal-Wallis test (not normal distribution) was used with Dunn's post-hoc test. For binary outcomes, the Chi-square test was used to test the difference between groups with Bonferroni's post-hoc correction for multiple comparisons. Details of the specific statistical tests used can be found in the legends.

Image analysis

Putative boutons and mitochondria were manually identified in custom-made software running on Matlab (Mathworks, MA, USA). A putative bouton had to be wider and at least 50 % brighter than the axon. A 1.2 µm diameter circle was positioned around the putative bouton or mitochondrion once it was identified. Putative boutons were only scored once they were bigger and brighter than the axonal backbone. Putative boutons were considered as lost once they did not fulfill these criteria. Mitochondria were considered moved/lost once they were no longer positioned in the initial circle. For analyzing the relationships between the stability of mitochondria and boutons, we considered mitochondria to be close to a bouton when the center to center distance of the circles positioned around the boutons or mitochondria were equal or smaller than 2 µm. To investigate whether mitochondria were positioned preferentially at specific distances to boutons, we compared the distribution of the distances of mitochondria to the nearest bouton to the situation where the boutons are randomly redistributed over the axons. This shuffling was done by first drawing each axon in 3D, together with the boutons and mitochondria. Next, mitochondria were kept in position, but for each axon separately, the boutons were redistributed over the axon and the distance of all mitochondria to the nearest bouton were recomputed. This shuffling and recalculation was repeated 1000 times to compute the Shuffle histogram in Figure 2B. For analysis of mitochondrial motility (Figure 1), time lapse images were drift corrected using a custom-made Matlab App (kindly provided by J. Winnubst). ImageJ was used to

obtain kymographs from all axonal stretches of > 40µm in length and mitochondrial displacements were manually traced. Only displacements of > 2µm were counted. Analysis was constricted to the first 2 minutes of imaging due to bleaching.

Author contributions

LSR, RR, **CAPS**, FG, EMR, DvV, and UTE performed experiments.

LSR, RR, **CAPS**, FG, LS, CvdT, and JAH performed data analyses.

LSR, RR, CNL, and CL conceived experiments.

LSR, RR, and CNL wrote the manuscript.

LSR and RR contributed equally.

CNL is corresponding author.

Affiliations

LSR, RR, LS, EMMR, DvV, CvdT, and CNL: Department of Molecular Visual Plasticity, Netherlands Institute for Neuroscience, Royal Netherlands Academy of Arts and Science, The Netherlands.

CAPS, FG, CL: Department of Synapse and Network Development, Netherlands Institute for Neuroscience, Royal Netherlands Academy of Arts and Science, The Netherlands.

UTE: Department of Neurophysiology, Faculty of Medicine, Ruhr University Bochum, Germany.

JAH: Department of Cortical Structure and Function, Netherlands Institute for Neuroscience, Royal Netherlands Academy of Arts and Science, The Netherlands.

CNL: Department of Molecular and Cellular Neurobiology, Center for Neurogenomics and Cognitive Research, VU University Amsterdam, The Netherlands.

Competing interests

The authors declare no competing interests.

Acknowledgements

We would like to thank Dr. T.W. Gadella Jr for providing the mTurquoise2 plasmid and J. Winnubst for providing the Matlab drift correction tool. This research was funded by an NWO Vici grant and an NWO ALW Open Program grant to Christian Lohmann and an AgentschapNL grant to the NeuroBasic NeuroPhenomics consortium (CNL) and a donation from Praktijkgenerator.nl.

References

1. Kann O. and Kovacs R. (2007). Mitochondria and neuronal activity. Am. J. Physiol Cell Physiol 292: C641-C657.

2. Tang Y. and Zucker R.S. (1997). Mitochondrial involvement in post-tetanic potentiation of synaptic transmission. Neuron 18: 483-491.

3. Levy M., Faas G.C., Saggau P., Craigen W.J., and Sweatt J.D. (2003). Mitochondrial regulation of synaptic plasticity in the hippocampus. J. Biol. Chem. 278: 17727-17734.

4. Kang J.S., Tian J.H., Pan P.Y., Zald P., Li C., Deng C., and Sheng Z.H. (2008). Docking of axonal mitochondria by syntaphilin controls their mobility and affects short-term facilitation. Cell 132: 137-148.

5. Lennie P. (2003). The cost of cortical computation. Curr. Biol. 13: 493-497.

6. Hollenbeck P.J. and Saxton W.M. (2005). The axonal transport of mitochondria. J. Cell Sci. 118: 5411-5419.

7. Li Z., Okamoto K., Hayashi Y., and Sheng M. (2004). The importance of dendritic mitochondria in the morphogenesis and plasticity of spines and synapses. Cell 119: 873-887.

8. Chang D.T., Honick A.S., and Reynolds I.J. (2006). Mitochondrial trafficking to synapses in cultured primary cortical neurons. J. Neurosci. 26: 7035-7045.

9. MacAskill A.F. and Kittler J.T. (2010). Control of mitochondrial transport and localization in neurons. Trends Cell Biol. 20: 102-112.

10. Sheng Z.H. (2014). Mitochondrial trafficking and anchoring in neurons: New insight and implications. J. Cell Biol. 204: 1087-1098.

11. Sajic M., Mastrolia V., Lee C.Y., Trigo D., Sadeghian M., Mosley A.J., Gregson N.A., Duchen M.R., and Smith K.J. (2013). Impulse conduction increases mitochondrial transport in adult mammalian peripheral nerves *in vivo*. PLoS. Biol. 11: e1001754.

12. Davis C.H., Kim K.Y., Bushong E.A., Mills E.A., Boassa D., Shih T., Kinebuchi M., Phan S., Zhou Y., Bihlmeyer N.A. et al. (2014). Transcellular degradation of axonal mitochondria. Proc. Natl. Acad. Sci. U. S. A 111: 9633-9638.

13. Saxton W.M. and Hollenbeck P.J. (2012). The axonal transport of mitochondria. J. Cell Sci. 125: 2095-2104.

14. Beal M.F. (1996). Mitochondria, free radicals, and neurodegeneration. Curr. Opin. Neurobiol. 6: 661-666.

15. Mattson M.P. (2007). Mitochondrial regulation of neuronal plasticity. Neurochem. Res. 32: 707-715.

16. Millecamps S. and Julien J.P. (2013). Axonal transport deficits and neurodegenerative diseases. Nat. Rev. Neurosci. 14: 161-176.

17. Babic M., Russo G.J., Wellington A.J., Sangston R.M., Gonzalez M., and Zinsmaier K.E. (2015). Miro's N-terminal GTPase domain is required for transport of mitochondria into axons and dendrites. J. Neurosci. 35: 5754-5771.

18. Manji H., Kato T., Di Prospero N.A., Ness S., Beal M.F., Krams M., and Chen G. (2012). Impaired mitochondrial function in psychiatric disorders. Nat. Rev. Neurosci. 13: 293-307.

19. Schon E.A. and Przedborski S. (2011). Mitochondria: the next (neurode)generation. Neuron 70: 1033-1053.

20. Obashi K. and Okabe S. (2013). Regulation of mitochondrial dynamics and distribution by synapse position and neuronal activity in the axon. Eur. J. Neurosci. 38: 2350-2363.

21. MacAskill A.F., Rinholm J.E., Twelvetrees A.E., Arancibia-Carcamo I.L., Muir J., Fransson A., Aspenstrom P., Attwell D., and Kittler J.T. (2009). Miro1 is a calcium sensor for glutamate receptor-dependent localization of mitochondria at synapses. Neuron 61: 541-555.

22. Li Z., Jo J., Jia J.M., Lo S.C., Whitcomb D.J., Jiao S., Cho K., and Sheng M. (2010). Caspase-3 activation via mitochondria is required for long-term depression and AMPA receptor internalization. Cell 141: 859-871.

23. Ishihara N., Nomura M., Jofuku A., Kato H., Suzuki S.O., Masuda K., Otera H., Nakanishi Y., Nonaka I., Goto Y. et al. (2009). Mitochondrial fission factor Drp1 is essential for embryonic development and synapse formation in mice. Nat. Cell Biol. 11: 958-966.

24. Faits M.C., Zhang C., Soto F., and Kerschensteiner D. (2016). Dendritic mitochondria reach stable positions during circuit development. Elife. 5.

25. Shepherd G.M. and Harris K.M. (1998). Three-dimensional structure and composition of CA3-->CA1 axons in rat hippocampal slices: implications for presynaptic connectivity and compartmentalization. J. Neurosci. 18: 8300-8310.

26. Stettler D.D., Yamahachi H., Li W., Denk W., and Gilbert C.D. (2006). Axons and synaptic boutons are highly dynamic in adult visual cortex. Neuron 49: 877-887.

27. Weeber E.J., Levy M., Sampson M.J., Anflous K., Armstrong D.L., Brown S.E., Sweatt J.D., and Craigen W.J. (2002). The role of mitochondrial porins and the permeability transition pore in learning and synaptic plasticity. J. Biol. Chem. 277: 18891-18897.

28. Sun T., Qiao H., Pan P.Y., Chen Y., and Sheng Z.H. (2013). Motile axonal mitochondria contribute to the variability of presynaptic strength. Cell Rep. 4: 413-419.

29. Keck T., Mrsic-Flogel T.D., Vaz A.M., Eysel U.T., Bonhoeffer T., and Hubener M. (2008). Massive restructuring of neuronal circuits during functional reorganization of adult visual cortex. Nat. Neurosci. 11: 1162-1167.

30. Yamahachi H., Marik S.A., McManus J.N., Denk W., and Gilbert C.D. (2009). Rapid axonal sprouting and pruning accompany functional reorganization in primary visual cortex. Neuron 64: 719-729.

31. Giannikopoulos D.V. and Eysel U.T. (2006). Dynamics and specificity of cortical map reorganization after retinal lesions. Proc. Natl. Acad. Sci. U. S. A 103: 10805-10810.

32. Kaas J.H., Krubitzer L.A., Chino Y.M., Langston A.L., Polley E.H., and Blair N. (1990). Reorganization of retinotopic cortical maps in adult mammals after lesions of the retina. Science 248: 229-231.

33. Plucinska G., Paquet D., Hruscha A., Godinho L., Haass C., Schmid B., and Misgeld T. (2012). *In vivo* imaging of disease-related mitochondrial dynamics in a vertebrate model system. J. Neurosci. 32: 16203-16212.

34. Misgeld T., Kerschensteiner M., Bareyre F.M., Burgess R.W., and Lichtman J.W. (2007). Imaging axonal transport of mitochondria *in vivo*. Nat. Methods 4: 559-561.

35. Takihara Y., Inatani M., Eto K., Inoue T., Kreymerman A., Miyake S., Ueno S., Nagaya M., Nakanishi A., Iwao K. et al. (2015). *In vivo* imaging of axonal transport of mitochondria in the diseased and aged mammalian CNS. Proc. Natl. Acad. Sci. U. S. A 112: 10515-10520.

36. Pekkurnaz G., Trinidad J.C., Wang X., Kong D., and Schwarz T.L. (2014). Glucose regulates mitochondrial motility via Milton modification by O-GlcNAc transferase. Cell 158: 54-68.

37. Tallent M.K., Varghis N., Skorobogatko Y., Hernandez-Cuebas L., Whelan K., Vocadlo D.J., and Vosseller K. (2009). *In vivo* modulation of O-GlcNAc levels regulates hippocampal synaptic plasticity through interplay with phosphorylation. J. Biol. Chem. 284: 174-181.

38. van Versendaal D., Rajendran R., Saiepour M.H., Klooster J., Smit-Rigter L., Sommeijer J.P., De Zeeuw C.I., Hofer S.B., Heimel J.A., and Levelt C.N. (2012). Elimination of inhibitory synapses is a major component of adult ocular dominance plasticity. Neuron 74: 374-383.

39. Keck T., Scheuss V., Jacobsen R.I., Wierenga C.J., Eysel U.T., Bonhoeffer T., and Hubener M. (2011). Loss of sensory input causes rapid structural changes of inhibitory neurons in adult mouse visual cortex. Neuron 71: 869-882.

40. Stoppini L., Buchs P.A., and Muller D. (1991). A simple method for organotypic cultures of nervous tissue. J. Neurosci. Methods 37: 173-182.

Chapter 3

Activity-dependent regulation of mitochondrial motility in developing cortical dendrites

Cátia A. P. Silva, Annik Carson, Victoria Busch, Mike van Zwieten, Matthijs Verhage and Christian Lohmann

Silva et al., 2021. eLife

CAPS contribution: designed and performed experiments, wrote paper.

List of figures

Abstract

Developing neurons form synapses at a high rate. Synaptic transmission is very energy-demanding and likely requires ATP production by mitochondria nearby. Mitochondria might be targeted to active synapses in young dendrites, but whether such motility regulation mechanisms exist is unclear. We investigated the relationship between mitochondrial motility and neuronal activity in the primary visual cortex of young mice *in vivo* and in slice cultures. During the first 2 postnatal weeks, mitochondrial motility decreases while the frequency of neuronal activity increases. Global calcium transients do not affect mitochondrial motility. However, individual synaptic transmission events precede local mitochondrial arrest. Pharmacological stimulation of synaptic vesicle release, but not focal glutamate application alone, stops mitochondria, suggesting that an unidentified factor co-released with glutamate is required for mitochondrial arrest. A computational model of synaptic transmission-mediated mitochondrial arrest shows that the developmental increase in synapse number and transmission frequency can contribute substantially to the age-dependent decrease of mitochondrial motility.

Introduction

Newborns can interact with their environment soon after birth, without any previous experience of sensory input. This ability relies on extensive preparation of the developing nervous system before the onset of sensory experience. Young networks are initially established by molecular guidance cues and refined by activity-driven synaptic plasticity. Before the onset of sensory processing, developing neuronal networks generate neuronal activity spontaneously that strengthens well-targeted synapses and weakens others to prepare the brain for sensory processing. Later, learning adjusts synaptic circuits to the prevalent environmental conditions (Katz and Shatz, 1996; Sengpiel and Kind, 2002; Sanes and Yamagata, 2009; Kilb et al., 2011; Kirkby et al., 2013; Leighton and Lohmann, 2016).

The development of synapses and synaptic transmission are highly energy demanding processes. A substantial amount of this energy is supplied by mitochondria, the main energy providers in neurons (Harris et al., 2012). Imaging experiments showed that neuronal mitochondria can be highly motile in intact tissue (Misgeld et al., 2007; Plucińska and Misgeld, 2016). For example, mitochondria are generated at the soma and transported to distal dendrites and axons via the microtubule network (Sheng and Cai,

2012). This motility allows for energy provision at high-energy demanding sites, in particular, synapses. Defects in mitochondrial motility have been shown to lead to impaired neurotransmission, further linking mitochondrial motility and synaptic function (Sheng and Cai, 2012). In addition, previous studies reported that experimentally enhancing neuronal activity (with high extracellular potassium, the voltage gated sodium channel activator veratridine, glutamate or electrical stimulation) stops mitochondria at synapses, whereas blocking action potential firing using tetrodotoxin increases mitochondrial motility and reduces the number of stationary mitochondria at synapses (Rintoul et al., 2003; Li et al., 2004; Chang et al., 2006; MacAskill et al., 2009). MIRO1, a calcium sensitive protein linking mitochondria to the microtubule network can mediate mitochondrial arrest in dendrites and axons (MacAskill et al., 2009; Wang and Schwarz, 2009): upon calcium binding, MIRO1 releases mitochondria from motor proteins (kinesins or dyneins), thus interrupting their motility.

In contrast, other evidence suggests that mitochondrial motility in neuronal dendrites is not affected by activity (Beltran-Parrazal et al., 2006; Faits et al., 2016). In retinal explants, neither spontaneously occurring nor stimulus-evoked activity affect mitochondrial motility (Faits et al., 2016). Moreover, mitochondrial motility remains high in an hyperactive retina with immature synapses (Morrow et al., 2005; Tran et al., 2014; Faits et al., 2016). These observations suggest that high mitochondrial motility may not be the consequence of low activity in immature tissue, but rather a characteristic of very young neurons (Faits et al., 2016). Thus, activity levels may co-vary with mitochondrial arrest rather than causing it.

To address the role of natural activity patterns in mitochondrial arrest, we investigated here whether spontaneous activity affects mitochondrial motility in the developing visual cortex both *in vivo* and in organotypic slice cultures. We found that mitochondrial motility decreased over the first two postnatal weeks while the frequency of spontaneous activity increased. Global spontaneous calcium transients did not affect mitochondrial motility; however, spontaneous activity at the synaptic level preceded mitochondrial motility arrest and pharmacological stimulation of synaptic vesicle release, but not focal glutamate application alone, was sufficient to stop mitochondrial motility. A computational model of synaptic activity-mediated control of mitochondrial motility suggests that the developmental increase in synapse number and transmission frequency contributes substantially to the age dependent decrease of mitochondrial motility.

Results

We investigated the relationship between spontaneous activity and mitochondrial motility *in vivo* and in organotypic slice cultures of the developing mouse primary visual cortex during the second postnatal week before eye opening at P14 (Figure 1A). We used in utero electroporation at embryonic day 16.5 to express the calcium indicator GCaMP6s and mitochondrial-DsRed in pyramidal neurons of layer II/III (Figure 1B-C). Time-lapse recordings were performed to reveal the spatio-temporal relationship between mitochondrial motility and calcium signaling in developing dendrites (Figure 1D-E).

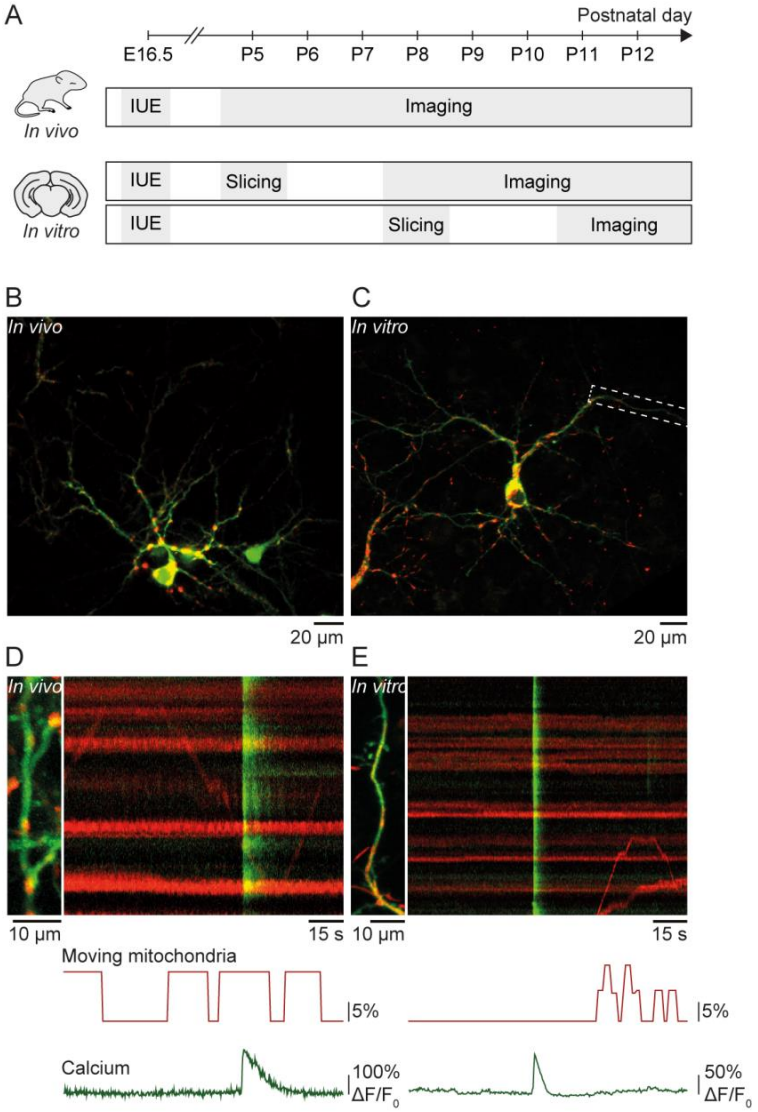

Figure 1. Simultaneous imaging of dendritic calcium transients and mitochondrial motility *in vitro* and *in vivo*.
A: Timeline of *in vivo* and *in vitro* experiments: in utero electroporation (IUE) was performed at embryonic day (E) 16.5 to deliver GCaMP6s (calcium indicator) and Mito-DsRed (mitochondrial marker) to pyramidal neurons of layer II/III in the visual cortex. *In vivo* experiments: acute imaging of transfected dendrites in pups between P5 and P12 using a 2-photon microscope. *In vitro* experiments: imaging of transfected dendrites using a confocal microscope in organotypic cortical slices cultured for 3-7 days after slice preparation from P5 or P8 pups.

B: GCaMP6- and Mito-DsRed-expressing layer II/III pyramidal neurons *in vivo* (P16).
C: GCaMP6- and Mito-DsRed-expressing layer II/III pyramidal neurons *in vitro* (P5 + DIV4).D: Dendrite of layer II/III pyramidal neuron *in vivo* and kymograph (right) representing dendritic calcium transients (green) as well as motile and stationary mitochondria (red). Immobile mitochondria appear as horizontal lines (no change in position over time) and moving mitochondria as diagonal lines. Below, graphic representation of the percentage of moving mitochondria and global calcium transients. The percentage of moving mitochondria was calculated as the number of moving mitochondria over the total number of mitochondria, binned for every second. The mean percentage of moving mitochondria across the duration of this recording was 8.5%. Vertical green lines show spontaneously occurring global calcium transients, most likely resulting from back-propagating action potentials.
E: Dendrite of the layer II/III pyramidal neuron shown in C. The mean percentage of moving mitochondria across the duration of the recording was 2.4%.

Previous studies reported that neuronal activity and calcium signaling reduce mitochondrial motility in dendrites *in vitro* (Li et al., 2004; Chang et al., 2006), but this idea has not been tested *in vivo*. Therefore, we first investigated the interaction between spontaneous network activity and mitochondrial motility in neonatal mice. Overall, we observed an anti-correlation between the frequency of spontaneous global calcium transients and the percentage of moving mitochondria in awake (unanesthetized) animals (Figure 2A). Upon closer inspection, it became clear that these parameters were linked systematically to the age of the animal: in older animals (≥ postnatal day (P) 8) activity levels were consistently higher and mitochondrial motility was low (Figure 2A-D). We observed a similar relationship between neuronal activity, mitochondrial motility and age in anesthetized mice (0.8 % isoflurane, Figure supplement 1A-D). Therefore, we combined both groups for the analyses shown below (Figure 2E-G).

Since overall calcium signaling correlated with mitochondrial motility, we asked whether neuronal activity could directly affect mitochondrial motility. First, we replicated previous experiments performed in cell cultures (DIV14-17) that showed an increase of mitochondrial motility after blocking action potential firing (Li et al., 2004; Chang et al., 2006). Application of the sodium channel blocker tetrodotoxin (TTX; 2 µM) to the surface of the brain (P5-P12) abolished global calcium transients (Figure 2E) and, as expected, led to a significant increase in mitochondrial motility (Figure 2F, see also Methods for an extended discussion on statistics). Furthermore, the effect of TTX on mitochondrial motility was highly proportional to the frequency of baseline activity (r^2 = 0.81; Figure 2G), suggesting that natural patterns of neuronal activity efficiently constrain mitochondrial motility.

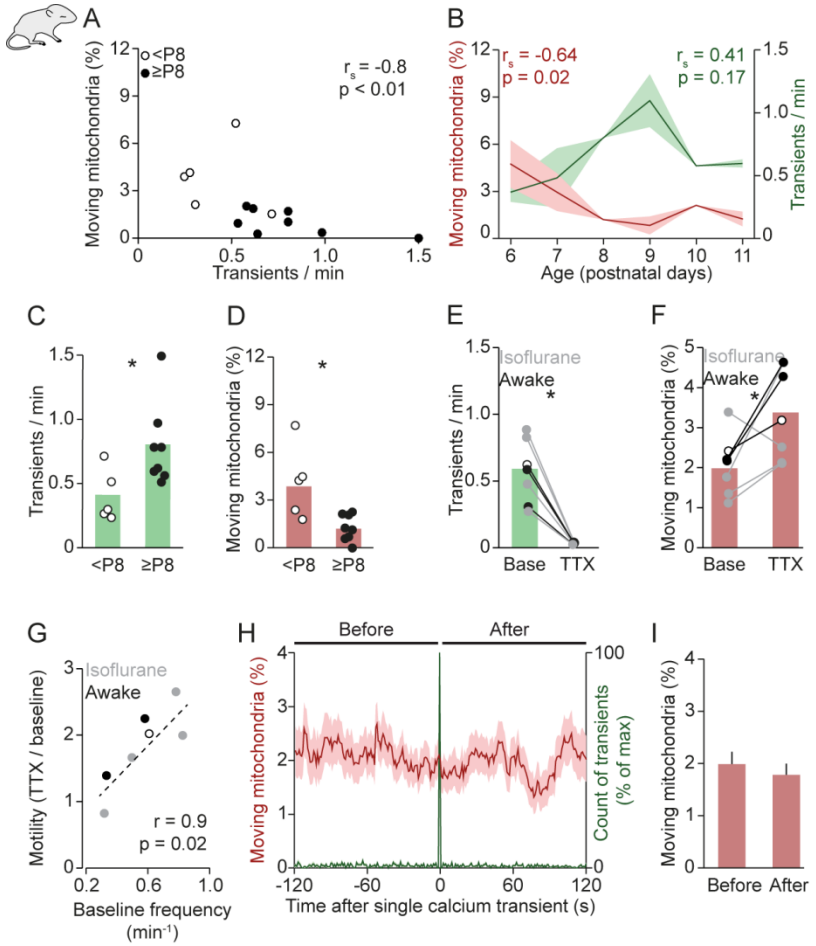

Figure 2. Mitochondrial motility and spontaneous activity are anti-correlated during *in vivo* early postnatal development.
A: Anti-correlation between the frequency of spontaneous global calcium transients and the percentage of moving mitochondria in imaging experiments of awake pups (n = 13 pups, Spearman's rank correlation; 1192 mitochondria in 131 dendrites).
B: The frequency of spontaneous global calcium transients increased until P9 (but not significantly for the entire age range, Spearman's rank correlation) and the percentage of moving mitochondria decreased over postnatal days 6-11 *in vivo* (Spearman's rank correlation).
C-D: When comparing awake animals younger than P8 to P8 and older, the frequency of spontaneous global calcium transients increased (t-test, n = 5 vs n = 8, p = 0.02) and the percentage of moving mitochondria decreased (t-test, n = 5 vs n = 8, p = 0.045).
E-F: Application of tetrodotoxin (TTX, 2 µM) on the surface of the cortex (n = 7 pups, 1625 mitochondria in 160 dendrites) completely abolished spontaneously occurring global calcium transients (paired t-test, p = 6*10-4) and increased the percentage of moving mitochondria (paired t-test, p = 0.035).
G: Higher baseline frequency of spontaneous global calcium transients was correlated with a larger effect of TTX on the percentage of moving mitochondria (n = 7 pups, Pearson correlation, r = 0.85, p = 0.015).
H-I: Mean mitochondrial motility time-locked to the onset of single global calcium transients. The percentage of moving mitochondria did not change significantly between the 2 minutes before and after spontaneously occurring global calcium transients in awake animals (n = 136 transients, paired t-test, p = 0.33).

We then examined whether spontaneously occurring single global calcium transients affected mitochondrial motility. We compared mitochondrial motility before and after global calcium transients across all recordings by aligning the occurrence of global

calcium transients in time and plotting the percentage of moving mitochondria around this time point (Figure 2H). We found that spontaneous global calcium transients did not precede a change in mitochondrial motility (Figure 2H-I) or mitochondrial speed (Figure supplement 1E-F). Together, these experiments showed that while neuronal activity modulated mitochondrial motility, global calcium transients - most likely reflecting single back-propagating action potentials and bursts of back-propagating action potentials - were ineffective in doing so. We therefore speculated that synaptic transmission, rather than postsynaptic action potential firing, might regulate mitochondrial motility. To address this possibility, we aimed at analyzing the relationship between synaptic activity and mitochondrial motility. Our *in vivo* recordings showed transmission events at individual synapses (Figure supplement 2), but we detected these events too rarely to quantify any possible effect of synaptic activity on mitochondrial motility.

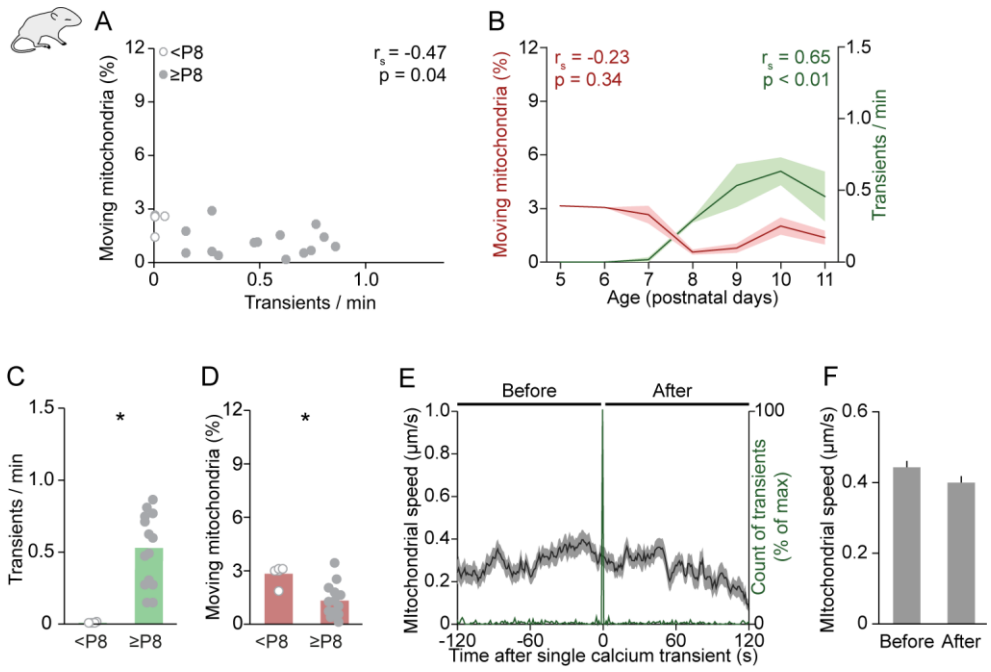

Figure supplement 1. Relationship between neuronal activity, mitochondrial motility, and age *In vivo*.
A: Anti-correlation between the frequency of spontaneous global calcium transients and the percentage of moving mitochondria in animals under isoflurane anesthesia (Spearman's rank correlation: rs = -0.47, p = 0.04).
B: The frequency of spontaneous global calcium transients increased with age (Spearman's rank correlation).C-D: When comparing animals younger than P8 to P8 and older, the frequency of spontaneous global calcium transients increased (t-test, n = 5 vs n = 14, p = 3*10-6) and the percentage of moving mitochondria decreased (t-test, n = 5 vs n = 14, p = 0.002) in animals under isoflurane anesthesia.
E-F: Mean mitochondrial speed time-locked to the onset of single global calcium transients. The speed of moving mitochondria did not change between the 2 minutes before and after a single spontaneously occurring calcium transient *in vivo* (right, student's t-test, n = 1029 mitochondria, p = 0.07).

Therefore, we moved to organotypic slice culture preparations, which allow higher signal-to-noise ratio imaging and more stable recordings to investigate the role of transmission at synapses. We obtained cortical slices at P5 or P8 and kept them in culture for at least three days before imaging. Slices obtained from older animals showed a trend towards higher spontaneous activity levels (Figure 3A, Figure supplement 3A-B) and significantly lower mitochondrial motility than slices obtained from younger animals (Figure 3B, Figure supplement 1A-B). As *in vivo*, spontaneous global calcium transients did not precede changes in mitochondrial motility (Figure 3C-D, Figure supplement 3C-D) or speed (Figure supplement 3E-F). Thus, mitochondrial motility and its independence of spontaneous global calcium signaling were maintained in slice cultures (Figure supplement 3A-B). Together, we reproduced our *in vivo* observations on mitochondrial motility in slice cultures and, thus, found them suitable to investigate the role of synaptic activity in regulating mitochondrial motility.

In slice cultures, visual cortex layer II/III neurons frequently showed spontaneous calcium transients in spines representing synaptic transmission events at excitatory synapses, as shown previously in the developing visual cortex and hippocampus (Kleindienst et al., 2011; Winnubst et al., 2015; Niculescu et al., 2018). In nine cells (P5 + 3-7 DIV), we identified 157 spines of which 71 (45 %) showed spontaneous synaptic calcium transients (376 transients). We asked whether synaptic activity affected the motility of passing mitochondria. We observed that mitochondria typically passed by inactive synapses (Figure 3E), but frequently halted when they reached a synapse that had just been active (Figure 3F). Therefore, we specifically determined whether synaptic calcium transients affected the likelihood that incoming mitochondria stopped at or passed by synapses. To quantify this effect, we compared the percentage of approaching mitochondria that stopped at a synapse before and after the occurrence of a synaptic calcium transient (Figure 3G-H). When we compared the percentage of stopping mitochondria during a 120 second interval before a single synaptic calcium transient occurred with an interval of the same duration after that calcium transient, we found that the percentage of stopping mitochondria increased significantly after the transient (Figure 3I). To answer whether the observed effect size (the difference between the

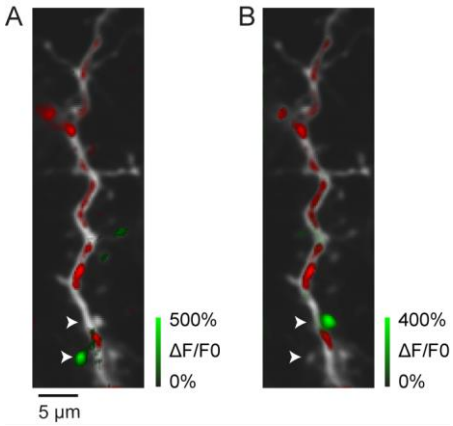

Figure supplement 2. Synaptic calcium transients *in vivo*.
A, B: Two examples of local calcium transients (green) in spines of a layer II/III pyramidal neuron dendrite at P13 (red: mitochondrial-DsRed). Arrow heads mark two spines that are activated in A or B.

arrest rates before and after a local calcium transient) was likely to occur by chance or not, we performed a boot-strap analysis where we randomized the time points of synaptic calcium transients in our recordings and determined the resulting effect size for a total of 1000 runs. We found that the observed effect size was above the 95 percentile of the randomized effect size distribution (Figure 3J) demonstrating that this effect was unlikely to be observed by chance.

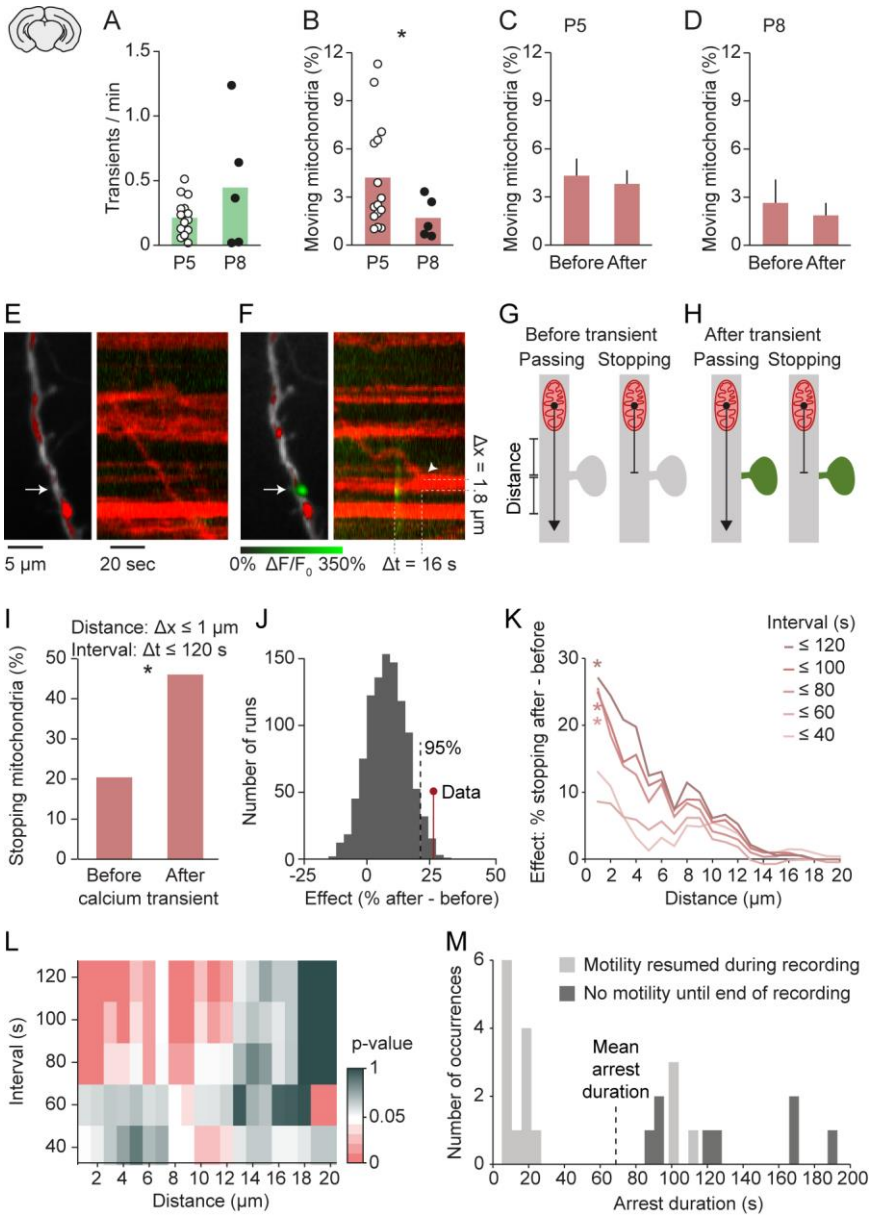

Figure 3. Mitochondria stop at synapses after synaptic transmission events.
A-B: Frequency of global calcium transients and mitochondrial motility in slices obtained from P5 and P8 pups. The frequency of spontaneous global calcium transients did not change significantly (n = 15 vs n = 5 cells, student's t-test, p = 0.37). The percentage of moving mitochondria was significantly decreased in slices from older animals (n = 15 (252 mitochondria) vs n = 5 (85 mitochondria), student's t-test, p = 0.02), similar to the *in vivo* results.
C-D: The percentage of moving mitochondria did not change significantly between the 2 minutes before and after spontaneously occurring calcium transients in P5 (n = 158 transients, paired t-test, p = 0.07) or P8 slices (paired t-test, n = 101 transients, p = 0.3).
E: Dendritic segment and kymograph showing a mitochondrion approaching and passing an

inactive synapse (arrow).
F: Same dendritic segment as in A. A mitochondrion arrived near the same synapse (arrow) after a synaptic calcium transient occurred and stopped within its vicinity (Δx: distance to synapse, Δt: time after synaptic calcium transient).
G-H: Mitochondria moving towards a synapse can show one of two behaviors: they may continue moving (left) or stop near the synapse (right). We compared the percentage of approaching mitochondria that stopped within a specific distance range before individual synaptic calcium transients occurred (G) with that of mitochondria that reached a synapse after a transient (H) within a specific time interval.
I: There was a significant increase in the percentage of stopping mitochondria after a single local calcium transient occurred (distance <= 1 µm; interval <= 120 s; *p = 6 * 10-5, chi-squared test).
J: We compared the effect size of mitochondrial arrest at active synapses to a distribution generated by shuffling the time points at which synaptic calcium transients occurred (1000 runs). The observed effect size was within the top 5 percentile of those generated from shuffled data for distances <= 1 µm and intervals <= 120 s.
K: Quantitative estimation of the spatio-temporal characteristics of mitochondrial arrest (chi-squared test for each distance/interval pair Bonferroni-corrected; distance <= 1 µm; interval <= 80 s, p = 0.0035; interval <= 100 s, p = 0.0016; interval <= 120 s, p = 0.0025).
L: Matrix showing the individual chi-squared test p-values from each distance/interval pair. Roughly, p < 0.05 for intervals between 80 and 120 s and distances of up to 5 µm. (Number of observations for K,L: see Figure supplement 4B)
M: Distribution of mitochondrial arrest durations after single spontaneous synaptic events. Shown in dark gray are underestimated durations for data points where mitochondria remained immotile until the end of the recording.

Next, we quantified the effect size for different distances from the synapse and different time intervals after a synaptic calcium transient and found that mitochondrial arrest was most prevalent within distances of up to 5 micrometers around a synapse and for intervals of 80-120 seconds after the synaptic event (Figure 3K, L). On average, synaptic activity was associated with an interruption of mitochondrial movement for about one minute (68 seconds; Figure 3M). However, this number underestimated the duration of arrest, since one third of the stopping mitochondria were still immobile at the end of a recording (mean 131 seconds at a recording duration of 350 seconds) preventing an exact estimate of the time point when they started moving again. Together, our observations at individual synapses suggested that spontaneous synaptic transmission can capture moving mitochondria in postsynaptic dendrites.

To address the potential mechanism of mitochondrial arrest at active synapses, we first tested whether membrane depolarization leads to mitochondrial arrest. Consistent with previous studies (Li et al., 2004; MacAskill et al., 2009; Faits et al., 2016), we found that an increase of extracellular potassium to 50 mM decreased mitochondrial motility by approximately 50% (Figure 4A, B). This result demonstrated that long-lasting depolarization arrests mitochondria. However, our finding that global calcium transients, which are most likely the consequence of depolarization induced opening of voltage gated calcium channels, suggest that depolarization alone is insufficient to stop mitochondria. To test whether synaptic transmission is sufficient to interrupt

mitochondrial motility and whether this effect is dependent or independent of action potential firing, we pharmacologically triggered synaptic release while action potential generation was prevented with TTX (Figure 4C-E). After three baseline recordings we applied TTX (1 µM), which blocked all global calcium transients as expected. Next, we stimulated release of synaptic vesicles by applying latrotoxin (Deak et al., 2009) to the bath. The molecular mechanism of latrotoxin induced transmitter release is unknown. Nevertheless, at the concentration used here (1 nM) latrotoxin specifically triggers synaptic vesicle release through activation of its receptors latrophilin and neurexin that are located at presynaptic terminals (Valtorta et al., 1984; Matteoli et al., 1988; Südhof, 2001). After application of latrotoxin to the bath, the intracellular calcium concentration increased within a few minutes and mitochondrial motility was either entirely suppressed or largely inhibited (Figure 4C-E). Mitochondrial motility recovered only partly after around one hour, whereas calcium levels returned to baseline levels within 15-20 minutes.

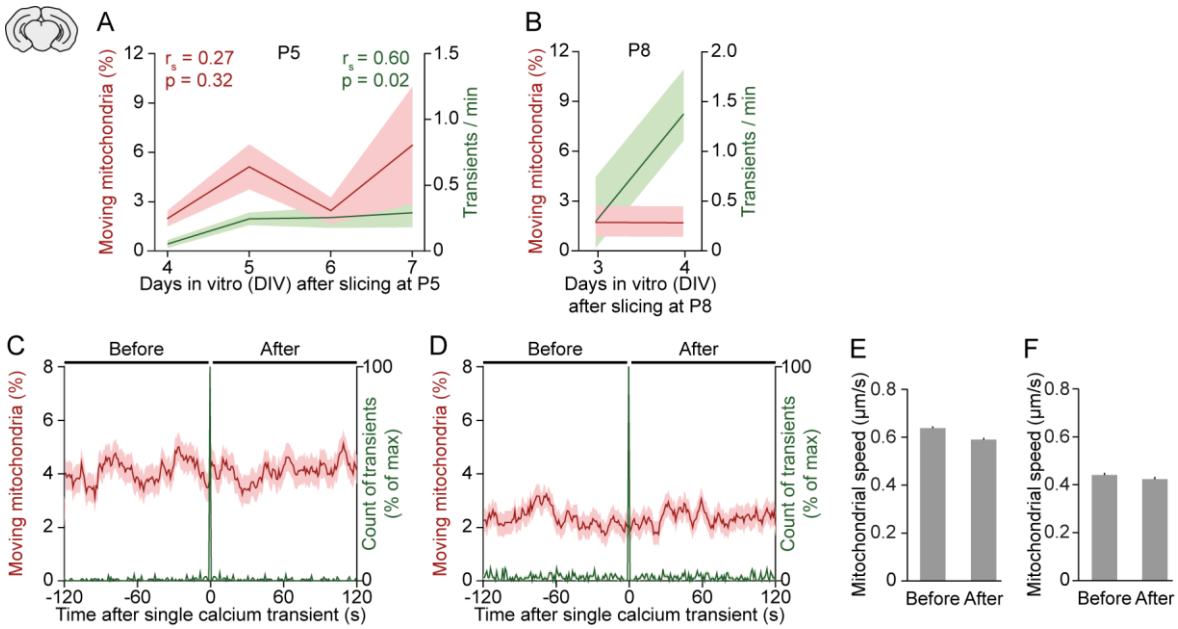

Figure supplement 3. Relationship between neuronal activity, mitochondrial motility, and age in organotypic slice cultures.
A-B: In slices obtained from P5 (A) or P8 pups (B), the frequency of spontaneous global calcium transients increased slightly over days *in vitro* whereas the motility of mitochondria did not change significantly (Spearman's rank correlation).
C-D: Mean mitochondrial motility time-locked to the onset of single global calcium transients for slices obtained from P5 (C) and P8 pups (D).
E-F: The speed of moving mitochondria did not change between the 2 minutes before and after a single spontaneously occurring calcium transient in cells from P5 (E, student's t-test, n = 1592 mitochondria, p = 0.1) or P8 pups (F, paired t-test, n = 769 mitochondria, p = 0.5).

These experiments indicated that single synaptic transmission events have the capacity to stop mitochondria for one to a few minutes and that massive synaptic

activation interrupts mitochondrial motility almost entirely for periods of tens of minutes. Finally, we asked whether the transmitter glutamate is responsible for presynaptic release mediated mitochondrial arrest. We applied single puffs of glutamate (100 µM) to individual dendrites using a pico-spritzer. Focal glutamate delivery triggered calcium increases in the dendrite extending 7-59 µm (27 ± 14 µm; mean ± standard deviation). We analyzed mitochondrial motility before and after glutamate application in the dendritic stretch that responded with a calcium rise. We found that mitochondrial motility was slightly, but not significantly, reduced after glutamate puffs (Figure 4F, G), demonstrating that glutamate is not sufficient to cause vesicle release mediated mitochondrial arrest.

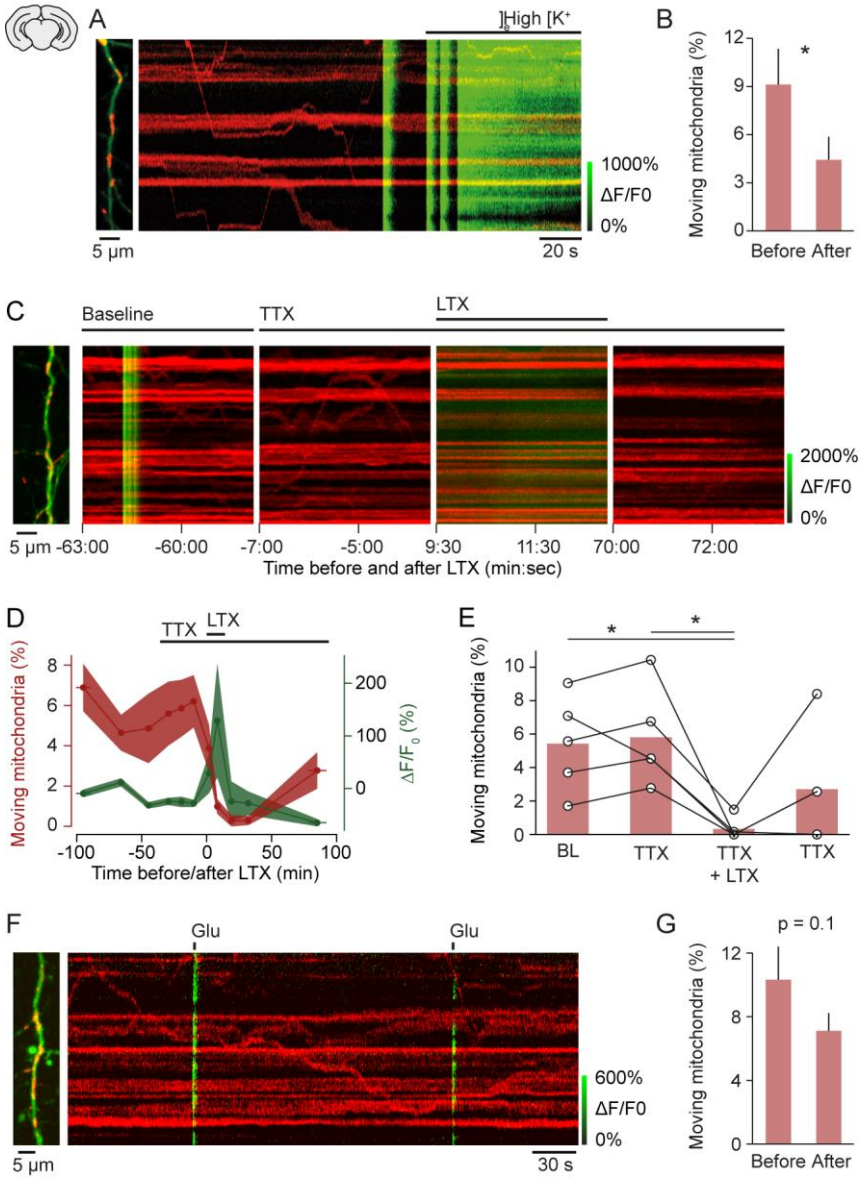

Figure 4. Mechanism of activity induced mitochondrial arrest
A, B: Perfusing layer II/III pyramidal neurons (P5 + 3-7 DIV) with high-potassium medium [50 mM] triggered a massive influx of calcium and significantly reduced mitochondrial motility within 2 minutes (n = 9 cells; 107 mitochondria, paired t-test, p = 0.04).
C-E: Stimulating synaptic vesicle release with latrotoxin (LTX) interrupted mitochondrial motility

entirely.
C: Example kymographs from recordings during baseline, in the presence of tetrodotoxin (TTX), TTX and LTX, and after washout of LTX. Basal calcium levels were elevated and mitochondrial motility was absent during the presence of LTX.
D: Averaged time-course of mitochondrial motility and GCaMP6 ΔF/F0 for the duration of the experiments. Shaded areas and horizontal bars indicate SEMs of values and time points, respectively.
E: Percentage of moving mitochondria across all conditions ($p = 0.0058$, repeated measures ANOVA, * $p = 0.028$ (Baseline vs LTX+TTX), * $p = 0.022$ (TTX vs TTX + LTX), Post-hoc t-test with Bonferroni multi-measures correction, n = 5 cells, 92 mitochondria).
F-G: Triggering calcium transients with focal application of Glutamate (100 μM) in the presence of TTX did not affect mitochondrial motility significantly (P5 + 3-7 DIV, n = 74 transients from 13 cells, 146 mitochondria, paired t-test, before vs after, 10.32 ± 2.09 vs 7.12 ± 1.12, $p = 0.1$).

While the factor that mediates mitochondrial arrest remains unknown, our experiments showed that synaptic vesicle release interrupts mitochondrial transport locally. Since synaptic density (De Felipe J. et al., 1997) as well as network activity (Rochefort et al., 2009) and thus synaptic vesicle release increase dramatically in the cortex during the second postnatal week, we hypothesized that the temporary recruitment of mitochondria to synapses by spontaneous synaptic activity could contribute to the overall decrease in mitochondrial motility we observed during *in vivo* development.

To investigate this idea, we designed a computational model for estimating mitochondrial motility in a developing dendrite at different synaptic input frequencies. Since we established a lower bound for the mean duration of immobilization of ~70 seconds, we modeled the effect of synaptic inputs on mitochondrial motility for mean arrest durations of one to five minutes using Gaussian distributions (μ = 1-5 minutes, σ = 2.5 minutes). We found that the distributions for 1-3 minutes were comparable with our observed duration distributions (Figure 5A, cf. Figure 3M). The model showed that changes in synaptic activity could affect mitochondrial motility critically: while low input frequencies (e.g. 0.035 Hz in a 100 μm dendritic segment) reduced mitochondrial motility only marginally from the default state (~10%), higher input frequencies showed clear effects (Figure 5B). For example, at 0.35 Hz, mitochondrial motility was reduced

by approximately 50% at steady state. We determined mitochondrial motility for increasing input frequencies and different durations of mitochondrial arrest (Figure 5C). To determine the putative effect of an increase in synaptic activity between the first and the second postnatal week on mitochondrial motility, we estimated the frequency of synaptic inputs received by a stretch of dendrite of 100 μm length. In our previous *in vivo* study, we found a mean density of 36 active synapses per 100 μm dendrite in visual cortex layer II/III pyramidal neurons at the end of the second postnatal week (P10-15)

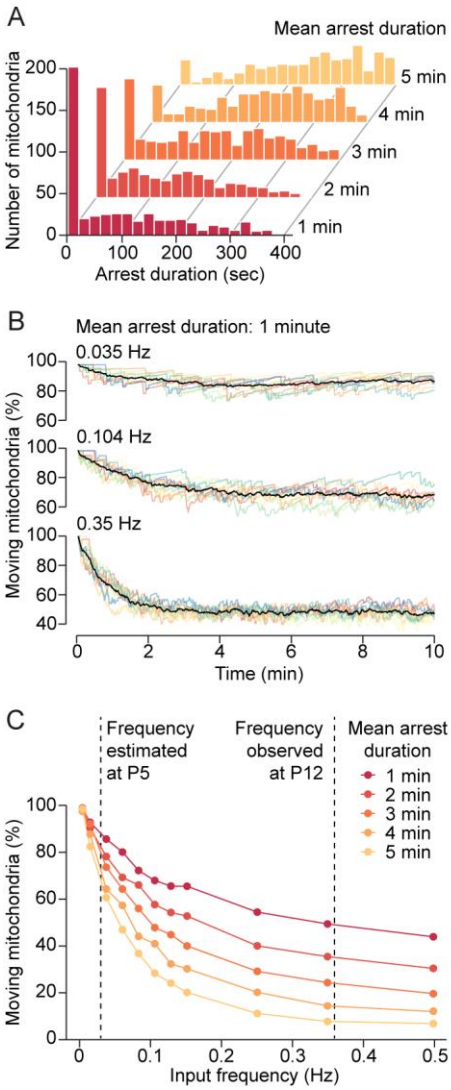

Figure 5: Model of synaptic input mediated modulation of mitochondrial motility.
A: Distribution of mitochondrial arrest durations generated by the model for mean durations of one to five minutes.
B: Changes of mitochondrial motility after onset of simulated synaptic inputs for a mean arrest duration of 1 minute. Input frequencies are given as total synaptic inputs along a 100 µm stretch of dendrite. Low input frequencies hardly changed overall mitochondrial motility. Higher input frequencies reduced motility substantially. Steady state was reached after a few minutes. Colored lines: individual simulations, black lines: average of 10 simulations.
C: Relationship between synaptic input frequency and mitochondrial motility for different arrest durations at steady state. The expected increase of synaptic activity from P5 to P12 reduced mitochondrial motility by 30 – 60%, depending on the actual duration of mitochondrial arrest after synaptic transmission.

and transmission occurred 0.6 times per minute at each synapse (Winnubst et al., 2015). We estimated, therefore, that a 100 µm dendrite receives synaptic inputs at a frequency of approximately 0.36 Hz. Anatomical studies showed a 5-10 times increase of synaptic density in the developing sensory cortex between P5 and P11 (De Felipe J. et al., 1997) and we found here that neuronal activity doubled from the first to the second postnatal week (Figure 2C). Assuming that release probabilities do not change dramatically during this period, synaptic input frequencies should be about 0.02–0.04 Hz at P5. Similarly, we find in *in vivo* patch-clamp and calcium imaging experiments a 16-times increase in synaptic transmission events in dendrites of V1 layer II/III pyramidal cells from P8 to P13 (AH Leighton et al. 2021, personal communication). As Figure 5C shows, an increase in synaptic input frequency in this range would reduce mitochondrial motility by 30 to 60% depending on the actual arrest times at synapses. Since we observed a 70% decrease in mitochondrial motility between the first and second postnatal week, our model showed that temporary immobilization of mitochondrial motility through synaptic signaling can mediate a large proportion of this effect. Together, our data suggest a primary role of synaptic vesicle release, but not action potential firing, in the reduction of mitochondrial motility with

dendrite maturation.

Discussion

Mitochondrial motility and positioning are fundamental for axon and dendrite development and synaptic plasticity (Courchet et al., 2013; Kimura and Murakami, 2014; Fukumitsu et al., 2015; López-Doménech et al., 2016; Vaccaro et al., 2017; Divakaruni et al., 2018). Moreover, mitochondrial dynamics are affected in many neurological disorders (Chen and Chan, 2009; Deheshi et al., 2013; Misgeld and Schwarz, 2017). Thus, regulation of mitochondrial motility is important for neuronal function; however, to what degree neuronal activity determines mitochondrial motility in intact neuronal circuits has been unclear. By directly observing mitochondrial motility and neuronal activity simultaneously in developing dendrites, we provide evidence that synaptic vesicle release, but not postsynaptic action potential firing, constrains mitochondrial motility and stabilizes mitochondria with increasing age.

Imaging neuronal activity and dendritic mitochondria *in vivo* demonstrated a dramatic motility reduction of visual cortex layer II/III pyramidal cells during the second postnatal week. Motility reduction progressed in parallel with a strong increase in overall neuronal activity. Given that dendritic mitochondria in retinal explants and axonal mitochondria in the visual cortex show similar decreases in motility (Chang and Reynolds, 2006; Faits et al., 2016; Lewis et al., 2016; Smit-Rigter et al., 2016), our results confirm a general progression towards more stationary mitochondria in intact tissue.

Since there have been conflicting reports on the regulation of mitochondrial motility by natural activity patterns, we set out to investigate their relationship directly. We found that global calcium transients reflecting back-propagating action potentials were unrelated to changes in mitochondrial motility. Considering that manipulations of neuronal action potential firing did trigger changes in mitochondrial motility in the present study and many studies in cell cultures (Li et al., 2004; Chang et al., 2006; MacAskill et al., 2009; Wang and Schwarz, 2009; but see: Beltran-Parrazal et al., 2006), this finding was surprising at first (but see below).

As global calcium transients appeared to be ineffective, we studied the role of transmission at individual synapses and discovered that the likelihood for a passing mitochondrion to stop at a synapse increased significantly when this synapse was active within two minutes before it arrived. That synaptic activation, but not action potential

firing, arrests mitochondrial motility is in fact consistent with the majority of observations of activity-dependent regulation of mitochondrial motility in hippocampal and cortical neurons (Li et al., 2004; Chang et al., 2006; MacAskill et al., 2009; Wang and Schwarz, 2009). Since activity manipulations, such as depolarizing neurons by increasing extracellular potassium, blocking action potential firing with TTX and electric field stimulation affect both action potential firing and synaptic transmission, it is possible that synaptic release changes, but not firing alone, altered mitochondrial motility in these studies.

How can local synaptic activation stop moving mitochondria when their motility is unaffected by spontaneously occurring global calcium transients? Our observations that pharmacological activation of synaptic vesicle release arrests mitochondria, but that neither spontaneous global activation nor focal glutamate application stops moving mitochondria, suggest that a local factor, either by itself or together with glutamate, mediates mitochondrial arrest. A possible candidate is ATP: it is present in synaptic vesicles and released simultaneously with glutamate at excitatory cortical synapses (Khakh, 2001; Burnstock, 2007; Lalo et al., 2016). ATP receptors of the P2X and P2Y families are expressed in cortical pyramidal cell dendrites (Guzman and Gerevich, 2016), trigger postsynaptic depolarizations (Pankratov et al., 2002) and calcium increases (Lalo et al., 1998; Lalo and Kostyuk, 1998), activate CaMKII (Pougnet et al., 2014) and mediate synaptic plasticity (Pankratov et al., 2009; Lalo et al., 2016). Thus, a local factor co-released with glutamate, such as ATP, is most likely required for mitochondrial arrest at active synapses. A co-released factor could, in principle, provide single synapse specificity by generating or – together with glutamate – boosting a local signal that stops mitochondria at active synapses.

Our analysis of changes in mitochondrial motility in relation to spontaneously occurring synaptic transmission events allowed us to determine the spatio-temporal characteristics of this effect quantitatively. We found that mitochondrial arrest was restricted to a segment of dendrite of roughly 5-10 micrometers distally and proximally from the insertion point of a spine. Mitochondria were stopped when they arrived within two minutes after a synaptic transmission event and remained stationary for one minute on average. Interestingly, several molecular signaling cascades at the synapse have been described that act on very similar scales in time and space. In particular, several small GTPases become activated within less than a minute after single spine stimulation in short stretches of dendrite (5-10 micrometer) and stay active for several minutes (e.g. Ras and RhoA; Harvey et al., 2008; Murakoshi et al., 2011). These and other small GTPases, including DRP-1 and Miro-1, which regulate mitochondrial activity and

motility, are controlled by intracellular calcium rises and CaMKII activation (MacAskill et al., 2009; Wang and Schwarz, 2009; Fukumitsu et al., 2016; Divakaruni et al., 2018). CaMKII expression increases dramatically in the visual cortex during the second postnatal week (© 2008 Allen Institute for Brain Science. Allen Developing Mouse Brain Atlas. Available from: https://developingmouse.brain-map.org/). Therefore, synaptic transmission-induced CaMKII phosphorylation requiring e.g. ATP receptor activation may stop mitochondria more frequently with increasing age by activating small GTPases for a few minutes and several micrometers along the dendrite.

To estimate whether mitochondrial arrest through synaptic activity can explain the progressive demobilization of mitochondria in dendrites during development, we employed a computational model. This model indicates that the estimated increase in synaptic activity from the first to the second postnatal week can reduce mitochondrial motility by 30-60%. These numbers are in line with our *in vivo* observation that blocking synaptic activity with TTX increased mitochondrial motility by 60%. Together, these data show that developmental increases in synaptic activity can explain a large proportion of the motility decrease observed during this period. We speculate that the here described reduction of mitochondrial motility through synaptic activity with increasing age is complemented by a shift in the number of potentially mobile mitochondria towards a pool of stationary mitochondria during development. While for example Miro1 controls temporary mitochondrial arrest, there is no molecular mechanism known for retaining mitochondria permanently at a location in dendrites. Theoretical models suggest that mitochondria are stationary in the absence of Miro1 (MacAskill et al., 2009); however, in Miro1 knockout neurons mitochondrial motility is only mildly affected (Saotome et al., 2008; MacAskill et al., 2009; López-Doménech et al., 2018). Furthermore, to our knowledge a reduction in Miro1 expression or function during development has not been reported. Alternatively, increased tethering of mitochondria may reduce the pool of potentially mobile mitochondria with increasing age. For example, myosin V anchors mitochondria (Pathak et al., 2010), has been proposed to keep mitochondria in a stationary state (Schwarz, 2013; Misgeld and Schwarz, 2017) and is enriched in dendrites (Wang et al., 2008; Konietzny et al., 2019).

The regulation of mitochondrial motility through synaptic activity we describe here may serve developing synapses to efficiently meet their energy demands and calcium handling. In addition, synaptic regulation of mitochondrial trafficking can account to a large degree for the reduction of mitochondrial motility during development and is probably a fundamental process in wiring the developing brain.

Materials and Methods

Plasmids

To investigate the relationship between neuronal activity and mitochondria we used the genetically encoded calcium indicator GCaMP6s (Addgene plasmid 40753; Douglas Kim) in combination with mitochondrial-DsRed (mitochondrial targeting sequence from subunit VIII of human cytochrome c oxidase causing mitochondrial localization as previously described; Rizzuto et al., 1995; Li et al., 2004; MacAskill et al., 2009). These plasmids were cloned into pCAGGS, to enable delivery to neurons via in utero electroporation.

Animals and in utero electroporation

All experimental procedures were approved by the institutional animal care and use committee of the Royal Netherlands Academy of Arts and Sciences. To sparsely deliver the plasmids of interest to pyramidal neurons of layer II/III of the visual cortex, pregnant C57Bl/6J female mice at 16.5 days gestation underwent in utero electroporation surgery. Pregnant females were anesthetized using 3% isoflurane mixed with 1 L/min oxygen and kept under anesthesia with 1.5-2% isoflurane. A midline incision was made and uterine horns were exposed. Plasmid DNA (mitochondrial-DsRed: 0.1 µg/µl, GCaMP6s: 2 µg/µl) was dissolved in 10 mM Tris and 0.05% Fast Green. Approximately 1 µl of this mixture was injected through a pulled capillary pipette in the lateral ventricle of each embryo using a picospritzer (PLI-100, BTX Harvard Apparatus, Holliston, MA). A custom-made square wave isolated pulse generator (voltage of 50 V, 5 pulses, pulse width 50 ms and 150 ms interval) was used for electroporation. After electroporation, the uterine horns were carefully placed back in the abdomen cavity and the abdomen was sutured. During the surgery embryos were kept moist with warm saline and the mothers were kept warm using a euthermic pad. Pregnant females were allowed to recover after Lidocaine ointment was applied on the wound for local analgesia and Metacam (1 mg/kg s.c.) was administered for post-operative analgesia. Once the pups were born, they were checked before postnatal day 2 for expression and targeting of V1.

Organotypic slice cultures

Organotypic slice cultures of transfected visual cortex were prepared as follows: at postnatal day 5 or 8, animals were decapitated quickly, and brains were placed in ice-cold Gey's balanced salt solution under sterile conditions. Coronal slices (400 µm for P5 and 250 µm for P8) were cut using a tissue chopper (McIlwain) and incubated with

serum-containing medium on Millicell culture inserts (Millipore, Merck, New York, NY). Slices were kept in culture for 3 to 7 days before imaging.

Confocal microscopy of organotypic slice cultures

For confocal imaging, slices were excised from their membrane supports and placed in a flow-through chamber. Slices were continuously perfused with heated (35°C) Hank's Balanced Salt Solution (HBSS, Fisher Scientific, Waltham, MA, supplemented with in mM: 4.2 $NaHCO_3$, 2.6 $CaCl_2$, 0.1 Trolox). Slices were imaged on a SP5 Leica confocal microscope with a 63x objective (0.9 NA, Leica, Wetzlar, Germany). For imaging we selected neurons that showed the following characteristics: soma localized in upper layer II, apical dendrite pointing to layer I, low basal GCaMP6s fluorescence as well as long and dim mitochondria. Preference was given to isolated cells, to minimize background fluorescence. Apical dendrites (at least 50 µm from the soma) were imaged using an argon laser at 488 nm and power levels between 0.3 and 1%. Time-lapse image stacks (up to 6 optical sections, 1.2 µm z-spacing), at 0.23 µm per pixel, 350 ms per stack were collected for 350 s, every 10 minutes, for a total of 10 times per cell. We observed no changes in fluorescence intensity, cell activity levels or mitochondrial motility levels with time under these conditions. At the end of the experiment, low magnification image stacks (0.23 µm pixel size and 1 µm z-spacing) were collected to localize the recorded dendrite within the dendritic arborization.

In vivo two-photon microscopy

For *in vivo* imaging, transfected neonatal mice (P5-12) were pre-anesthetized using 3% isoflurane mixed with 1 L/min oxygen and kept under anesthesia with 1-2% isoflurane. A head bar with an opening (Ø 4 mm) was attached to the skull above the visual cortex (0–2 mm rostral from lambda and 0–2 mm lateral from the midline) with superglue (Henkel, Düsseldorf, Germany) and dental cement (Heraeus, Hanau, Germany). A small craniotomy above the visual cortex (approximately 1–2 mm Ø) was performed with a needle and forceps and care was taken not to damage the dura mater. The exposed cortical surface was kept moist with cortex buffer (in mM: 125 NaCl, 5 KCl, 10 glucose, 10 HEPES, 2 $MgSO_4$, 2 $CaCl_2$, pH 7.4). For additional stability, a thin layer of 1.5% high electroendosmosis agarose (Biomol, Hamburg, Germany) was applied to the cortical surface. Before imaging, isoflurane was decreased to 0.8% (under anesthesia condition) or 0% (awake condition). A pulsed titanium sapphire laser (Chameleon Vision II, Coherent, Palo Alto, CA) at 900 nm and power up to 30% was used with a 25x water-immersion objective (1.10 NA, Nikon). Time-lapse image stacks (up to 5 optical sections, 2 µm z-spacing) were obtained at a pixel size of 0.13-0.17 µm and stack rate

of 5 to 10 Hz. Throughout the entire experiment, physiological parameters such as heartbeat and body temperature were monitored, and temperature was controlled using a heating pad.

Pharmacological manipulations

High extracellular potassium *in vitro*: cells were imaged as described above for at least 20 minutes and then the imaging medium was replaced by one supplemented with KCl to a final concentration of 50 mM. After 20 minutes of high potassium incubation and imaging, normal medium was restored and cells were imaged for at least 20 more minutes. Cells did not show dendritic blebbing and in most cells spontaneous activity reappeared, suggesting that they were healthy until the end of the experiment.

To test the role of presynaptic release on mitochondrial motility in dendrites, we imaged the effects of latrotoxin, a synaptic vesicle release stimulator (Deak et al., 2009), on mitochondrial motility and calcium levels in slice cultures during the following conditions sequentially: Baseline, TTX, TTX + LTX, and after LTX washout. TTX was applied (1078, 1 μM, Bio-Techne, Minneapolis, MN) through the bath perfusion. Then LTX (ALX-630-027-C040, 1 nM, Enzo Life Sciences b.v., Farmingdale, NY) was added to the bath and the perfusion was stopped for 10 minutes. Subsequently, perfusion resumed with TTX containing solution.

Focal glutamate application: TTX (1 μM; No. 1078, Bio-Techne, Minneapolis, MN) was applied through the bath perfusion. A glass pipette with a resistance of approximately 4 MΩ containing glutamate (100 μM) in bath solution was inserted into the slice, approximately 50 μm from the dendrite, and glutamate was applied focally with a Picospritzer at 20 psi (PLI-100, BTX Harvard Apparatus, Holliston, MA). Pulse duration was chosen between 1–20 milliseconds to evoke local calcium transients. After placing the glutamate-containing pipette, adjusting the pulse duration and a wait period of at least 10 minutes, 1-3 single pulses were applied during each recording of 350 seconds duration.

To block action potential firing *in vivo*, TTX (2 μM) was prepared in cortex buffer and in agarose. After baseline imaging, the agarose was carefully removed from the top of the brain and the TTX solution in cortex buffer was applied to the surface of the brain for 2 minutes. Then, this cortex buffer was removed and agarose with TTX was applied to the surface of the brain. Imaging continued as previously. This procedure blocked neuronal activity for the entire imaging period, while the pups' physiological parameters did not change.

Image analysis

All images were processed using ImageJ software. Images were filtered using a median filter (radius 1 pixel). Maximal intensity projections of image stacks were generated. All stacks recorded at one dendrite were corrected for motion artefacts due to drift as well as aligned with respect to each other using NoRMCorre (Pnevmatikakis and Giovannucci, 2017).

From the resulting stacks, two-dimensional projections of time (x-axis) versus displacement (y-axis) were generated for individual dendrites to examine spontaneous global calcium transients as well as mitochondrial motility. Global calcium transients appeared as vertical lines, as there was an increase in intracellular calcium levels throughout the entire dendrite. Immotile mitochondria appeared as horizontal lines, and mitochondrial motility as diagonal lines. The percentage of moving mitochondria was calculated as the number of moving mitochondria divided by the total number of present mitochondria, for each second.

For the analysis of local calcium transients, $\Delta F/F_0$ images were calculated where F_0 was the average fluorescence of the first 200 frames without apparent calcium transients of the first recording for each cell. Custom-made Matlab scripts aided the manual identification of synaptic events: signals had to last for more than the duration of two frames, did not spread from other sites and were localized to the spine head.

Statistics

Calcium transients per minute and percent moving mitochondria per one second bins are shown in all Figures where we compare global calcium transient activity or mitochondrial motility across time or different experimental conditions, respectively. Spearman's rank correlation was used to detect correlations across time. For single comparisons t-tests (two-tailed, paired or unpaired) and for multiple comparisons repeated measures ANOVA with posthoc t-tests and Bonferroni multi-measure correction were used. Since for the *in vivo* measurements (Figure 2) the initial percentages of moving mitochondria were very low, the observed effect may be susceptible to discretization. To test whether age and TTX do indeed affect mitochondrial motility *in vivo*, we performed additional analyses. The number of moving and stable mitochondria were counted in 2 minute bins (MacAskill et al., 2009) and then summed across all recordings for both conditions, respectively and the resulting contingency tables (see Source Data Tables) were used to perform Fisher's exact test. We found that the number of observed mitochondria moving was significantly decreased in animals that

were P8 or older compared to younger animals ($p < 0.00001$) and that TTX increased the number of moving mitochondria significantly ($p = 0.0034$). To test whether there is a significant relationship between the occurrence of individual synaptic calcium transients and the arrest of mitochondria we used chi-squared tests and performed a bootstrap analysis as described in the Results section.

Modeling mitochondrial motility modulation by synaptic inputs (MitoMotil)

The model of mitochondrial motility was written with Python 3.6 (Python Software Foundation). First, a population of mitochondria ($n = 500$) was generated where each mitochondrion was initialized with a recovery time drawn from a normal distribution. We ran simulations varying recovery time distribution means over 1-5 minutes ($\sigma = 2.5$ minutes in each condition). All mitochondria were in the motile pool at the beginning of the simulation run. Synaptic transmission events were generated from a homogeneous Poisson process (from the Elephant library, https://elephant.readthedocs.io/en/latest/) with synaptic input frequencies ranging from 0.001-0.5 Hz. We ran each simulation for 1500 seconds to allow the percentage of immobile mitochondria to reach steady state. Each synaptic transmission event immobilized a variable number of mitochondria randomly selected from the total pool. The proportion of affected mitochondria was drawn from a normal distribution ($\mu = 0.05$, $\sigma = 0.01$). These values were based on our observation that single synaptic transmission events affected approximately 5-10 µm of a 100 µm stretch of dendrite. This variable proportion of affected mitochondria was used to calculate the number of mitochondria from the population for immobilization. Affected mitochondria remained immobilized for the duration of the recovery time variable with which they were initialized. If a mitochondrion was already immobilized and selected from the total pool for immobilization by a subsequent event, the immobilization time was extended by the second event.

Author contributions

CAPS and CL designed the experiments.

CAPS, VB, MvZ and CL performed experiments.

AC made the computational model.

CAPS, MV, and CL wrote the paper.

CL is corresponding author.

Affiliations

CAPS, VB, MvZ, and CL: Department of Synapse and Network Development, Netherlands Institute for Neuroscience, The Netherlands.

MV and CL: Department of Functional Genomics, Center for Neurogenomics and Cognitive Research, VU University Amsterdam, the Netherlands.

AC: Department of Biological Sciences, University of Toronto Scarborough, Toronto, ON1C1A4, Canada.

Competing interests

The authors declare no competing interests.

Acknowledgements

We thank Ginny Farias, Koen Kole, Thomas Misgeld, and Rajeev Rajendran for critically reading the manuscript. Johan Winnubst, Juliette Cheyne, and Alexandra Leighton for custom-made Matlab scripts and Matthew Self for advice on statistics. Thomas Misgeld for the original mitochondrial-DsRed plasmid, and Christiaan Levelt for the pCAGGS construct. In addition, we thank Christiaan Levelt for teaching us the in utero electroporation surgery.

References

Beltran-Parrazal L, López-Valdés HE, Brennan KC, Díaz-Muñoz M, de Vellis J, Charles AC (2006) Mitochondrial transport in processes of cortical neurons is independent of intracellular calcium. Am J Physiol Cell Physiol 291:C1193-1197.

Burnstock G (2007) Physiology and pathophysiology of purinergic neurotransmission. Physiol Rev 87:659–797.

Chang DTW, Honick AS, Reynolds IJ (2006) Mitochondrial trafficking to synapses in cultured primary cortical neurons. J Neurosci 26:7035–7045.

Chang DTW, Reynolds IJ (2006) Differences in mitochondrial movement and morphology in young and mature primary cortical neurons in culture. Neuroscience 141:727–736.

Chen H, Chan DC (2009) Mitochondrial dynamics--fusion, fission, movement, and mitophagy--in neurodegenerative diseases. Hum Mol Genet 18:R169-176.

Courchet J, Lewis TL, Lee S, Courchet V, Liou D-Y, Aizawa S, Polleux F (2013) Terminal Axon Branching Is Regulated by the LKB1-NUAK1 Kinase Pathway via Presynaptic Mitochondrial Capture. Cell 153:1510–1525.

De Felipe J., Marco P, Fairen A, Jones EG (1997) Inhibitory synaptogenesis in mouse somatosensory cortex. Cereb Cortex 7:619–634.

Deak F, Liu X, Khvotchev M, Li G, Kavalali ET, Sugita S, Sudhof TC (2009) {alpha}-Latrotoxin Stimulates a Novel Pathway of Ca2+-Dependent Synaptic Exocytosis Independent of the Classical Synaptic Fusion Machinery. J Neurosci 29:8639–8648.

Deheshi S, Pasqualotto BA, Rintoul GL (2013) Mitochondrial trafficking in neuropsychiatric diseases. Neurobiol Dis 51:66–71.

Divakaruni SS, Van Dyke AM, Chandra R, LeGates TA, Contreras M, Dharmasri PA, Higgs HN, Lobo MK, Thompson SM, Blanpied TA (2018) Long-Term Potentiation Requires a Rapid Burst of Dendritic Mitochondrial Fission during Induction. Neuron 100:860-875.e7.

Faits MC, Zhang C, Soto F, Kerschensteiner D (2016) Dendritic mitochondria reach stable positions during circuit development. eLife 5.

Fukumitsu K, Fujishima K, Yoshimura A, Wu YK, Heuser J, Kengaku M (2015) Synergistic Action of Dendritic Mitochondria and Creatine Kinase Maintains ATP Homeostasis and Actin Dynamics in Growing Neuronal Dendrites. J Neurosci 35:5707–5723.

Fukumitsu K, Hatsukano T, Yoshimura A, Heuser J, Fujishima K, Kengaku M (2016) Mitochondrial fission protein Drp1 regulates mitochondrial transport and dendritic arborization in cerebellar Purkinje cells. Mol Cell Neurosci 71:56–65.

Guzman SJ, Gerevich Z (2016) P2Y Receptors in Synaptic Transmission and Plasticity: Therapeutic Potential in Cognitive Dysfunction. Neural Plast 2016:e1207393.

Harris JJ, Jolivet R, Attwell D (2012) Synaptic energy use and supply. Neuron 75:762–777.

Harvey CD, Yasuda R, Zhong H, Svoboda K (2008) The Spread of Ras Activity Triggered by Activation of a Single Dendritic Spine. Science 321:136–140.

Katz LC, Shatz CJ (1996) Synaptic activity and the construction of cortical circuits. Science 274:1133–1138.

Khakh BS (2001) Molecular physiology of P2X receptors and ATP signalling at synapses. Nat Rev Neurosci 2:165–174.

Kilb W, Kirischuk S, Luhmann HJ (2011) Electrical activity patterns and the functional maturation of the neocortex. Eur J Neurosci 34:1677–1686.

Kimura T, Murakami F (2014) Evidence that dendritic mitochondria negatively regulate dendritic branching in pyramidal neurons in the neocortex. J Neurosci 34:6938–6951.

Kirkby LA, Sack GS, Firl A, Feller MB (2013) A Role for Correlated Spontaneous Activity in the Assembly of Neural Circuits. Neuron 80:1129–1144.

Kleindienst T, Winnubst J, Roth-Alpermann C, Bonhoeffer T, Lohmann C (2011) Activity-dependent clustering of functional synaptic inputs on developing hippocampal dendrites. Neuron 72:1012–1024.

Konietzny A, González-Gallego J, Bär J, Perez-Alvarez A, Drakew A, Demmers JAA, Dekkers DHW, Hammer JA, Frotscher M, Oertner TG, Wagner W, Kneussel M, Mikhaylova M (2019) Myosin V regulates synaptopodin clustering and localization in the dendrites of hippocampal neurons. J Cell Sci 132:3790–3798.

Lalo U, Kostyuk P (1998) Developmental changes in purinergic calcium signalling in rat neocortical neurones. Brain Res Dev Brain Res 111:43–50.

Lalo U, Palygin O, Verkhratsky A, Grant SGN, Pankratov Y (2016) ATP from synaptic terminals and astrocytes regulates NMDA receptors and synaptic plasticity through PSD-95 multi-protein complex. Sci Rep 6:33609.

Lalo U, Voitenko N, Kostyuk P (1998) Iono- and metabotropically induced purinergic calcium signalling in rat neocortical neurons. Brain Res 799:285–291.

Leighton AH, Lohmann C (2016) The Wiring of Developing Sensory Circuits-From Patterned Spontaneous Activity to Synaptic Plasticity Mechanisms. Front Neural Circuits 10:71.

Lewis TL, Turi GF, Kwon S-K, Losonczy A, Polleux F (2016) Progressive Decrease of Mitochondrial Motility during Maturation of Cortical Axons *In vitro* and *In vivo*. Curr Biol 26:2602–2608.

Li Z, Okamoto K, Hayashi Y, Sheng M (2004) The importance of dendritic mitochondria in the morphogenesis and plasticity of spines and synapses. Cell 119:873–887.

López-Doménech G, Covill-Cooke C, Ivankovic D, Halff EF, Sheehan DF, Norkett R, Birsa N, Kittler JT (2018) Miro proteins coordinate microtubule- and actin-dependent mitochondrial transport and distribution. EMBO J 37:321–336.

López-Doménech G, Higgs NF, Vaccaro V, Roš H, Arancibia-Cárcamo IL, MacAskill AF, Kittler JT (2016) Loss of Dendritic Complexity Precedes Neurodegeneration in a Mouse Model with Disrupted Mitochondrial Distribution in Mature Dendrites. Cell Rep 17:317–327.

MacAskill AF, Rinholm JE, Twelvetrees AE, Arancibia-Carcamo IL, Muir J, Fransson A, Aspenstrom P, Attwell D, Kittler JT (2009) Miro1 is a calcium sensor for glutamate receptor-dependent localization of mitochondria at synapses. Neuron 61:541–555.

Matteoli M, Haimann C, Torri-Tarelli F, Polak JM, Ceccarelli B, Camilli PD (1988) Differential effect of alpha-latrotoxin on exocytosis from small synaptic vesicles and from large dense-core vesicles containing calcitonin gene-related peptide at the frog neuromuscular junction. Proc Natl Acad Sci 85:7366–7370.

Misgeld T, Kerschensteiner M, Bareyre FM, Burgess RW, Lichtman JW (2007) Imaging axonal transport of mitochondria *in vivo*. Nat Meth 4:559–561.

Misgeld T, Schwarz TL (2017) Mitostasis in Neurons: Maintaining Mitochondria in an Extended Cellular Architecture. Neuron 96:651–666.

Morrow EM, Furukawa T, Raviola E, Cepko CL (2005) Synaptogenesis and outer segment formation are perturbed in the neural retina of Crx mutant mice. BMC Neurosci 6:5.

Murakoshi H, Wang H, Yasuda R (2011) Local, persistent activation of Rho GTPases during plasticity of single dendritic spines. Nature 472:100–104.

Niculescu D, Michaelsen-Preusse K, Güner Ü, Dorland R van, Wierenga CJ, Lohmann C (2018) A BDNF-mediated push-pull plasticity mechanism for synaptic clustering. Cell Rep 24:2063–2074.

Pankratov Y, Lalo U, Krishtal O, Verkhratsky A (2002) Ionotropic P2X purinoreceptors mediate synaptic transmission in rat pyramidal neurones of layer II/III of somato-sensory cortex. J Physiol 542:529–536.

Pankratov Y, Lalo U, Krishtal OA, Verkhratsky A (2009) P2X receptors and synaptic plasticity. Neuroscience 158:137–148.

Pathak D, Sepp KJ, Hollenbeck PJ (2010) Evidence that myosin activity opposes microtubule-based axonal transport of mitochondria. J Neurosci 30:8984–8992.

Plucińska G, Misgeld T (2016) Imaging of neuronal mitochondria in situ. Curr Opin Neurobiol 39:152–163.

Pnevmatikakis EA, Giovannucci A (2017) NoRMCorre: An online algorithm for piecewise rigid motion correction of calcium imaging data. J Neurosci Methods 291:83–94.

Pougnet J-T, Toulme E, Martinez A, Choquet D, Hosy E, Boué-Grabot E (2014) ATP P2X receptors downregulate AMPA receptor trafficking and postsynaptic efficacy in hippocampal neurons. Neuron 83:417–430.

Rintoul GL, Filiano AJ, Brocard JB, Kress GJ, Reynolds IJ (2003) Glutamate Decreases Mitochondrial Size and Movement in Primary Forebrain Neurons. J Neurosci 23:7881–7888.

Rizzuto R, Brini M, Pizzo P, Murgia M, Pozzan T (1995) Chimeric green fluorescent protein as a tool for visualizing subcellular organelles in living cells. Curr Biol CB 5:635–642.

Rochefort NL, Garaschuk O, Milos RI, Narushima M, Marandi N, Pichler B, Kovalchuk Y, Konnerth A (2009) Sparsification of neuronal activity in the visual cortex at eye-opening. Proc Natl Acad Sci 106:15049–15054.

Sanes JR, Yamagata M (2009) Many paths to synaptic specificity. Annu Cell DevBiol 25:161–195.

Saotome M, Safiulina D, Szabadkai G, Das S, Fransson A, Aspenstrom P, Rizzuto R, Hajnoczky G (2008) Bidirectional Ca2+-dependent control of mitochondrial dynamics by the Miro GTPase. Proc Natl Acad Sci 105:20728–20733.

Schwarz TL (2013) Mitochondrial Trafficking in Neurons. Cold Spring Harb Perspect Biol 5:a011304.

Sengpiel F, Kind PC (2002) The role of activity in development of the visual system. CurrBiol 12:R818–R826.

Sheng ZH, Cai Q (2012) Mitochondrial transport in neurons: impact on synaptic homeostasis and neurodegeneration. Nat Rev Neurosci 13:77–93.

Smit-Rigter L, Rajendran R, Silva CAP, Spierenburg L, Groeneweg F, Ruimschotel EM, van Versendaal D, van der Togt C, Eysel UT, Heimel JA, Lohmann C, Levelt CN (2016)

Mitochondrial dynamics in visual cortex are limited *In vivo* and not affected by axonal structural plasticity. Curr Biol 26:2609–2616.

Südhof TC (2001) alpha-Latrotoxin and its receptors: neurexins and CIRL/latrophilins. Annu Rev Neurosci 24:933–962.

Tran NM, Zhang A, Zhang X, Huecker JB, Hennig AK, Chen S (2014) Mechanistically Distinct Mouse Models for CRX-Associated Retinopathy. PLOS Genet 10:e1004111.

Vaccaro V, Devine MJ, Higgs NF, Kittler JT (2017) Miro1-dependent mitochondrial positioning drives the rescaling of presynaptic Ca2+ signals during homeostatic plasticity. EMBO Rep 18:231–240.

Valtorta F, Madeddu L, Meldolesi J, Ceccarelli B (1984) Specific localization of the alpha-latrotoxin receptor in the nerve terminal plasma membrane. J Cell Biol 99:124–132.

Wang X, Schwarz TL (2009) The mechanism of Ca2+ -dependent regulation of kinesin-mediated mitochondrial motility. Cell 136:163–174.

Wang Z, Edwards JG, Riley N, Provance DW, Karcher R, Li X dong, Davison IG, Ikebe M, Mercer JA, Kauer JA, Ehlers MD (2008) Myosin Vb Mobilizes Recycling Endosomes and AMPA Receptors for Postsynaptic Plasticity. Cell 135:535–548.

Winnubst J, Cheyne JE, Niculescu D, Lohmann C (2015) Spontaneous activity drives local synaptic plasticity *in vivo*. Neuron 87:399–410.

Chapter 4

The relationship between calcium transients and mitochondrial distribution in developing cortical dendrites

Cátia A. P. Silva, Victoria Busch, Mike van Zwieten and Christian Lohmann

CAPS contribution: designed and performed experiments, wrote the manuscript.

List of figures

Abstract

Young neurons are highly dynamic, repeatedly establishing and eliminating synaptic contacts to ensure that only the correct ones are maintained. This process is highly energy demanding and requires spontaneous neuronal activity. Mitochondria are the main energy providing organelles in neurons, and their distribution and motility have been shown to be modulated by neuronal activity. Here, we investigated the relationship between neuronal activity, both global and local, and mitochondrial presence and motility, in the primary visual cortex of young mice. During the first two postnatal weeks, mitochondrial motility is unaffected by global calcium transients that were manipulated within the physiological range both *in vivo* and in slice cultures. Dendritic mitochondria are not more likely to stabilize near functionally identified synapses. However, stable mitochondria do co-localize with spontaneous local calcium transients in the dendritic shaft, which are likely to have a synaptic origin. Mitochondria-mediated provision of energy may therefore play an important role in the fine-tuning of developing networks.

Introduction

Mice open their eyes approximately two weeks after birth, so there is a lack of sensory input to the visual cortex during this time. Despite of this, the visual cortex is highly active due to spontaneous activity of cortical neurons. Spontaneous activity is crucial for fine-tuning neuronal connectivity, for example by strengthening synapses between neurons that fire synchronously, while weakening others (Kleindienst et al., 2011). This process prepares the brain for proper processing of visual inputs once the eyes open.

The development of synapses and synaptic transmission are highly energy-demanding processes. Mitochondria are the main energy providers in neurons (Harris et al., 2012). They are initially generated at the soma and transported to distal parts of neurons via the cytoskeleton (Sheng and Cai, 2012). This motility is thought to allow for energy provision at high-energy demanding sites, such as synapses. Thus, it seems likely that proper mitochondrial distribution is crucial in young neurons and that it is modulated by spontaneous activity. Indeed, previous research has shown that there is a link between neuronal activity and the resulting calcium influx, and mitochondrial distribution. However, the details of this relationship are not yet clear, thus requiring further investigation.

We previously studied spontaneous activity in developing dendrites in relation to mitochondrial motility. We studied spontaneous activity in two forms: (first) global, resulting from back-propagating action potentials; and (second) local, from synaptic activity. First (with global activity), we observed that with postnatal development, the frequency of spontaneous global activity increased, while mitochondrial motility decreased (Silva et al., 2021). However, spontaneous global activity did not seem to directly affect mitochondrial motility (Silva et al., 2021). Second (with local activity), we showed (with latrotoxin) that local activity in young spines can stop dendritic mitochondria, which is likely to be contributing to the decrease in mitochondrial motility observed over development (Silva et al., 2021). Here we further investigated these relationships. First, we asked whether manipulating global activity within the physiological range would alter mitochondrial motility. We found mitochondrial motility to be unaffected by global calcium transients both *in vivo* (manipulated with anesthesia) and in cultured slices (with electrical stimulation). Second, we asked whether mitochondria stabilize closer to synapses. We did not find stable mitochondria to be preferably located near functionally identified synapses (active spines). However, stable mitochondria did preferentially co-localize with spontaneous local calcium transients in the dendritic shaft, which are likely to have a synaptic origin.

Altogether, this study further builds on the body of knowledge supporting a strong relationship between mitochondrial distribution and local (synaptic) calcium activity.

Results

Here we further investigate the details of the relationship between spontaneous neuronal activity and mitochondrial distribution. We used in utero electroporation at embryonic day (E) 16.5 to express GCaMP6s (a genetically encoded calcium indicator) and mitochondrial-DsRed in pyramidal neurons of layer II/III of the primary visual cortex (V1). This enabled the imaging of mitochondrial dynamics and neuronal activity (as global or local calcium transients), *in vivo* and in cortical slice cultures (Figure 1).

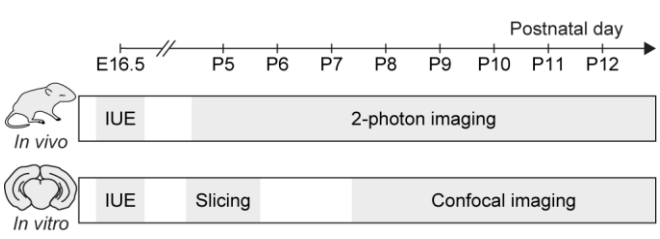

Figure 1. Experimental timeline. In utero electroporation (IUE) at embryonic day (E) 16.5 enables delivery of GCaMP6s and mitochondrial-DsRed to layer II/III pyramidal neurons of the visual cortex, to then perform 2-photon dendritic imaging *in vivo* (between postnatal 5 and 12), and confocal imaging in slice cultures (obtained at P5, and kept for 3- 7 days *in vitro*).

We first investigated the relationship between postnatal day (P), global spontaneous activity levels, and mitochondrial motility. We showed previously that with developmental age (P5 until P12), the frequency of global spontaneous activity increases while mitochondrial motility decreases (Silva et al., 2021). To disentangle whether developmental age or frequency of global activity was the main event leading to decreased mitochondrial motility, we manipulated spontaneous activity levels of pups to match that of older or younger animals. We decreased the frequency of activity *in vivo* using isoflurane anesthesia, taking advantage of the fact that spontaneous activity is reduced in isoflurane anesthetized animals (Siegel et al., 2012). We compared individual animals (n = 8, P5 - 12) under 0.8 % isoflurane anesthesia (Iso), and one hour after they woke up from it (0 % isoflurane, Awake). In both conditions, we observed spontaneously occurring global calcium transients and mitochondrial motility. As expected, the frequency of spontaneous calcium transients increased significantly after waking up (Figure 2A). Mitochondrial motility, however, did not change (Figure 2B). To control for the duration of the experiment, i.e. to check whether spontaneous activity would naturally change with time, we compared animals that remained under 0.8 % isoflurane for similar durations (n = 8 animals, P5 – 12, data in Chapter 3, Figure 2, Figure Supplement 1). These showed no differences in either frequency of spontaneous global calcium transients (Figure 2C), nor mitochondrial motility (Figure 2D).

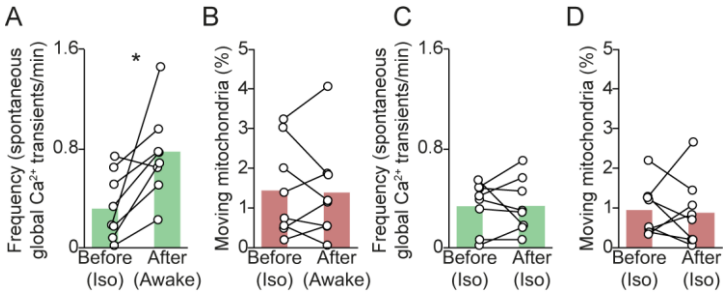

Figure 2. Increased global neuronal activity does not affect mitochondrial motility *in vivo*.
A: The frequency of spontaneous global calcium transients increased from under 0.8 % isoflurane anesthesia (Before, Iso) to 0 % isoflurane anesthesia or awake state (After, Awake; n = 8 animals, P5 - P12, 0.32 ± 0.1 vs 0.78 ± 013, paired t-test p = 0.02).
B: The percentage of moving mitochondria did not change from under 0.8 % isoflurane anesthesia to awake state (1.45 ± 0.43 vs 1.40 ± 0.45, paired t-test p = 0.87).
C: The frequency of spontaneous global calcium transients under 0.8 % isoflurane anesthesia in times comparable with Iso vs Awake did not change (Before vs After, n = 8 animals, P5 – P12, 0.33 ± 0.07 vs 0.34 ± 0.08, paired t-test p = 0.49).
D: The percentage of moving mitochondria under 0.8 % isoflurane anesthesia in times comparable with Iso vs Awake did not change (0.96 ± 0.24 vs 0.88 ± 0.32, paired t-test p = 0.41)

Next, we investigated whether we could separate age from frequency of spontaneous global activations in slice cultures. We previously investigated how spontaneous activity

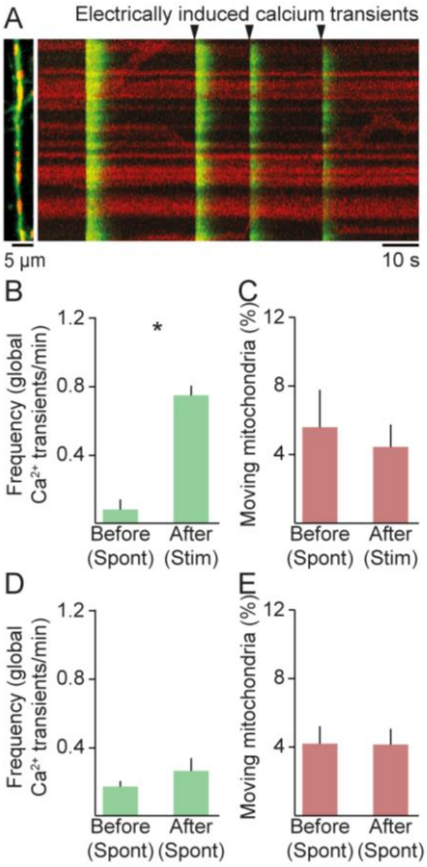

Figure 3. Increased global neuronal activity does not affect mitochondrial motility *in vitro*.
A: Example dendrite and corresponding two-dimensional representation of time versus displacement, showing a spontaneously occurring global calcium transient and three electrically induced global calcium transients (arrowheads), as well as stopped and moving mitochondria.
B: Electrical stimulation significantly increased the frequency of global calcium transients (Before (Spont) vs After (Stim), 0.08 ± 0.06 vs 0.75 ± 0.06 transients/min, paired t-test p = 0.0003).
C: Electrical stimulation did not affect the percentage of moving mitochondria (Spont vs Stim, 5.60 ± 2.25 vs 4.33 ± 1.30 %, paired t-test p = 0.31).
D: Unstimulated cells in comparable time-lapse imaging showed unchanged frequency of spontaneous global calcium transients (0.17 ± 0.03 vs 0.27 ± 0.07, paired t-test p = 0.14).
E: Unstimulated cells in comparable time-lapse imaging showed unchanged percentage of moving mitochondria (4.21 ± 1.02 vs 4.16 ± 0.92, paired t-test p = 0.48).

and mitochondrial motility differed in dendrites in slices obtained from P5 and P8 mice (Silva et al., 2021). Similar to the situation *in vivo*, the frequency of spontaneous global

calcium transients tended to increase with age (P5 vs P8, 0.21 ± 0.04 vs 0.45 ± 0.23 transients/ min, Student's t-test p = 0.37) while mitochondrial motility decreased (P5 vs P8, 4.21 ± 0.85 vs 1.69 ± 0.56 % moving mitochondria, Student's t-test p = 0.02) (data in Chapter 3, Figure 3). To study whether mitochondrial motility decreased due to the increase of global calcium transients, we increased the latter's frequency by electrical stimulation in slices obtained from P5 to match the levels at P8. We then assessed whether mitochondrial motility decreased accordingly. Electrical stimulation was performed by inserting a glass electrode into the slice and verifying that we could reliably induce global calcium transients (n = 5 cells, Figure 3A).

Electrical stimulation successfully increased the frequency of global calcium transients in P5 slices (Figure 3B), which matched the frequency observed in P8 cells (P8 data in Chapter 3, Figure 3; Stim P5 vs P8, 0.5 ± 0.05 vs 0.45 ± 0.23 transients/ min, Student's t-test p = 0.83). In line with our *in vivo* observations, the change in frequency did not affect mitochondrial motility (Figure 3C), which remained comparable to unstimulated P5 slices (P5 data in Chapter 3, Figure 3; Stim P5 vs P5, 3.94 ± 1.30 vs 4.21 ± 0.85 % moving mitochondria, Student's t-test p = 0.8). To control for the duration of the experiment, i.e. to check whether spontaneous activity would naturally change with time, we analyzed unstimulated P5 cells over comparable

durations (P5 data in Chapter 3, Figure 3; n = 15 cells). These unstimulated cells showed no differences in either frequency of spontaneous global calcium transients (Figure 3D), nor mitochondrial motility (Figure 3E).

So far, we could not detect an effect of global activity - either spontaneous or artificially manipulated within the physiological range - on mitochondrial motility, both *in vivo* and *in vitro*. This is in line with our previous results (Silva et al., 2021) and supports the hypothesis that the decrease in mitochondrial motility occurring with developmental age is not caused by the observed increase in the frequency of global spontaneous activity that happens around the same time.

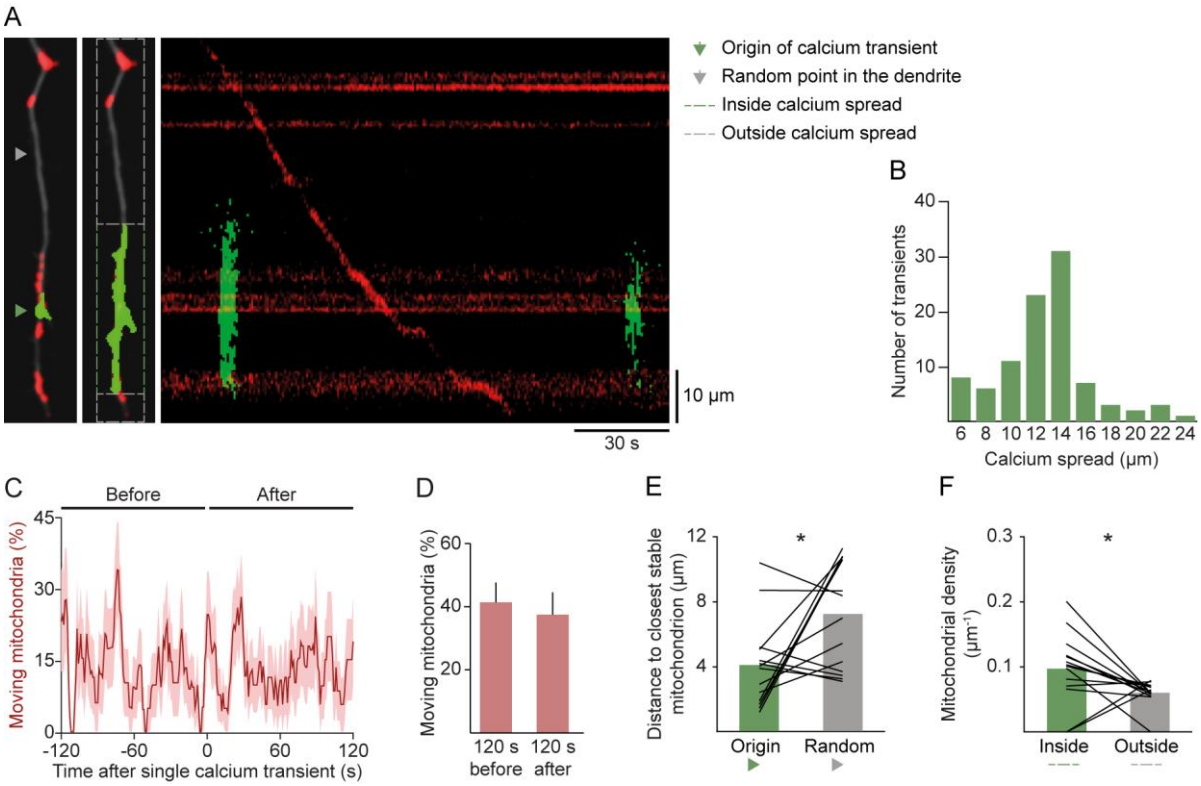

Figure 4. Spontaneous local calcium transients in the dendritic shaft spatially relate to stable mitochondria.
A: Example dendrite and corresponding two-dimensional projection of time-lapse imaging, showing spontaneously occurring local calcium transients in the dendritic shaft. Typically, these transients repeatedly originate at a location (left: origin labelled with green arrowhead), and spread antero- and retrogradely (middle: green dashed line delineates maximum calcium spread).
B: Distribution of the calcium spread of these spontaneous local calcium transients.
C: Mean mitochondrial motility time-locked to the onset of single local calcium transients in the dendritic shaft.
D: Quantification of C. The percentage of moving mitochondria did not change significantly between the 2 minutes before and after spontaneous local calcium transients in the dendritic shaft (n = 95 transients, paired t-test p = 0.37).
E: The origin of spontaneous local calcium transients in the shaft is closer to the closest stable mitochondrion than a random point on the dendrite (n = 14 origins, paired t-test p = 0.02).
F: The density of mitochondria is higher within the calcium spread than outside of it (n = 14 origins, paired t-test p = 0.04).

Conversely, we previously reported that spontaneous activity restricted to spines, i.e. local spontaneous activity, temporarily stops mitochondria in their vicinities (Silva et al., 2021). Thus, we then investigated whether another type of local activity, which occurs in the dendritic shaft, would affect mitochondrial motility. In four cells, we observed spontaneously occurring local calcium transients in the dendritic shaft (typically called dendritic spikes), probably mediated by synapses lacking the morphological distinction of spines (Figure 4A) (Hausser et al., 2000). On each dendrite, these transients often started in the same location, which we named "origin" (11 origins, Figure 4A, green arrowhead). Transients spread within the dendrite (95 transients, Figure 4A, green traced line) and were 11.79 µm wide on average (Figure 4B). Spreading occurred in both antero- and retrograde directions. Mitochondrial motility did not change between the two minutes before and after single local calcium transients in the dendritic shaft (Figure 4C-D).

Given that with this local activity in the dendritic shaft we observed areas with high (Figure 4A, inside calcium spread) and low (Figure 4A, outside calcium spread) calcium in the same stretch of dendrite, we investigated the differential density of stable mitochondria. We hypothesized that stable mitochondria preferably localize closer to or within the calcium spread. We found that the origin of these transients was on average closer to stable mitochondria than a random point outside of the calcium spread (Figure 4E, legend in Figure 4A). We also found more stable mitochondria within the calcium spread than outside of it (Figure 4F, legend in Figure 4A). We conclude that these transients (spontaneous local activity in the dendritic shaft) do not affect nearby moving mitochondria, as there were no changes in mitochondrial motility after these transients. However, these calcium transients seem spatially related to stable mitochondria, as they often co-localize.

As spontaneous local transients in the shaft are closer to stable mitochondria, and we previously described that spontaneous activity in spines precedes mitochondrial motility arrest, we then asked whether active spines are closer to stable mitochondria. We studied nine cells that exhibited spontaneous local calcium transients in spines (Figure 5A, dashed box, data in Chapter 3, Figure 4). We checked whether the distance to the closest stable mitochondrion was shorter for active spines, when compared to inactive ones, but that was not the case (Figure 5B). We noticed spines exhibited different morphologies and often changed their morphological appearance throughout the imaging period (Figure 5C). We wondered whether these characteristics would be related to the distance to stable mitochondria. To analyze this, we first divided spines based on differences of structural plasticity throughout the imaging period: stable (did

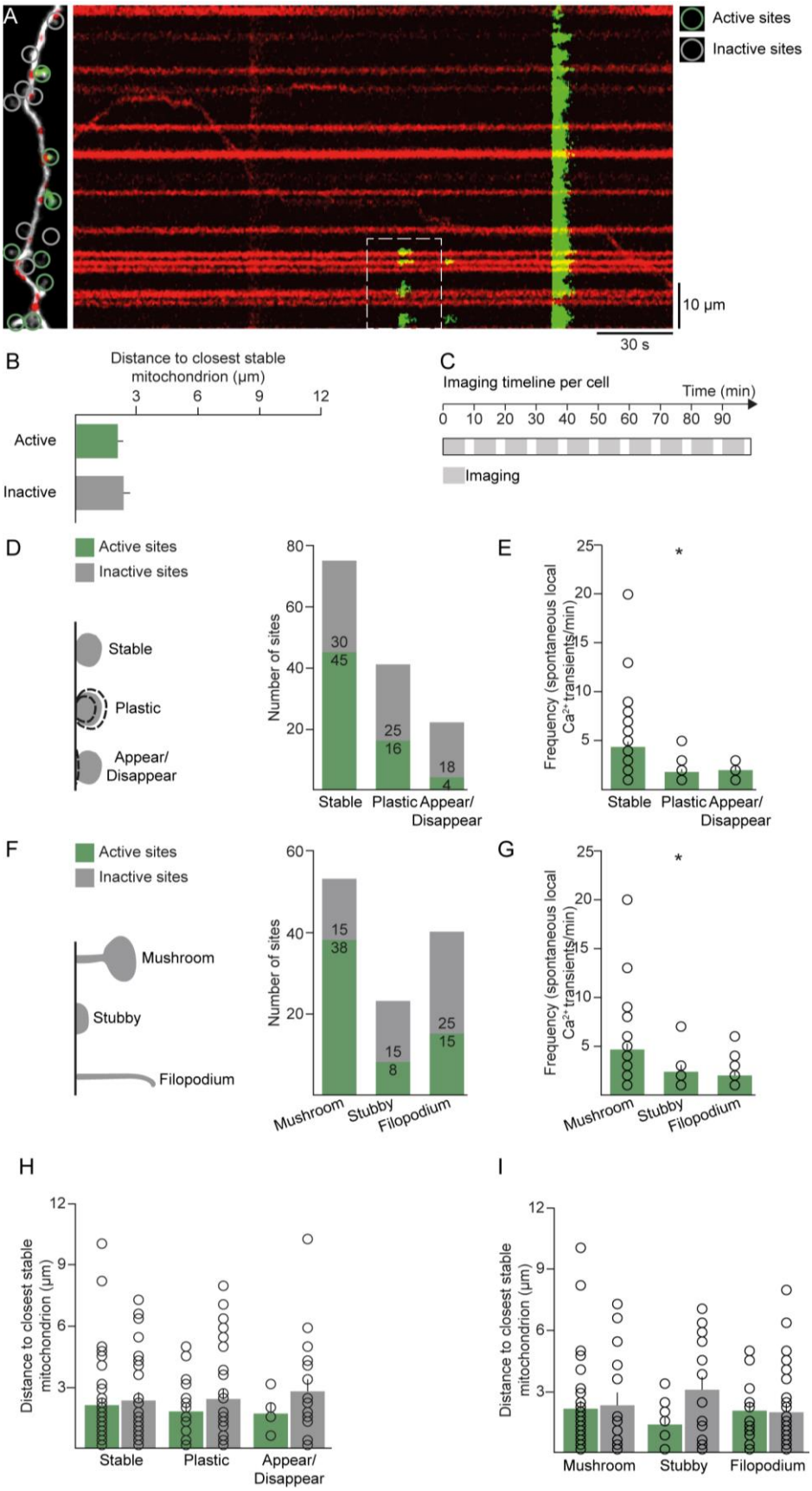

Figure 5. Functionally identified synapses in spines do not spatially relate to stable mitochondria.
A: Example dendrite and corresponding two-dimensional projection of time-lapse imaging, showing spontaneously occurring local calcium transients in spines.
B: Distance to the closest stable mitochondrion is not different between active and inactive

spines (Active vs Inactive, 2.02 ± 0.27 vs 2.37 ± 0.31 µm, Student's t-test p = 0.40).
C: Timeline of imaging: approximately 6 minute-time-lapse images every 10 minutes, for a total of 10 time-lapse images.
D-E: Spines were divided according to structural plasticity: stable, plastic, appear/ disappearing. Stable sites were the most active, and with the highest frequency of spontaneous local calcium transients (Stable vs Plastic vs (Dis)appear, 4.38 ± 0.55 vs 1.81 ± 0.29 vs 2.00 ± 0.41, Kruskal-Wallis test p = 0.004).
F-G: Stable and plastic spines were divided according to morphology: mushroom-, stubby-, and filopodium-like. Mushroom-like sites were the most active, and with the highest frequency of spontaneous local calcium transients (Mushroom vs Stubby vs Filopodium, 4.66 ± 0.62 vs 2.38 ± 0.71 vs 2.00 ± 0.38, Kruskal-Wallis test p = 0.005).
H: The distance to the closest stable mitochondrion did not vary with structural plasticity (Mann-Whitney test, p = 0.18).
I: The distance to the closest stable mitochondrion did not vary with morphology (Mann-Whitney test, p = 0.64).

not change morphology), plastic (changed morphology), and appear/ disappearing (not always present) (Figure 5D). Most spines were stable, and stable spines showed a higher frequency of spontaneous local calcium transients (Figure 5D-E). Second, we subdivided spines that were present throughout the entire imaging period based on their different morphology: mushroom- (head and neck), stubby- (head, without clear neck) and filopodium-like (long and thin neck without head) (Figure 5F). Most spines were mushroom-like, and these also showed a higher frequency of spontaneous local calcium transients (Figure 5F-G).We did not find a spatial relationship between stable mitochondria, and the different states of plasticity of spines (Figure 5H), nor the different morphological categories of spines (Figure 5I). Therefore, we have no evidence to suggest that mitochondria preferably stabilize around active spines.

Discussion

In line with our previous study, we do not find a relationship between global neuronal activity and mitochondria (Silva et al., 2021). We do find a spatial relationship between spontaneous local activity in the dendritic shaft and stable mitochondria. Finally, we do not have enough evidence to suggest that mitochondria stabilize around synapses.

Previous studies have consistently shown that (1) artificially enhanced global neuronal activity (by activating NMDA receptors) decreases mitochondrial motility (Ashby et al., 2006; Chang et al., 2006a; Faits et al., 2016; Li et al., 2004a; MacAskill et al., 2009a), and (2) spontaneously occurring global neuronal activity does not affect mitochondrial motility (Faits et al., 2016; Silva et al., 2021). Here, we aimed to find the boundary between these extremes, i.e. to find where, in the range between a spontaneous global calcium transient and a massive potassium-induced calcium transient, calcium

transients start affecting mitochondrial motility (Figure 6A). We altered the frequency of global calcium transients within the physiological range, both *in vivo* and in cultured slices, and found that it did not affect mitochondrial motility. We conclude that global calcium transients, resulting from back-propagating action potentials, do not regulate mitochondrial motility during brain development. Thus, there are two contrasting phenomena: artificial manipulations of activity affect mitochondrial motility, while spontaneous activity does not. A unifying theory between the two might include synaptic activity as the main reason for mitochondrial motility arrest (Figure 6B). Artificial manipulations of activity inevitably affect synaptic activity, which in turn promptly affects mitochondrial motility. In contrast, spontaneously occurring neuronal activity probably does not lead to such an increase in synaptic activity that would affect mitochondrial motility. Over development, however, we observe an increase in frequency of spontaneous global calcium transients and a concomitant mitochondrial motility decrease, without the first directly affecting the second. This could be explained by the gradual increase in synaptic density (De Felipe J. et al., 1997) and activity (Rochefort et al., 2009) over development, which progressively affects mitochondrial motility.

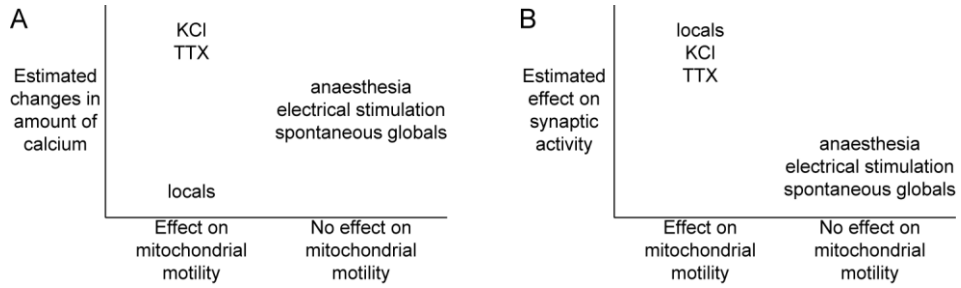

Figure 6. Visual representation of the relationship between different activity manipulations and their effect (or lack thereof) on mitochondrial motility.A. Mitochondrial motility changes do not seem to exclusively relate to activity manipulations that lead to big changes in calcium.
B. Mitochondrial motility changes seem to relate to activity manipulations that lead to big changes in synaptic activity.

We then studied spontaneous activity at the synaptic level as spontaneously occurring local calcium transients. In cortical slice cultures, we observed two types of spontaneous local activity: in spines and in the shaft. We can confidently say that spines with spontaneous calcium transients are synapses (Kleindienst et al., 2011). Similarly, we are confident that the observed spontaneous calcium transients in the shaft are synaptically driven, as they reappeared at the same location in each dendrite, suggesting an underlying regulator from which they originate. Moreover, they look similar to synaptically triggered dendritic spikes that have been previously described (Hausser et al., 2000, personal communication by D. Dombeck).

We previously showed that mitochondria stop after spontaneous local calcium transients in spines (Silva et al., 2021). Here we did not find mitochondria to stop after spontaneous local calcium transients in the shaft. The main difference we observe is the direct contact of calcium with mitochondria. In spines, the calcium rise is restricted to the head of the spine, while mitochondrial motility occurs at the shaft. We have speculated the mechanism by which spine activation leads to mitochondrial arrest to be through activation of small GTPases, and not direct action of calcium (Silva et al., 2021). In the shaft, however, the calcium rise occurs where mitochondria are, which seems to lead to a different effect. To test this, one could selectively induce calcium transients either at individual spines or in synapses in the shaft, for example using glutamate uncaging, while evaluating mitochondrial motility.

We then asked whether these functionally identified synapses, either in spines or in the shaft, were spatially related to stable mitochondria. Previous studies reported mitochondria preferentially co-localizing with excitatory post-synaptic sites under basal conditions (Chang et al., 2006b; Mironov, 2006), or at least when synaptic activity was mimicked (Li et al., 2004b; MacAskill et al., 2009b). We found that shaft (1), but not spine (2), synapses were closer to stable mitochondria than expected by chance (Figure 7A). Regarding shaft activity (1), we found stable mitochondria around the origin of these transients, and a higher density of stable mitochondria within the calcium spread rather than outside. Local calcium transients with similar dynamics and relationship to mitochondria, have been observed in astrocytes (Jackson and Robinson, 2015; Jackson et al., 2014). There, mitochondria accumulated at these locations by binding of calcium to MIRO, arresting mitochondrial motility (Jackson and Robinson, 2015; Jackson et al., 2014). Mitochondria then buffered the resulting calcium, given that compromising mitochondrial function increased calcium spread (Jackson and Robinson, 2015; Jackson et al., 2014). In our dataset, we believe these calcium transients originate from synapses, which could show a molecular fingerprint that recruits or has previously recruited mitochondria. The opposite could also be true, with another signal recruiting more mitochondria to these locations where later shaft synapses are established. All in all, our observation suggests co-localization of high synaptic density- and high mitochondrial density areas. Conversely (2), we did not find active spines to be closer to stable mitochondria. This could be because the density of both spines and mitochondria was quite high, probably preventing the measurement of a spatial bias (Figure 7B). Moreover, if we want to look at the relationship between synapses and stable mitochondria, comparing mitochondrial presence between active and non-active spines might not be the best approach. Non-active spines might be synapses with lower

amplitude and/ or frequency of calcium transients, so the proper comparison could have been spines vs non-spines. However, that was not possible in our setup because spines were homogeneously distributed and in a higher density than mitochondria. Taken (1 and 2) together, it is possible that mitochondria are systematically closer to synapses than expected by chance, and we just were not able to pick this up. Basically, in dendrites where synapses are clustered together (shaft synapses, 1), one could see co-localizing mitochondria also clustered together; while in dendrites with pseudo-homogeneously distributed synapses (for example in spines, 2), mitochondria are also found in a pseudo-homogeneous manner; thus preventing the observation of the possible co-localization between synapses and mitochondria. To test the hypothesis that mitochondria are systematically closer to synapses, one should be able to clearly identify and manipulate stretches of dendrites with and without synapses, both in the shaft and in spines. One could also evaluate long stretches of dendrite at different developmental ages and find synapse- and mitochondria hotspots.

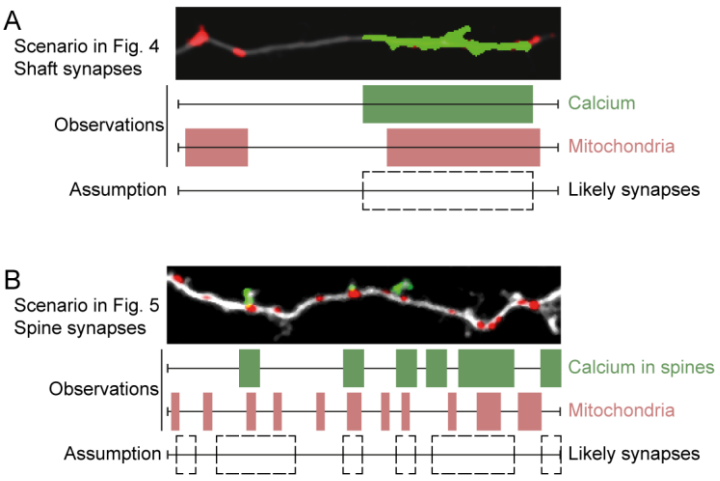

Figure 7. Visual representation of the relationship between spontaneous local calcium transients and stable mitochondria. A. With data in fig. 4, the spontaneously occurring calcium transient supposes the existence of clustered shaft synapses; which co-localize with stable mitochondria. B. With data in fig. 5, the spontaneously occurring calcium transients at spines are spread-out throughout the stretch of dendrite. Mitochondria are also spread-out throughout the stretch of dendrite. We are not able to observe a spatial bias between them, i.e., mitochondria and synapses being closer than expected by chance.

It is likely that this calcium-dependent mitochondrial positioning enables mitochondria to tune ATP production to their surroundings. Thus, the relationship between calcium dynamics and mitochondrial distribution we describe here may serve developing dendrites to efficiently meet calcium handling and energy demands. Our findings suggest that mitochondria play an important role in compartmentalizing calcium signals coming from synapses. As synaptic activity plays a major role in fine-tuning connectivity at these ages, this relationship is likely to have functional implications in wiring the developing brain.

Materials and Methods

Plasmids

To investigate the relationship between neuronal activity and mitochondria we used the genetically encoded calcium indicator GCaMP6s (Addgene plasmid 40753; Douglas Kim) in combination with mitochondrial-DsRed (mitochondrial targeting sequence from subunit VIII of human cytochrome c oxidase causing mitochondrial localization as previously described; Rizzuto et al., 1995; Li et al., 2004; MacAskill et al., 2009). These plasmids were cloned into pCAGGS, to enable delivery to neurons via in utero electroporation.

Animals and in utero electroporation

All experimental procedures were approved by the institutional animal care and use committee of the Royal Netherlands Academy of Arts and Sciences. To sparsely deliver the plasmids of interest to pyramidal neurons of layer II/III of the visual cortex, pregnant C57Bl/6J female mice at 16.5 days gestation underwent in utero electroporation surgery. Pregnant females were anesthetized using 3% isoflurane mixed with 1 L/min oxygen and kept under anesthesia with 1.5-2% isoflurane. A midline incision was made and uterine horns were exposed. Plasmid DNA (mitochondrial-DsRed: 0.1 µg/µl, GCaMP6s: 2 µg/µl) was dissolved in 10 mM Tris and 0.05% Fast Green. Approximately 1 µl of this mixture was injected through a pulled capillary pipette in the lateral ventricle of each embryo using a picospritzer (PLI-100, BTX Harvard Apparatus, Holliston, MA). A custom-made square wave isolated pulse generator (voltage of 50 V, 5 pulses, pulse width 50 ms and 150 ms interval) was used for electroporation. After electroporation, the uterine horns were carefully placed back in the abdomen cavity and the abdomen was sutured. During the surgery embryos were kept moist with warm saline and the mothers were kept warm using a euthermic pad. Pregnant females were allowed to recover after Lidocaine ointment was applied on the wound for local analgesia and Metacam (1 mg/kg s.c.) was administered for post-operative analgesia. Once the pups were born, they were checked before postnatal day 2 for expression and targeting of V1.

Organotypic slice cultures

Organotypic slice cultures of transfected visual cortex were prepared as follows: at postnatal day 5, animals were decapitated quickly, and brains were placed in ice-cold Gey's balanced salt solution under sterile conditions. Coronal slices (400 µm) were cut using a tissue chopper (McIlwain) and incubated with serum-containing medium on

Millicell culture inserts (Millipore, Merck, New York, NY). Slices were kept in culture for 3 to 7 days before imaging.

Confocal microscopy of organotypic slice cultures

For confocal imaging, slices were excised from their membrane supports and placed in a flow-through chamber. Slices were continuously perfused with heated (35°C) Hank's Balanced Salt Solution (HBSS, Fisher Scientific, Waltham, MA, supplemented with in mM: 4.2 NaHCO3, 2.6 CaCl2, 0.1 Trolox). Slices were imaged on a SP5 Leica confocal microscope with a 63x objective (0.9 NA, Leica, Wetzlar, Germany). For imaging we selected neurons that showed the following characteristics: soma localized in upper layer II, apical dendrite pointing to layer I, low basal GCaMP6s fluorescence as well as long and dim mitochondria. Preference was given to isolated cells, to minimize background fluorescence. Apical dendrites (at least 50 µm from the soma) were imaged using an argon laser at 488 nm and power levels between 0.3 and 1%. Time-lapse image stacks (up to 6 optical sections, 1.2 µm z-spacing), at 0.23 µm per pixel, 350 ms per stack were collected for 350 s, every 10 minutes, for a total of 10 times per cell. We observed no changes in fluorescence intensity, cell activity levels or mitochondrial motility levels with time under these conditions. At the end of the experiment, low magnification image stacks (0.23 µm pixel size and 1 µm z-spacing) were collected to localize the recorded dendrite within the dendritic arborization.

In vivo two-photon microscopy

For *in vivo* imaging, transfected neonatal mice (P5-12) were pre-anesthetized using 3% isoflurane mixed with 1 L/min oxygen and kept under anesthesia with 1-2% isoflurane. A head bar with an opening (Ø 4 mm) was attached to the skull above the visual cortex (0–2 mm rostral from lambda and 0–2 mm lateral from the midline) with superglue (Henkel, Düsseldorf, Germany) and dental cement (Heraeus, Hanau, Germany). A small craniotomy above the visual cortex (approximately 1–2 mm Ø) was performed with a needle and forceps and care was taken not to damage the dura mater. The exposed cortical surface was kept moist with cortex buffer (in mM: 125 NaCl, 5 KCl, 10 glucose, 10 HEPES, 2 MgSO4, 2 CaCl2, pH 7.4). For additional stability, a thin layer of 1.5% high electroendosmosis agarose (Biomol, Hamburg, Germany) was applied to the cortical surface. Before imaging, isoflurane was decreased to 0.8% (under anesthesia condition) or 0% (awake condition). A pulsed titanium sapphire laser (Chameleon Vision II, Coherent, Palo Alto, CA) at 900 nm and power up to 30% was used with a 25x water-immersion objective (1.10 NA, Nikon). Time-lapse image stacks (up to 5 optical sections, 2 µm z-spacing) were obtained at a pixel size of 0.13-0.17 µm and stack rate

of 5 to 10 Hz. Throughout the entire experiment, physiological parameters such as heartbeat and body temperature were monitored, and temperature was controlled using a heating pad.

Electrical stimulation

Electrical stimulation was performed by insertion of a glass electrode 40-100 µm from the cell soma. Electrical pulses of 1 ms were delivered at 10 Hz for 1 second, with intensity being adjusted as the minimum required to reliably induce global calcium transients (10 - 30 µA).

Image analysis

All images were processed using ImageJ software. Images were filtered using a median filter (radius 1 pixel). Maximal intensity projections of image stacks were generated. All stacks recorded at one dendrite were corrected for motion artefacts due to drift as well as aligned with respect to each other using NoRMCorre (Pnevmatikakis and Giovannucci, 2017).

From the resulting stacks, two-dimensional projections of time (x-axis) versus displacement (y-axis) were generated for individual dendrites to examine spontaneous global calcium transients as well as mitochondrial motility. Global calcium transients appeared as vertical lines, as there was an increase in intracellular calcium levels throughout the entire dendrite. Immotile mitochondria appeared as horizontal lines, and mitochondrial motility as diagonal lines. The percentage of moving mitochondria was calculated as the number of moving mitochondria divided by the total number of present mitochondria, for each second.

For the analysis of local calcium transients, $\Delta F/F_0$ images were calculated where F_0 was the average fluorescence of the first 200 frames without apparent calcium transients of the first recording for each cell. Custom-made Matlab scripts aided the manual identification of synaptic events: signals had to last for more than the duration of two frames, did not spread from other sites and were localized to the spine head.

Author contributions

CAPS and CL designed the experiments.

CAPS, VB and MZ performed experiments.

CAPS wrote the manuscript.

Affiliations

CAPS, VB, MZ, and CL: Department of Synapse and Network Development, Netherlands Institute for Neuroscience, 1105 BA Amsterdam, the Netherlands.

CL: Department of Functional Genomics, Center for Neurogenomics and Cognitive Research, VU University Amsterdam, the Netherlands.

Competing interests

The authors declare no competing interests.

Acknowledgements

We thank Johan Winnubst, Juliette Cheyne, and Alexandra Leighton for custom-made Matlab scripts; Thomas Misgeld for the original mitochondrial-DsRed plasmid; and Christiaan Levelt for the pCAGGS construct. In addition, we thank Christiaan Levelt for teaching us the in utero electroporation surgery.

References

Ashby, M.C., Maier, S.R., Nishimune, A., and Henley, J.M. (2006). Lateral Diffusion Drives Constitutive Exchange of AMPA Receptors at Dendritic Spines and Is Regulated by Spine Morphology. J. Neurosci. 26, 7046–7055.

Chang, D.T.W., Honick, A.S., and Reynolds, I.J. (2006a). Mitochondrial trafficking to synapses in cultured primary cortical neurons. J. Neurosci. 26, 7035–7045.

Chang, D.T.W., Honick, A.S., and Reynolds, I.J. (2006b). Mitochondrial Trafficking to Synapses in Cultured Primary Cortical Neurons. J. Neurosci. 26, 7035–7045.

De Felipe J., Marco, P., Fairen, A., and Jones, E.G. (1997). Inhibitory synaptogenesis in mouse somatosensory cortex. Cereb. Cortex 7, 619–634.

Faits, M.C., Zhang, C., Soto, F., and Kerschensteiner, D. (2016). Dendritic mitochondria reach stable positions during circuit development. ELife 5.

Harris, J.J., Jolivet, R., and Attwell, D. (2012). Synaptic energy use and supply. Neuron 75, 762–777.

Hausser, M., Spruston, N., and Stuart, G.J. (2000). Diversity and dynamics of dendritic signaling. Science 290, 739–744.

Jackson, J.G., and Robinson, M.B. (2015). Reciprocal Regulation of Mitochondrial Dynamics and Calcium Signaling in Astrocyte Processes. J. Neurosci. 35, 15199–15213.

Jackson, J.G., O'Donnell, J.C., Takano, H., Coulter, D.A., and Robinson, M.B. (2014). Neuronal Activity and Glutamate Uptake Decrease Mitochondrial Mobility in Astrocytes and Position Mitochondria Near Glutamate Transporters. J. Neurosci. 34, 1613–1624.

Kleindienst, T., Winnubst, J., Roth-Alpermann, C., Bonhoeffer, T., and Lohmann, C. (2011). Activity-dependent clustering of functional synaptic inputs on developing hippocampal dendrites. Neuron 72, 1012–1024.

Li, Z., Okamoto, K., Hayashi, Y., and Sheng, M. (2004a). The importance of dendritic mitochondria in the morphogenesis and plasticity of spines and synapses. Cell 119, 873–887.

Li, Z., Okamoto, K., Hayashi, Y., and Sheng, M. (2004b). The Importance of Dendritic Mitochondria in the Morphogenesis and Plasticity of Spines and Synapses. Cell 119, 873–887.

MacAskill, A.F., Rinholm, J.E., Twelvetrees, A.E., Arancibia-Carcamo, I.L., Muir, J., Fransson, A., Aspenstrom, P., Attwell, D., and Kittler, J.T. (2009a). Miro1 is a calcium sensor for glutamate receptor-dependent localization of mitochondria at synapses. Neuron 61, 541–555.

MacAskill, A.F., Rinholm, J.E., Twelvetrees, A.E., Arancibia-carcamo, I.L., Muir, J., Fransson, A., Aspenstrom, P., Attwell, D., and Kittler, J.T. (2009b). Miro1 Is a Calcium Sensor for Glutamate Receptor-Dependent Localization of Mitochondria at Synapses. Neuron 61, 541–555.

Mironov, S.L. (2006). Spontaneous and evoked neuronal activities regulate movements of single neuronal mitochondria. Synapse. 59, 403–411.

Rochefort, N.L., Garaschuk, O., Milos, R.I., Narushima, M., Marandi, N., Pichler, B., Kovalchuk, Y., and Konnerth, A. (2009). Sparsification of neuronal activity in the visual cortex at eye-opening. Proc. Natl. Acad. Sci. 106, 15049–15054.

Sheng, Z.H., and Cai, Q. (2012). Mitochondrial transport in neurons: impact on synaptic homeostasis and neurodegeneration. Nat. Rev. Neurosci. 13, 77–93.

Siegel, F., Heimel, J.A., Peters, J., and Lohmann, C. (2012). Peripheral and central inputs shape network dynamics in the developing visual cortex *in vivo*. Curr. Biol. 22, 253–258.

Silva, C.A., Yalnizyan-Carson, A., Fernández Busch, M.V., van Zwieten, M., Verhage, M., and Lohmann, C. (2021). Activity-dependent regulation of mitochondrial motility in developing cortical dendrites. ELife 10, e62091.

Chapter 5

Characterization of the EB3-YFP/ Mito-CFP mouse line as a tool to study microtubule- and mitochondrial dynamics in the developing visual cortex

Cátia A. P. Silva and Christian Lohmann

CAPS contribution: designed and performed experiments, wrote the manuscript.

List of figures

Abstract

To form functional neuronal networks, young neurons are extremely morphologically dynamic in an effort to establish appropriate synaptic contacts. These morphological changes are energy-dependent and are mostly mediated by microtubules, part of the neuron's cytoskeleton. Mitochondria are the main energy-providing organelles in neurons, and are transported via microtubules to all parts of the neuron. Thus, understanding the relationship between microtubule- and mitochondrial dynamics is crucial to understand the rules of neuronal connectivity. We characterized the novel EB3-YFP/ Mito-CFP mouse line, to test whether it is a suitable tool to study microtubule- and mitochondrial dynamics in the developing visual cortex. This mouse line combines fluorescent labeling of microtubules by YFP-tagged EB3, and mitochondria by CFP-tagged COXVIII. This mouse line shows mitochondrial dynamics consistent with previous literature, but overexpression of EB3-YFP over time, and very few YFP and CFP co-expressing cortical neurons. Thus, this mouse line is not a suitable tool for our study. Nonetheless, these issues do not seem to occur in other brain areas, such the hippocampus, suggesting that this mouse line could be a valuable tool for others.

Introduction

During early development, neurons undergo morphological maturation as the axon elongates and the dendritic tree becomes denser and larger. These changes allow for many synapses to be formed between cells, connecting neurons, and generating early functional networks. At first, these connections are highly changeable; synapses are formed, eliminated or stabilized as networks are refined (Elston and Fujita, 2014; Hua and Smith, 2004; Lohmann and Kessels, 2014).

These changes in neuronal morphology and connectivity are mediated by the cytoskeleton, a complex and dynamic network of fibers that gives the cell its shape (Gallo and Letourneau, 2000). The cytoskeleton consists of three main types of fibers: actin filaments, neurofilaments and microtubules, and each plays a specific role in maintaining and adapting cell structure and function. Actin filaments mediate mostly activity-dependent morphological changes in filopodia and spines. Neurofilaments serve to anchor organelles, maintaining the internal organization of the cell. Microtubules are the neuronal 'highways', crucial for the transport of organelles and vesicles to all parts of the cell. They are highly dynamic, and continuously assembled and dismantled (Gu and Zheng, 2009). Microtubule dynamics are mostly regulated by a group of

microtubule-associated end-binding (EB) proteins, such as end-binding protein 3 (EB3) which binds to the plus-end of microtubules to enable their growth.

The development of synapses, synaptic transmission, and microtubule-dependent transport of organelles are highly energy demanding processes. A substantial amount of this energy is supplied by mitochondria, the main energy providers in neurons (Harris et al., 2012). Mitochondria are also dynamic. They undergo fusion and fission (to control their function, size, and number), and are motile (transported via microtubules to all parts of the cell) (Sheng and Cai, 2012). Microtubule- and mitochondrial dynamics are extremely critical in young neurons, as they ensure energy is available, so the correct synaptic connections are established (Blockus and Polleux, 2021).

Our laboratory has unpublished evidence of a relationship between microtubule- and mitochondrial dynamics during brain development. At each branch point in a dendrite, a mitochondrion travelling from the soma can exhibit one of three behaviors: stop at the branch point, continue through the right branch, or the left branch. Individual mitochondria were significantly more likely to display the same behavior as the previous mitochondrion, suggesting they followed the available microtubule track. Extracellular application of glucose to one of the branches lead to a significant increase in mitochondrial motility towards said branch. In the future, we aim to further investigate the relationship between microtubule- and mitochondrial dynamics, as well as their role in establishing networks in the visual cortex before the onset of vision. We therefore require a tool that allows us to visualize both microtubule- and mitochondrial dynamics.

Here, we characterized the novel EB3-YFP/ Mito-CFP mouse line, to test whether it is a suitable tool to study microtubule- and mitochondrial dynamics in the developing visual cortex. This mouse line combines fluorescent labeling of microtubules by YFP-tagged EB3, and mitochondria by CFP-tagged COXVIII (cytochrome oxidase 8, a mitochondria-specific protein). The two original lines were used to study microtubule- and mitochondrial dynamics respectively, mostly in peripheral axons (Kleele et al., 2014; Misgeld et al., 2007). Our investigation indicates that YFP overexpression over time interferes with the study of EB3 dynamics, and that cortical neurons co-expressing both YFP and CFP are rare, preventing the systematic study of the relationship. Nonetheless, we provide proof of concept that microtubule- and mitochondrial dynamics can be studied in individual young neurons. We concluded that this mouse line is not suitable for our study, but a promising tool for others.

Results

To test whether EB3-YFP/ Mito-CFP mice are suitable to investigate the relationship between microtubule- and mitochondrial dynamics in the developing cortex, we performed several dual imaging experiments: two-photon imaging *in vivo*; and confocal imaging in acute slices and in slice cultures of the visual cortex before eye opening at postnatal day (P) 14 (Figure 1). This mouse line expresses YFP-tagged EB3, a microtubule plus-end binding protein that enables visualization of dynamic microtubules (specifically growing), and CFP-tagged mitochondria.

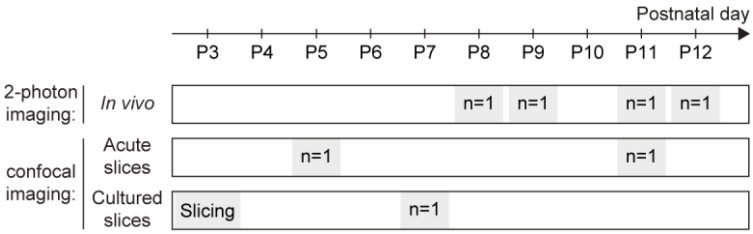

Figure 1. Experimental timeline. We performed two-photon microscopy imaging *in vivo* in four animals (postnatal day (P) 8 -12); and confocal imaging in acute slices (obtained from one P5 and one P11 mouse), and in slice cultures (from one P3 mouse, kept for 4 days *in vitro* (DIV)).

First, we imaged the superficial layers *in vivo* of the visual cortex of mouse pups, aged 8, 9, 11 or 12 days old. Each animal was used for only one timepoint. To study microtubule- and mitochondrial dynamics, we obtained time-lapse recordings of both the EB3-YFP and Mito-CFP channels. From these recordings, we generated average fluorescence images to enable visualization of moving mitochondria. As was expected in dendrites, we observed mitochondrial motility in both anterograde and retrograde directions. The average speed was 0.35 ± 0.03 µm/ s (Figure 2A) (P8: n = 5, 0.23 ± 0.04 µm/ s; P9: n = 4, 0.17 ± 0.08 µm/ s; P11: n = 22, 0.44 ± 0.05 µm/ s; P12: n = 16, 0.31 ± 0.03 µm/ s). To measure EB3 dynamics, we generated average fluorescence images using the EB3-YFP channel and traced the outline of neuronal processes resulting from dynamic EB3 (Figure 2B-C). We identified dynamic EB3 in animals younger than P10 (Figure 2B, note the outline of neuronal processes). In animals older than P10, EB3 fluorescence was too abundant and diffuse to observe single microtubule dynamics (Figure 2C, note the absence of the outline of neuronal processes). We traced single dendrites and created two dimensional projections of time versus displacement to measure EB3 turnover in animals younger than P10 (Figure 2D). Also as expected in dendrites, EB3 dynamics were observed in both directions and the average speed was 0.12 ± 0.01 µm/ s (P8: n = 6, 0.13 ± 0.02 µm/ s; P9: n = 4, 0.10 ± 0.01 µm/ s). Surprisingly, we did not detect neurons co-expressing EB3-YFP and Mito-CFP. These data suggest that the expression of each transgene occurs at different time-points, and the

pools of neurons in which they are initially expressed are different. As a consequence, the superficial layers of the visual cortex of this mouse line do not co-express EB3-YFP and Mito-CFP in sufficient individual neurons to study the relationship between microtubule- and mitochondrial dynamics. With time, it seems that expression would increase enough so that it would overlap in the same neuron, but by then, high and diffuse EB3-YFP expression prevents analysis of microtubule dynamics in animals older than P10.

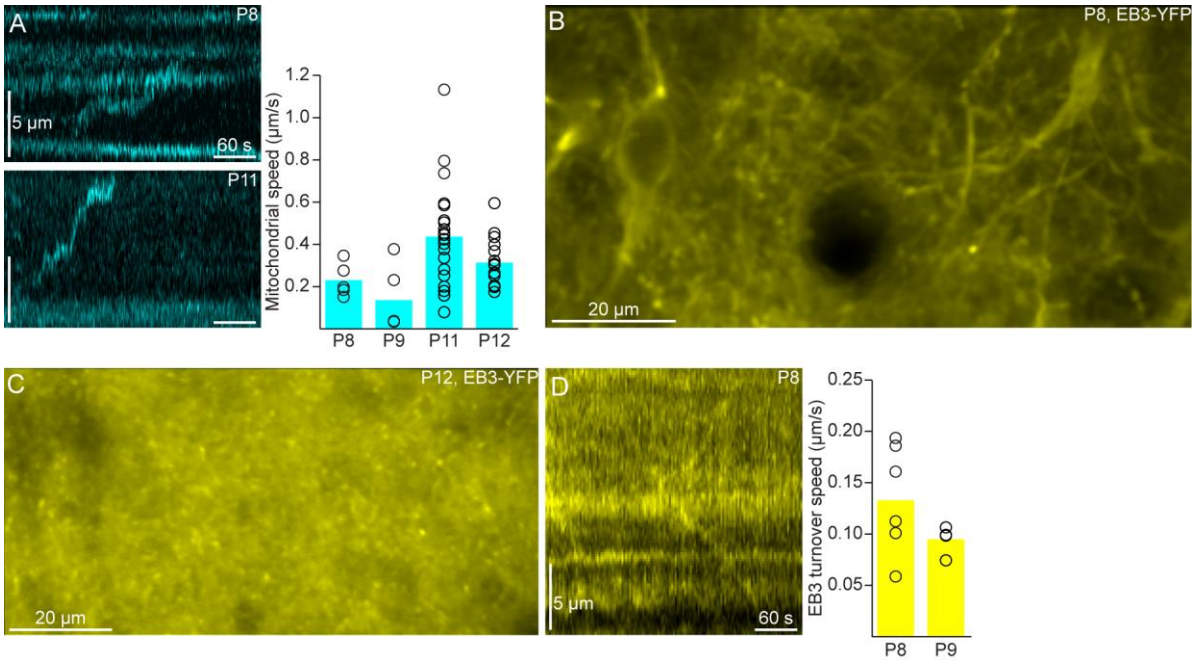

Figure 2. YFP-tagged microtubule and CFP-tagged mitochondrial dynamics *in vivo*.
A. Two-dimensional representation of CFP-tagged mitochondrial motility in a P8 (top) and a P11 (bottom) animal, and quantification of mitochondrial speed.
B. Average fluorescence of EB3-YFP in a P8 mouse from *in vivo* two-photon imaging showing identifiable EB3 dynamics as the outline of neuronal processes.
C. Average fluorescence of EB3-YFP in a P12 mouse from *in vivo* two-photon imaging showing no identifiable EB3 dynamics.
D. Two-dimensional representation of YFP-tagged EB3 dynamics (example) in a P8 animal, and EB3 turnover speed quantification.

To better characterize EB3-YFP and Mito-CFP expression patterns in different cortical layers and throughout development, we prepared acute coronal cortical slices from a P5 and a P11 mouse. At P5, deeper cortical layers showed both EB3-YFP and Mito-CFP labeling, while superficial cortical layers were mostly void of both (Figure 3A-B). We did not find neurons co-expressing EB3-YFP and Mito-CFP at P5. At P11, EB3-YFP fluorescence was observed in all cortical layers, but single dendrites could not be identified (Figure 3C). Mito-CFP-positive neurons were more abundant in deeper than more superficial cortical layers (Figure 3D). We also did not find neurons co-expressing EB3-YFP and Mito-CFP at P11. We produced two dimensional projections of time versus

displacement to measure EB3 and mitochondrial dynamics in either mouse (Figure 3E-F). Dynamic EB3-fluorescence and Mito-CFP fluorescence were scarce at both time points. From the few dynamic EB3-YFP-tagged plus ends and Mito-CFP tagged mitochondria, we computed the speed. YFP-tagged EB3 turnover speed was 0.16 ± 0.01 µm/ s at P5 (n = 6), and 0.09 ± 0.02 µm/ s at P11 (n = 3) (Figure 3E). Mito-CFP tagged mitochondrial speed was 0.62 ± 0.16 µm/ s at P5 (n = 3), and 0.29 ± 0.05 µm/ s at P11 (n = 2) (Figure 3F). These observations suggest an asynchronous developmental profile of EB3-YFP and Mito-CFP expression, from deeper to more superficial cortical layers.

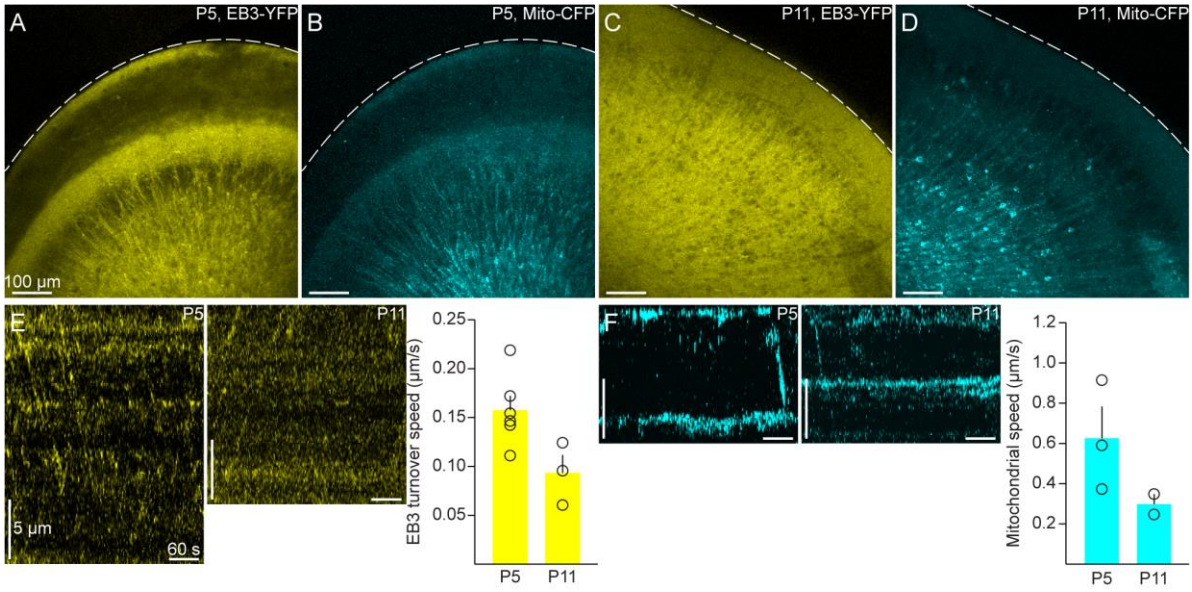

Figure 3. Microtubule- and mitochondrial dynamics in acute slices.
A-B. Overview picture of EB3-YFP (A) and Mito-CFP (B) in a P5 acute slice.
C-D. Overview picture of EB3-YFP (C) and Mito-CFP (D) in a P11 acute slice.
A-D: Dashed line indicates top edge of layer I. No double labelled cells were found in either cortex.
E. Two-dimensional representation of EB3 dynamics at P5 (left) and P11 (middle) and quantification of EB3 turnover speed (right). Few dynamic EB3 were found.
F. Two-dimensional representation of mitochondrial dynamics at P5 (left) and P11 (middle) and quantification of mitochondrial speed (right). Few dynamic mitochondria were found.

To test if the simultaneous study of microtubule- and mitochondrial dynamics would be possible in deeper cortical layers of younger animals, we obtained cortical slices from a P3 mouse and kept them in culture for 4 days (P3 + DIV 4). We only found one neuron co-expressing EB3-YFP and Mito-CFP in cortical slice cultures (Figure 4A, dashed box). Similar to experiments described above, EB3 turnover was 0.14 ± 0.01 µm/ s (n = 17) (Figure 4B). Mitochondrial motility, however, was lower than expected, as well as slower 0.09 ± 0.02 µm/ s (n = 4) (Figure 4C). As this was the only co-expressing neuron found, we could not study the relationship between microtubule- and mitochondrial dynamics.

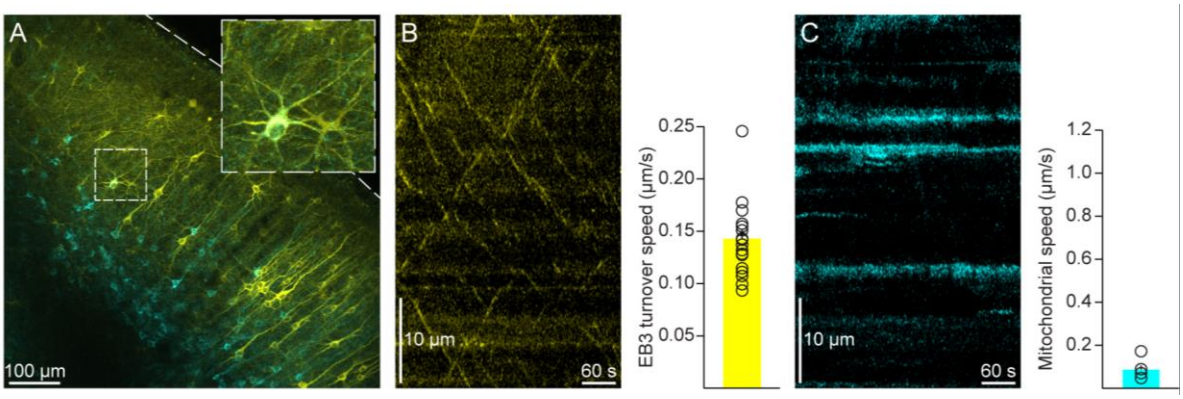

Figure 4. YFP-tagged microtubule and CFP-tagged mitochondrial dynamics in cortical slice cultures.
A. Overview picture of an organotypic cortical slice showing EB3-YFP and Mito-CFP fluorescence. Dashed box identifies the only double labelled neuron found. Dashed line indicates the top edge of layer I.
B. Two-dimensional representation of YFP-tagged EB3 dynamics (left) and dynamic EB3 speed quantification (right).
C. Two-dimensional representation of CFP-tagged mitochondrial dynamics (left) and mitochondrial speed quantification (right).

Subsequently, we analyzed the hippocampus for co-expression of EB3-YFP and Mito-CFP (Figure 5A). We obtained hippocampal slices at P3 and cultured them for 3 days (P3 + DIV 3). We found a small number of co-expressing neurons in which the relationship between microtubule- and mitochondrial dynamics could be studied (Figure 5B).

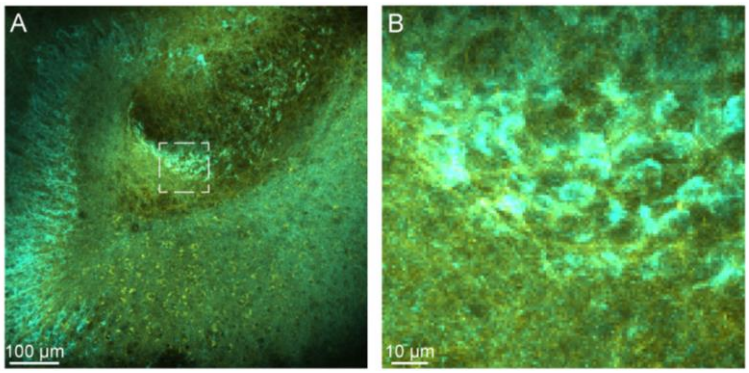

Figure 5. YFP-tagged Microtubule and CFP-tagged mitochondrial dynamics in hippocampal slice cultures.
A. Overview picture of an organotypic hippocampal slice showing EB3-YFP and Mito-CFP.
B. Digital zoom of dashed box, showing double-labeled neurons.

A summary of our evaluation of EB3-YFP and Mito-CFP expression patterns across cortical layers and developmental age is shown in a schematic (Figure 6). Both EB3-YFP and Mito-CFP were found to be expressed from deeper to more superficial cortical layers over developmental age, with Mito-CFP being expressed later. With time, EB3-YFP becomes diffuse, i.e., clear puncta were not observed, preventing its use to measure EB3 dynamics. Both constructs were only co-expressed in deep cortical layers of young animals, and co-expression within single neurons was rare. Thus, the applicability of this transgenic mouse line to study the relationship between

microtubule- and mitochondrial dynamics in the developing cortex is limited and can be used only in specific regions and developmental time windows.

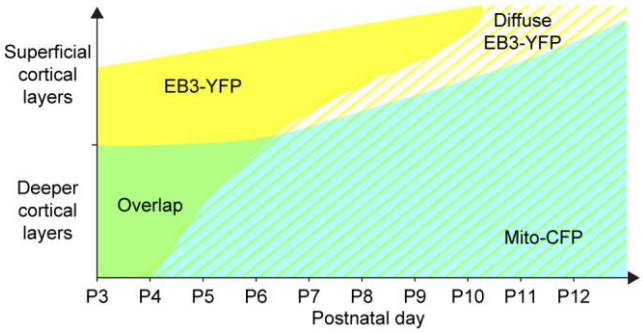

Figure 6. EB3-YFP and Mito-CFP expression patterns.
Mito-CFP-expression (cyan area) spreads from deeper to more superficial cortical layers with time. At P12, layer II is still not populated by Mito-CFP. EB3-YFP (yellow area) also shows a developmental profile from deeper to more superficial layers, but after some time, EB3-YFP becomes diffuse (yellow striped area), preventing the analysis of microtubule dynamics. Both Mito-CFP and non-diffuse EB3-YFP co-exist in deeper cortical layers (albeit without co-expression within the same neuron).

Discussion

The EB3-YFP/ Mito-CFP transgenic mouse line originated from the crossing of two mouse lines that were previously used to study microtubule- and mitochondrial dynamics, respectively, mostly in peripheral axons (Kleele et al., 2014; Misgeld et al., 2007). Here, we were the first to characterize EB3-YFP and Mito-CFP co-expression in developing dendrites of the visual cortex of this mouse line. We also assessed whether EB3-YFP/ Mito-CFP mice could be used to study microtubule- and mitochondrial dynamics during the first two postnatal weeks, before the onset of visual input. These transgenic mice showed dendritic mitochondrial dynamics comparable to previous observations (Chang and Reynolds, 2006; Chang et al., 2006). Also as expected in dendrites, EB3-mediated microtubule growth occurred in both directions. The average speed was 0.13 ± 0.007 µm/ s (all experiments), which is similar to estimations in *ex vivo* distal axons in adult mice (0.112 ± 0.003 µm/ s) (Kleele et al., 2014). By P11, we were not able to measure dynamic EB3-YFP in cortical dendrites, as labeling became diffuse. Co-expression of EB3-YFP and Mito-CFP in single cortical neurons was rare. Taken together, we conclude that this mouse line is not suitable to study the relationship between microtubule- and mitochondrial dynamics during cortical development. However, this mouse is a suitable tool for other studies, as hippocampal neurons co-expressed EB3-YFP and Mito-CFP.

The Mito-CFP expression appears to work well, making this mouse a suitable tool to study mitochondrial dynamics. Here, we focused on mitochondrial speed. Mitochondria can move in bouts of high speed (over 1 µm /s) and pause in between. As we only

consider frames that showed mitochondrial displacement at the frequency with which we acquired (mostly under 1 Hz), these may be averaged into lower speed (one second at 1 µm/ s and one second paused, as 0 µm/ s, is read as 0.5 µm/ s). The higher mitochondrial speed in older animals observed here could be explained by the faster imaging acquisition *in vivo* (0.5 Hz *in vitro* vs 0.7 – 1.5 Hz *in vivo*).

We were not able to detect dynamic EB3 in cortical dendrites by P11 in this transgenic mouse line. The most likely cause for this is that the cell continues to produce EB3-YFP, even when binding sites are saturated. This EB3-YFP overexpression leads to diffuse EB3-YFP labeling as EB3-YFP concentration in the cytoplasm increases, while no further binding to microtubules occurs. This ubiquitous cytoplasm fluorescence dominates the signal and prevents visualization of EB3-YFP at binding sites. Overexpression has been observed in other EB3-YFP mouse lines, and ones with lower expression levels are being generated (Kleele et al., 2014, personal communication). This phenomenon might be EB3-specific, and fluorescently labeling other proteins that regulate microtubule dynamics could be a solution.

Co-expression of EB3-YFP and Mito-CFP was extremely rare in cortical neurons during the first two postnatal weeks. In EB3-YFP/ Mito-CFP mice, the Thy1 promoter drives both EB3-YFP and Mito-CFP expression. Previous mouse lines using this promoter showed mosaic transgene expression in varying subsets of neurons (Feng et al., 2000). When the two lines are crossed, the level of co-expression within single neurons is unpredictable.

In this mouse line, it seems neurons start expressing the YFP-EB3 transgene earlier than they do the CFP-Mito transgene. By the time neurons express CFP-Mito, YFP-EB3 expression in single neurons is no longer suitable for imaging of dynamic EB3. It also seems that different neurons preferably express one of the transgenes, which could be due to their integration site within the genome.

To study the relationship between microtubule- and mitochondrial dynamics in the developing cortex, we must ensure both that neurons contain both transgenes, and that only a sparse population of neurons are labelled, so that we can clearly identify individual cells. There are (at least) two ways of achieving this using transgenic mice. The first uses conditional expression of both CFP-Mito and YFP-EB3 transgenes, for example in combination with a sparse Cre or CaMKII transgenic mouse line (Chakravarthy et al., 2008), or conditional EB3-YFP expression only in Mito-CFP-positive neurons. The second method is to use the 2A construct, which is a single peptide that ensures cloning of two genes within single cells. All these approaches ensure that the constructs are expressed together.

An alternative to the use of transgenic mice would be to deliver plasmid DNA in wild-type mice, for example via viral injections in pups, or in utero electroporation. The latter might be the best suited for *in vivo* dendritic imaging of the visual cortex, since it allows for sparse labeling of layer II/III pyramidal neurons with stable expression levels over time.

In conclusion, the EB3-YFP/ Mito-CFP transgenic mouse line shows the mitochondrial dynamics that we would expect both based on literature and our own experience. However, this mouse line also shows overexpression of EB3 over time, and almost no co-expression within cortical neurons. Therefore, it is not a suitable tool to study the role of microtubule- and mitochondrial dynamics in establishing networks in the visual cortex. Conversely, it appears to be a valuable tool to study other brain areas, such as the hippocampus.

Materials and Methods

Generation of the transgenic EB3-YFP/ Mito-CFP mouse

To label growing microtubule ends and mitochondria within the same animal, two transgenic mouse lines were crossed in the laboratory of Prof. Dr. Thomas Misgeld, at the Technical University of Munich, Germany: EB3-YFP (YFP-tagged end-binding protein 3) and Mito-CFP (CFP-tagged subunit VIII of human cytochrome c oxidase gene). Mice carrying both transgenes were used for our experiments.

Mouse import and handling

EB3-YFP/ Mito-CFP transgenic mice were transported from Munich to Amsterdam while pregnant, and subsequently kept in individually ventilated cages (IVC) in a temperature-controlled room with a light-night cycle of 12 h. Pups were used in the first two postnatal weeks, after which the entire nest was euthanized. All experimental procedures were approved by the institutional animal care and use committee of the Royal Netherlands Academy of Arts and Sciences.

Slice cultures

Organotypic slice cultures containing the visual cortex were prepared as follows. At postnatal day (P) 3, animals were quickly decapitated, and the brain was placed in ice-cold Gey's balanced salt solution under sterile conditions (in mM: 4.96 KCl, 0.22 KH_2P0_4, 1.03 $MgCl_2*6H_2O$, 0.28 $MgSo_4*7H_2O$, 137 NaCl, 0.85 Na_2HPO_4, 2.12 Na_2HCO_3, 8.33 glucose, 1.5 $CaCl_2*2H_2O$, 0.5 kynurenic acid, pH 7.2). Coronal slices (400 µm) were cut using a

tissue chopper (McIlwain) and the four most caudal ones were incubated with serum-containing medium on Millicell culture inserts (Millipore). Slices were kept in culture for at least 3 days before imaging.

Acute slices

Acute coronal slices (300 µm) containing the visual cortex were obtained from P5 and P11 mice. Animals were quickly decapitated, and their brains were immersed in ice-cold cutting solution (in mM: 2.5 KCl, 1.25 NaH_2PO_4, 26 $NaHCO_3$, 20 glucose, 215 sucrose, 1 $CaCl_2$, 7 $MgCl_2$, pH 7.3-7.4) bubbled with 95%/ 5% O_2/ CO_2. Slices were obtained with a vibratome (Microm HM 650V, Thermo Scientific) and subsequently incubated at 35°C for 45 minutes in artificial cerebrospinal fluid (ACSF, in mM: 125 NaCl, 3.5 KCl, 1.25 NaH_2PO_4, 26 $NaHCO_3$, 20 glucose, 2 $CaCl_2$, 1 $MgCl_2$, pH 7.3-7.4).

Confocal microscopy of slices

For confocal imaging, both slice cultures and acute slices were placed in a flow-through chamber and continuously perfused with imaging solution at 35°C. Slice cultures were first excised from their culture inserts and perfused with Hank's Balanced Salt Solution (HBSS, Fisher Scientific, supplemented with in mM: 4.2 $NaHCO_3$, 2.6 $CaCl_2$, 0.1 Trolox). Acute slices were perfused with ACSF solution (see above) bubbled with 95%/ 5% O_2/ CO_2.

Slices were imaged on a SP5 Leica confocal microscope using a 63x objective (0.9 NA, Leica), with 458 and 514 nm laser lines. Time-lapse image stacks (up to 6 optical sections, 1 µm z-spacing) were obtained at 0.12 µm per pixel and stack rate of 0.5 Hz.

Acute *in vivo* two-photon microscopy

For acute *in vivo* imaging of young mice, pups of 8 to 12 days old were anesthetized using 3 % isoflurane mixed with 1 L/ min oxygen and kept under anesthesia with 1-2 % isoflurane. A head bar with an opening (Ø 4 mm) was attached to the skull above the visual cortex (0–2 mm rostral from lambda and 0–2 mm lateral from the midline) with superglue (Pattex) and dental cement (Heraeus Kulzer). A small craniotomy above the visual cortex (approximately 1–2 mm Ø) was performed with needle and forceps while care was taken not to damage the dura mater. The exposed cortical surface was kept moist with cortex buffer (in mM: 125 NaCl, 5 KCl, 10 glucose, 10 HEPES, 2 $MgSO_4$ and 2 $CaCl_2$, pH 7.4). For additional stability, a thin layer of 1.5 % high electroendosmosis agarose (Biomol) was applied to the cortical surface. A 2-photon microscope using a 25x water-immersion objective (1.10 NA, Nikon) and a 3 W titanium sapphire laser on a 960 nm laser line was used. Time-lapse image stacks (up to 3 optical sections, 2 µm z-

spacing) were obtained at 0.17 µm pixel and stack rate of 0.7 to 1.5 Hz. Throughout the entire experiment, physiological parameters such as heartrate and body temperature were monitored, and temperature was controlled using a heating pad.

Image analysis

All images were processed using ImageJ software. Maximum projections of image stacks were generated and corrected for motion artefacts due to drift or breathing of the animal. From the resulting stacks, two dimensional projections of time versus displacement were constructed for identifiable dynamic microtubule tips or moving mitochondria.

Author contributions

CAPS and CL designed and performed experiments, and wrote the manuscript.

Affiliations

CAPS and CL: Department of Synapse and Network Development, Netherlands Institute for Neuroscience, The Netherlands.

CL: Department of Functional Genomics, Center for Neurogenomics and Cognitive Research, VU University Amsterdam, the Netherlands.

Competing interests

The authors declare no competing interests.

Acknowledgements

We thank Thomas Misgeld and Tatjana Kleele for generating and providing the mice, as well as valuable discussions regarding the obtained unexpected results.

References

Blockus, H., and Polleux, F. (2021). Developmental mechanisms underlying circuit wiring: Novel insights and challenges ahead. Curr. Opin. Neurobiol. 66, 205–211.

Chakravarthy, S., Keck, T., Roelandse, M., Hartman, R., Jeromin, A., Perry, S., Hofer, S.B., Mrsic-Flogel, T., and Levelt, C.N. (2008). Cre-Dependent Expression of Multiple Transgenes in Isolated Neurons of the Adult Forebrain. PLOS ONE 3, e3059.

Chang, D.T.W., and Reynolds, I.J. (2006). Differences in mitochondrial movement and morphology in young and mature primary cortical neurons in culture. Neuroscience 141, 727–736.

Chang, D.T.W., Honick, A.S., and Reynolds, I.J. (2006). Mitochondrial trafficking to synapses in cultured primary cortical neurons. J. Neurosci. 26, 7035–7045.

Elston, G.N., and Fujita, I. (2014). Pyramidal cell development: postnatal spinogenesis, dendritic growth, axon growth, and electrophysiology. Front. Neuroanat. 8.

Feng, G., Mellor, R.H., Bernstein, M., Keller-Peck, C., Nguyen, Q.T., Wallace, M., Nerbonne, J.M., Lichtman, J.W., and Sanes, J.R. (2000). Imaging neuronal subsets in transgenic mice expressing multiple spectral variants of GFP. Neuron 28, 41–51.

Gallo, G., and Letourneau, P.C. (2000). Neurotrophins and the dynamic regulation of the neuronal cytoskeleton. J. Neurobiol. 44, 159–173.

Gu, J., and Zheng, J.Q. (2009). Microtubules in Dendritic Spine Development and Plasticity. OpenNeurosci J 3, 128–133.

Harris, J.J., Jolivet, R., and Attwell, D. (2012). Synaptic energy use and supply. Neuron 75, 762–777.

Hua, J.Y., and Smith, S.J. (2004). Neural activity and the dynamics of central nervous system development. Nat.Neurosci. 7, 327–332.

Kleele, T., Marinković, P., Williams, P.R., Stern, S., Weigand, E.E., Engerer, P., Naumann, R., Hartmann, J., Karl, R.M., Bradke, F., et al. (2014). An assay to image neuronal microtubule dynamics in mice. Nat. Commun. 5, 4827.

Lohmann, C., and Kessels, H.W. (2014). The developmental stages of synaptic plasticity. J. Physiol. 592, 13–31.

Misgeld, T., Kerschensteiner, M., Bareyre, F.M., Burgess, R.W., and Lichtman, J.W. (2007). Imaging axonal transport of mitochondria *in vivo*. Nat Meth 4, 559–561.

Sheng, Z.H., and Cai, Q. (2012). Mitochondrial transport in neurons: impact on synaptic homeostasis and neurodegeneration. Nat. Rev. Neurosci. 13, 77–93.

Chapter 6

General discussion

Preface

In this thesis we studied how neuronal mitochondria relate to developing synapses, and synaptic and neuronal activity. We focused on the use of more intact study systems (cultured slices and the *in vivo* mouse brain) and more physiologically relevant protocols than previously used (spontaneous activity and activity within the physiological range).

This resulted in three main conclusions:

1. Mitochondrial motility decreases over development (chapter 2 (Smit-Rigter et al., 2016) and chapter 3 (Silva et al., 2021))).

2. Global neuronal activity does not affect mitochondrial motility (chapter 3 (Silva et al., 2021)) and chapter 4).

3. Synaptic activity arrests mitochondrial motility (chapter 3 (Silva et al., 2021)) and chapter 4).

and two open questions:

1. Are mitochondria closer to synapses than expected by chance (chapter 2 (Smit-Rigter et al., 2016) and chapter 4)?

2. What is the relationship between microtubule- and mitochondrial dynamics (chapter 5)?

Last, I discuss this thesis' relevance for the field of synapse development and mitochondria, and propose several future directions.

Conclusions

1. Mitochondrial motility decreases over development

Previously, it was thought that neuronal mitochondria were highly motile organelles. This conclusion was drawn mostly from experiments using dissociated neurons obtained from embryonic tissue. However, more recent studies, including ours in chapters 2 and 3 that include *in vivo* (1) and *in vitro* (2) studies (discussed below) in the visual cortex, showed that mitochondrial motility decreases over time, mostly stabilizing within two weeks after birth (Faits et al., 2016; Silva et al., 2021; Smit-Rigter et al., 2016).

To the best of our knowledge, we are the first to image dendritic mitochondria *in vivo* (1) in the developing brain (Silva et al., 2021). During the first two postnatal weeks (postnatal day (P) 5 to 12), we observed a steady decrease in the number of moving mitochondria over days (Silva et al., 2021). We also imaged axonal mitochondria during

the second postnatal week (P10-13) and in adulthood (8-10 weeks old), where moving mitochondria were equally rare (~1%) (Smit-Rigter et al., 2016). This was in line with previous studies (Lewis et al., 2016), and suggests initial high mitochondrial motility that stabilizes by the end of the second postnatal week. Our data specifically suggest that mitochondrial motility in the primary visual cortex stabilizes around eye opening (~ P13).

In our hands, cortical slice cultures (2) retained the mitochondrial motility levels characteristic of the age at which they were obtained (Silva et al., 2021). Increasing days *in vitro* (P5 or P8 + 3 to 7 days *in vitro* (DIV)) did not have a significant effect on mitochondrial motility in dendrites, i.e., there was no decrease detected as observed *in vivo* (Silva et al., 2021). Axonal mitochondria in slice cultures obtained during the first postnatal week and kept in culture for another week (P5 + DIV7-8), showed higher motility levels than the ones observed in P10-13 animals *in vivo* (Smit-Rigter et al., 2016). This is because mitochondrial motility remained at levels characteristic of the age at which the slices were obtained (P5), and not the total age of the slice (12 - 13 days); thus being higher *in vitro* (at P5 + DIV7-8) than *in vivo* (at P10-13). In other studies, mitochondrial motility in neuronal projections of dissociated neurons decreased over days *in vitro* (E14/16 + DIV3-28)(Chang and Reynolds, 2006; Lewis et al., 2016). This was associated with an increase in synaptic density and synaptic co-localization with mitochondria (Chang and Reynolds, 2006; Lewis et al., 2016). The discrepancy between these studies (where mitochondrial motility changes over DIVs) and ours (where it does not) is probably due to the number of DIVs (over 10 vs 5 days, respectively); but it could also be due to differences between dissociated neurons and organotypic slice cultures, which we did not test in our setups. We thus conclude that mitochondrial motility in slice cultures is likely to follow the same profile as *in vivo* (decrease over time), but definitely slower. Therefore, *in vitro* approaches, although valuable, show a discrepancy in the developmental profile of mitochondrial motility.

Taken together, the following scenario emerges: mitochondria are initially generated at the soma and transported to distal parts of neurons during early brain development. At this moment, mitochondrial motility is typically high, but decreases over development (Chang and Reynolds, 2006; Faits et al., 2016; Lewis et al., 2016; Silva et al., 2021; Smit-Rigter et al., 2016).

2. Global neuronal activity does not affect mitochondrial motility

Results from studies using artificially-induced changes in global activity were used to support the hypothesis that neuronal activity affects mitochondrial motility. More recent studies, including ours in chapters 3 and 4, have challenged this view and shed light on the reasons for the apparent discrepancy between the effect of artificial- and naturally occurring neuronal activity on mitochondrial motility.

Many studies have performed activity manipulations that led to changes in mitochondrial motility (Chang et al., 2006; Li et al., 2004; MacAskill et al., 2009). Their main conclusion was that neuronal activity arrests mitochondrial motility at synaptic sites, likely through binding of synaptic calcium to MIRO1 which releases the mitochondrion from its transport machinery (MacAskill et al., 2009). Conversely, blocking neuronal activity increased mitochondrial motility, as the absence of intracellular calcium would prevent mitochondrial arrest (Chang et al., 2006; Li et al., 2004). Others, however, failed to detect such relationship between artificial activity manipulations and mitochondrial motility (Beltran-Parrazal et al., 2006). Reasons for the discrepancy include the concentration of drugs used for synaptic stimulation (e.g. 30 µM (MacAskill et al., 2009) vs 10 µM of glutamate (Beltran-Parrazal et al., 2006)).

Although there are fewer studies on naturally occurring activity, those that examined spontaneous activity consistently did not find an effect of global activity on mitochondrial motility (Faits et al., 2016; Silva et al., 2021). In the visual cortex, prior to vision onset, we observed no relationship between mitochondrial motility and spontaneous global activity in any of a wide range of experiments in chapters 3 and 4. In cultured slices obtained from P5 and P8 mice and in the *in vivo* brain between P5 and 12 with or without anesthesia, spontaneous global activity did not alter mitochondrial motility (Silva et al., 2021). This is in line with the previous finding that in retinal explants, spontaneously generated global activity at retinal ganglion cells did not affect mitochondrial motility (Faits et al., 2016).

This discrepancy between artificial- and natural activity may be explained by the fact that artificial manipulations of activity probably activate molecular pathways that are not activated through physiological activity, perhaps because artificial manipulations affect many neurons in a very synchronous manner. In chapter 4, we attempted to manipulate activity within the physiological range, by waking pups up from isoflurane anesthesia. This led to an increase in the frequency of spontaneous global calcium transients but had no effect on mitochondrial motility. Also in chapter 4, but now in slice cultures, increasing the frequency of spontaneous global calcium transients with

electrical stimulation within the physiological range also did not change mitochondrial motility. Others, however, observed decreased mitochondrial motility and increased mitochondrial overlap with synapses after electrical stimulation of synapses (Li et al., 2004). This discrepancy may be due to the frequency of stimulation used (discussed in the next subsection).

We have postulated that mitochondrial motility is affected by other than global neuronal activity. Since most activity manipulations affect both action potential firing and synaptic transmission, perhaps changes in synaptic transmission, but not firing alone, altered mitochondrial motility in these studies. That synaptic activation, but not action potential firing arrests mitochondrial motility is consistent with most observations of activity-dependent regulation of mitochondrial motility. In summary, artificial manipulations of global activity affect mitochondrial motility, while spontaneously occurring global neuronal activity does not; and synaptic activity might be the missing link between the two.

3. Synaptic activity arrests mitochondrial motility

The evidence that synaptic activity affects mitochondrial motility is vast and based mostly on experiments that artificially manipulated neuronal activity (previous subsection). This entails two limitations: the use of artificial manipulations (versus spontaneous activity) and affecting overall neuronal activity (versus specifically synaptic activity).

To the best of our knowledge, in chapter 3 (Silva et al., 2021) we are the first to show a relationship between spontaneously occurring neuronal activity at the synaptic level, and mitochondrial motility. We showed that spontaneous activity at single synapses precedes mitochondrial immobilization of nearby moving mitochondria (Silva et al., 2021). This effect was restricted in both space and time (approximately 10 micrometers from the spine's insertion point, and within one to two minutes after synaptic activation) (Silva et al., 2021). By provoking synaptic vesicle exocytosis, we showed that synaptic activity directly affected mitochondrial motility (Silva et al., 2021). These results differ from those found in the retina, where mitochondria did not stop upon spontaneously occurring synaptic activity and motility was not affected by blocking neurotransmitter receptors (Faits et al., 2016). This suggests that the regulation of mitochondrial motility is somewhat different between retinal and cortical neurons.

Our observation that synaptic activity arrests mitochondria may help integrate our findings with those before us that used artificial manipulations of activity. In our hands, electrical stimulations at either 10 Hz or 100 Hz led to global calcium transients of the same amplitude and duration as spontaneous ones (data not shown). Thus, in chapter 4, we performed 10 Hz stimulation to induce global calcium transients, which did not affect mitochondrial motility. We did not test whether 100 Hz stimulation affected mitochondrial motility. However, in another study, 100 Hz stimulation at spines did decrease mitochondrial motility (Li et al., 2004). Neuropeptide/ neurotrophin release is known to specifically be triggered by higher activity, e.g., 100 but not by 10 Hz (Gartner and Staiger, 2002). Synaptic stabilization (NR2B to A, and/ or PSD95 recruitment) also occurs with 100 but not 10 Hz stimulation (Matsuzaki et al., 2004). We therefore propose that electrical stimulation that induces global calcium transients does not affect mitochondrial motility, but electrical stimulation that affects synaptic transmission and plasticity does.

Mitochondrial arrest might also occur through a second messenger. We have shown that mitochondria did not stop immediately after a synaptic transmission event, but required approximately a minute to do so, supporting the idea that intermediate steps, e.g. including activation of small GTPases, might happen in the meantime.

Finally, we also estimated whether the regulation of mitochondrial motility by synaptic activity could be the leading cause for the decrease in mitochondrial motility over development (Silva et al., 2021). Our computational simulation included the progressive increase in synaptic transmission that occurs during the first two postnatal weeks, and the observed decrease in mitochondrial motility (Silva et al., 2021). It could explain how the increase in the frequency of global calcium transients and decrease in mitochondrial motility over development occur concomitantly but without the first directly affecting the second. Instead, the increase in synaptic density and activity (correlated with increased frequency of global calcium transients) directly affects mitochondrial motility.

Taken together, decreased mitochondrial motility over development might be due to increased synaptic density and activity. This reconciles existing literature with apparently contradictory results: artificial manipulations of activity affect mitochondrial motility because they massively affect all synaptic activity; spontaneous global calcium transients do not affect mitochondrial motility because the number of synapses affected is too small to have a measurable impact on mitochondria; and only electrical stimulation that affects synaptic activity affects mitochondria. This

differential effect of synaptic activity and global action potential firing opens a range of new questions about the characteristics of each, both in terms of information content as well as molecular markers.

Open questions

1. Are mitochondria closer to synapses than expected by chance?

Given the local modulation that synapses can have on nearby mitochondria, one could expect to find mitochondria closer to synapses than expected by chance. However, this does not seem to be always the case. In axons, we have found mitochondria and boutons to be closer than expected by chance (Smit-Rigter et al., 2016). Many studies find that boutons with closer mitochondria have some synaptic advantage, e.g. stability (Lees et al., 2019). In dendrites, we did not find mitochondria to be closer to synapses than expected by chance (chapter 4). Previous studies have both found the same as us in basal conditions (MacAskill et al., 2009), while others found mitochondria to be closer to synapses than to non-synaptic sites (Chang et al., 2006; Mironov, 2006). Differences between dendrites and axons could be due to the fact that mitochondrial occupancy and synaptic density in dendrites are higher than in axons (Chang et al., 2006; Li et al., 2004). This could imply that in axons, we can observe one mitochondrion and one synapse close together. In dendrites, however, this spatial bias might not be so obvious because there are many synapses and many mitochondria per stretch. Hence, synapses may temporarily arrest mitochondria (as discussed above), but the spatial relationship between them is not one mitochondrion to one synapse. In chapter 4, we observed mitochondrial accumulation at calcium compartments in the dendritic shaft. These calcium compartments are probably composed of many shaft synapses, suggesting mitochondria to be spatially related to synapses. Moreover, having high synaptic density compartments co-localizing with mitochondria supports the hypothesis that mitochondria and synapses can preferably co-localize, but this cannot be observed by looking at single synapses and single mitochondria.

Taken together, it seems that dendritic mitochondria may preferentially locate in areas of high synaptic density, but this might vary with age, type of neuron, activity profile, or other factors. In addition, ease of detection of this potential preferential localization likely depends on the physiology and morphology of the neuronal processes. Thus, the spatial relationship between dendritic mitochondria deserves further investigation.

2. What is the relationship between microtubule- and mitochondrial dynamics?

The cytoskeleton plays an essential role in stabilizing neuronal shape and providing structures required for long-range transport of organelles and vesicles, including mitochondria. Some elements of the cytoskeleton, such as microtubules, are extremely dynamic, polymerizing and de-polymerizing to grow and retract as required by the cell. Mitochondrial arrest through synaptic activity may involve microtubules (see Chapter 1, section 2.5). For example, ATP depletion, which is more likely to happen near synapses, might inhibit microtubule-based mitochondrial transport (Mironov, 2007). Similarly, high synaptic calcium concentrations could affect mitochondrial- and/ or microtubule function in such a way that microtubule-dependent mitochondrial transport is inhibited (MacAskill et al., 2009; Mironov, 2007; Wang and Schwarz, 2009). Long term immobilization of mitochondria could also involve their connection to microtubules (MacAskill et al., 2009; Wang and Schwarz, 2009). Studying the relationship between microtubule- and mitochondrial dynamics is thus necessary to understand the reciprocal modulation of synapses and mitochondria and, consequently, the setting up of young neuronal networks.

Relevance

Mitochondria in dendrite and synapse development

Mitochondrial motility and positioning are fundamental for neurite development and synaptic plasticity (Courchet et al., 2013; Divakaruni et al., 2018; Kimura and Murakami, 2014; López-Doménech et al., 2016; Vaccaro et al., 2017). Thus, the regulation of mitochondrial distribution is most likely crucial to ensure proper wiring in the developing brain. Setting up functional neuronal networks involves growing neurites and establishing synaptic contacts. Initially, neurons overgrow their neurites and establish many more synaptic contacts than they will then keep. These processes are mostly dependent on cell adhesion molecules, such as cadherins (Ye and Jan, 2005). The formation of new synapses (i.e. synaptogenesis) is thought to usually begin with contact between axonal and dendritic filopodia (Vaughn et al., 1988). Then, structural proteins are delivered to the presynaptic site, and activation of glutamate receptors further recruits neurotransmitter receptors from the postsynaptic density. Not all synapses are maintained and this process of elimination (i.e. synaptic pruning) occurs due to competition between axons (e.g. for neuronal growth factors). Which synapses are

maintained or eliminated is of obvious great importance for the resulting brain. Synaptic pruning, besides requiring hormones and neurotrophic factors, is also activity dependent. Our lab has previously shown evidence for an "out of sync lose your link" mechanism, where synapses that are not co-active with their synapse neighbors are more likely to be eliminated (Kleindienst et al., 2011). This modulation is especially interesting as it occurs at the level of single synapses, and not the entire dendrite or even neuron (further discussed in the next subsection).

Exacerbated neurite growth and synaptogenesis, as well as synaptic pruning, are energy demanding processes, and are probably established through the most metabolically efficient way. But how can the brain afford to make long neurites and many synapses that will then be eliminated? Indeed, mitochondria play an important role in these processes. Mitochondria were shown to negatively modulate neurite growth and branching (Kimura and Murakami, 2014), i.e., mitochondrial presence hinders neurite outgrowth. In parallel, mitochondria have been positively related to synaptogenesis (Li et al., 2004), with mitochondria and synaptic presence being strongly linked. Taken together, one could speculate that mitochondria could be involved in optimizing resources in the developing brain. Specifically, mitochondria could minimize neurite length and branching, to maximize resources for establishing synaptic contacts.

Mitochondria have also been positively related to synaptic function and increased synaptic efficacy (Cserép et al., 2018). So, can mitochondria be involved in the decision of which synapses are kept and which are eliminated? Although we lack direct empirical evidence for this, one could hypothesize that during development, mitochondrial proximity to some synapses could provide a survival advantage. For example, synapses with mitochondria nearby would be kept, while synapses without nearby mitochondria could be pruned. This could be due to mitochondria locally providing synapses with ATP and buffer the calcium resulting from synaptic activity. Thus, understanding the role of mitochondria during dendrite and synapse development is an important building block of our efforts to understand the rules of brain wiring.

Global and local activity have different characteristics

Experiments in this thesis demonstrate that local synaptic activity can have effects that differ from those of an action potential. This is not a new idea, as we know that neurons are not linear integrators that just sum inputs. Indeed, dendritic compartments can act as non-linear integrating computational units (Winnubst and Lohmann, 2012). For example, in adult mammals, simultaneously active spatially clustered synapses have

functional advantages, as they produce a depolarization that exceeds the linear summation of the synapses involved (Major et al., 2013; Sheffield and Dombeck, 2015; Xu et al., 2012). For this to occur, both strategic organization of synapses along the dendrite and synchronized spontaneous activity during development are required. This supports the idea that much of the computation happening in the brain is sub-cellular and does not always require action potential firing.

Experimental approaches and manipulations within the scope of this thesis

Two important limitations are associated with almost all the studies that have contributed to the current body of knowledge on the role of neuronal activity on mitochondrial motility: the almost exclusive use of dissociated neurons and artificial manipulations.

First, most previous studies used dissociated neurons. Dissociated neurons are obtained from embryonic tissue, and kept in culture for a variable number of days. They are easy to obtain and handle, as well as to manipulate pharmacologically and genetically. They enabled numerous important studies. However, dissociated neurons grow in non-natural media, and can establish aberrant connections with each other. Thus, dissociated neurons provide very good experimental control and are likely to be the best tool to perform artificial manipulations, and high-throughput essays, with very high resolution. However, they are probably not the best for developmental studies of postnatal neurons, as neuronal development occurs differently *in vitro* versus within an intact brain.

Slice cultures can be obtained at different days during the first postnatal weeks, enabling developmental studies of mitochondria- and synapse profiles. They retain natural activity patterns (unlike dissociated neurons) and show spontaneous activity (unlike acute slices). They also provide good experimental control and are a good tool to perform artificial manipulations. However, slices are also cultured in non-natural media; they do not retain long-range connectivity, as thalamic and other cortical projections are severed; and aberrant connections are probably made between neurons during the culturing phase. Thus, slices are a better choice for studying developing neurons at different stages.

The study of the *in vivo* brain allows for the investigation of an intact brain. Here, all brain cells are kept within their networks and molecular environments. However, *in vivo* experiments are likely to occur under anesthesia or stressful conditions for the animal,

potentially affecting normal brain functioning, thus making it more difficult to perform good experimental controls. In addition, these studies are expensive and of high technical difficulty, besides ethically unadvised.

As of now, there is no perfect approach, and one must critically consider which is the most suitable for each research question. In the particular question of mitochondrial motility and distribution in the developing brain, as well as its relationship to developing synapses, the best model system might be the slice culture, when kept in culture for a limited number of days as to avoid aberrant activity and connectivity. These allow for the delivery of genetic markers for synapses, synaptic activity, mitochondria, microtubules, and a combination; as well as for artificial manipulations.

Secondly, most previous studies used artificial manipulations of activity to affect mitochondria. Artificial manipulations are mostly well described and induce massive changes in neurons, which usually lead to clear effects that are easy to measure and replicate. These also generated important and relevant knowledge, but left the door open for the role of physiological activity. Indeed, most artificial manipulations affected mitochondria, while spontaneous activity and activity in the physiological range did not. More studies using naturally occurring activity are now necessary to bridge the gap in knowledge regarding their effect on mitochondrial motility, and the wiring of the developing brain.

Future directions

To further explore the relationship between synapses and synaptic activity, and mitochondrial motility and -distribution in the developing brain, a pondered decision on which experimental setup to use is essential (dissociated neurons, cultured slices, or the *in vivo* brain), and which (if any) artificial manipulations.

Recent developments have made it possible to record spontaneous synaptic events in single synapses of layer II/III pyramidal neurons during the first two postnatal weeks (A. H. Leighton, 2020, personal communication), which can be combined with a mitochondrial tracker. Do single synapses in the *in vivo* brain of young pups affect nearby moving mitochondria? What are the details of this relationship?

As argued above, the cultured slice is an excellent model system to study these topics. Specifically, the mechanisms by which synaptic transmission, but not global activity, modulates mitochondrial distribution can be studied. For how long do mitochondria remain stationary after spontaneous synaptic events? Do synapses with

nearby immobile mitochondria affect moving ones? Are synapses with mitochondria at the postsynaptic side different from ones without (increased releasing probability, morphological size, protein content, etc.)? Is the fate (eliminated vs stabilized) of post-synaptic sites dependent on mitochondrial proximity? Furthermore, we could test how activating single synapses affects nearby moving mitochondria. To do this, our lab developed a semi-automated technique that involves electrically activating the presynaptic partner of a single post-synaptic site (Winnubst et al., 2015), which could be done when a mitochondrion is passing by. Together with this technique, pharmacological manipulations would help dissect the molecular partners necessary for the effect of synaptic activity on mitochondrial motility. Can it be predicted which synapses affect nearby mitochondria? What is the molecular mechanism by which mitochondria are immobilized (both initially, and long term)? Is there increased mitochondrial substrate around synapses, such as provided by glucose transporters? Can we purposely place mitochondria in different locations and measure its impact on nearby structures (e.g. synapses and filopodia)?

Investigating how long-term stabilization of mitochondria occurs near the postsynaptic site is also important. Is long-term stabilization of mitochondria dependent on synaptic structures and/ or activity, MIRO1, microtubules, and/ or the actin cytoskeleton? Is it locally regulated, or is mitochondrial density high enough not to be? Are there anchoring structures that facilitate mitochondrial immobilization near synapses?

The relationship between microtubule and mitochondrial dynamics should also be investigated with a combination of microtubule and mitochondrial trackers for imaging experiments. What is the spatiotemporal relationship between microtubule- and mitochondrial dynamics? How are mitochondria, microtubules, and/ or other entities, regulating microtubule-dependent mitochondrial transport and distribution in the developing brain?

Lastly, as we better understand the functioning of single neurons and the rules of connectivity between young neurons, it will be important to invest in better computational models that provide accurate predictions of the biological mechanisms, which will allow us to further expand humanity’s scientific knowledge while reducing animal experimentation.

References

Beltran-Parrazal, L., López-Valdés, H.E., Brennan, K.C., Díaz-Muñoz, M., de Vellis, J., and Charles, A.C. (2006). Mitochondrial transport in processes of cortical neurons is independent of intracellular calcium. Am. J. Physiol. Cell Physiol. *291*, C1193-1197.

Chang, D.T.W., and Reynolds, I.J. (2006). Differences in mitochondrial movement and morphology in young and mature primary cortical neurons in culture. Neuroscience *141*, 727–736.

Chang, D.T.W., Honick, A.S., and Reynolds, I.J. (2006). Mitochondrial trafficking to synapses in cultured primary cortical neurons. J. Neurosci. *26*, 7035–7045.

Courchet, J., Lewis, T.L., Lee, S., Courchet, V., Liou, D.-Y., Aizawa, S., and Polleux, F. (2013). Terminal Axon Branching Is Regulated by the LKB1-NUAK1 Kinase Pathway via Presynaptic Mitochondrial Capture. Cell *153*, 1510–1525.

Cserép, C., Pósfai, B., Schwarcz, A.D., and Dénes, Á. (2018). Mitochondrial Ultrastructure Is Coupled to Synaptic Performance at Axonal Release Sites. ENeuro *5*.

Divakaruni, S.S., Van Dyke, A.M., Chandra, R., LeGates, T.A., Contreras, M., Dharmasri, P.A., Higgs, H.N., Lobo, M.K., Thompson, S.M., and Blanpied, T.A. (2018). Long-Term Potentiation Requires a Rapid Burst of Dendritic Mitochondrial Fission during Induction. Neuron *100*, 860-875.e7.

Faits, M.C., Zhang, C., Soto, F., and Kerschensteiner, D. (2016). Dendritic mitochondria reach stable positions during circuit development. ELife *5*.

Gartner, A., and Staiger, V. (2002). Neurotrophin secretion from hippocampal neurons evoked by long-term-potentiation-inducing electrical stimulation patterns. ProcNatl AcadSciUSA *99*, 6386–6391.

Kimura, T., and Murakami, F. (2014). Evidence that dendritic mitochondria negatively regulate dendritic branching in pyramidal neurons in the neocortex. J. Neurosci. *34*, 6938–6951.

Kleindienst, T., Winnubst, J., Roth-Alpermann, C., Bonhoeffer, T., and Lohmann, C. (2011). Activity-dependent clustering of functional synaptic inputs on developing hippocampal dendrites. Neuron *72*, 1012–1024.

Lees, R.M., Johnson, J.D., and Ashby, M.C. (2019). Presynaptic Boutons That Contain Mitochondria Are More Stable. Front. Synaptic Neurosci. *11*, 37.

Lewis, T.L., Turi, G.F., Kwon, S.-K., Losonczy, A., and Polleux, F. (2016). Progressive Decrease of Mitochondrial Motility during Maturation of Cortical Axons *In vitro* and *In vivo*. Curr. Biol. *26*, 2602–2608.

Li, Z., Okamoto, K., Hayashi, Y., and Sheng, M. (2004). The importance of dendritic mitochondria in the morphogenesis and plasticity of spines and synapses. Cell *119*, 873–887.

López-Doménech, G., Higgs, N.F., Vaccaro, V., Roš, H., Arancibia-Cárcamo, I.L., MacAskill, A.F., and Kittler, J.T. (2016). Loss of Dendritic Complexity Precedes Neurodegeneration in a Mouse Model with Disrupted Mitochondrial Distribution in Mature Dendrites. Cell Rep. *17*, 317–327.

MacAskill, A.F., Rinholm, J.E., Twelvetrees, A.E., Arancibia-Carcamo, I.L., Muir, J., Fransson, A., Aspenstrom, P., Attwell, D., and Kittler, J.T. (2009). Miro1 is a calcium sensor for glutamate receptor-dependent localization of mitochondria at synapses. Neuron *61*, 541–555.

Major, G., Larkum, M.E., and Schiller, J. (2013). Active properties of neocortical pyramidal neuron dendrites. Annu. Rev. Neurosci. *36*, 1–24.

Matsuzaki, M., Honkura, N., Ellis-Davies, G.C., and Kasai, H. (2004). Structural basis of long-term potentiation in single dendritic spines. Nature *429*, 761–766.

Mironov, S.L. (2006). Spontaneous and evoked neuronal activities regulate movements of single neuronal mitochondria. Synapse. *59*, 403–411.

Mironov, S.L. (2007). ADP regulates movements of mitochondria in neurons. Biophys. J. *92*, 2944–2952.

Sheffield, M.E.J., and Dombeck, D.A. (2015). Calcium transient prevalence across the dendritic arbour predicts place field properties. Nature *517*, 200–204.

Silva, C.A., Yalnizyan-Carson, A., Fernández Busch, M.V., van Zwieten, M., Verhage, M., and Lohmann, C. (2021). Activity-dependent regulation of mitochondrial motility in developing cortical dendrites. ELife *10*, e62091.

Smit-Rigter, L., Rajendran, R., Silva, C.A.P., Spierenburg, L., Groeneweg, F., Ruimschotel, E.M., van Versendaal, D., van der Togt, C., Eysel, U.T., Heimel, J.A., et al. (2016). Mitochondrial dynamics in visual cortex are limited *In vivo* and not affected by axonal structural plasticity. Curr. Biol. *26*, 2609–2616.

Vaccaro, V., Devine, M.J., Higgs, N.F., and Kittler, J.T. (2017). Miro1-dependent mitochondrial positioning drives the rescaling of presynaptic Ca2+ signals during homeostatic plasticity. EMBO Rep. *18*, 231–240.

Vaughn, J.E., Barber, R.P., and Sims, T.J. (1988). Dendritic development and preferential growth into synaptogenic fields: A quantitative study of Golgi-impregnated spinal motor neurons. Synapse *2*, 69–78.

Wang, X., and Schwarz, T.L. (2009). The mechanism of Ca2+ -dependent regulation of kinesin-mediated mitochondrial motility. Cell *136*, 163–174.

Winnubst, J., and Lohmann, C. (2012). Synaptic clustering during development and learning: The why, when and how. Front. Mol. Neurosci. *5:70*.

Winnubst, J., Cheyne, J.E., Niculescu, D., and Lohmann, C. (2015). Spontaneous activity drives local synaptic plasticity *in vivo*. Neuron *87*, 399–410.

Xu, N.L., Harnett, M.T., Williams, S.R., Huber, D., O'Connor, D.H., Svoboda, K., and Magee, J.C. (2012). Nonlinear dendritic integration of sensory and motor input during an active sensing task. Nature *492*, 247–251.

Ye, B., and Jan, Y.N. (2005). The cadherin superfamily and dendrite development. Trends Cell Biol *15*, 64–67.